

Wetting of Brushes by Polymer Melts

Promotoren: prof. dr. M.A. Cohen Stuart
 hoogleraar in de Fysische Chemie,
 met bijzondere aandacht voor de
 Kolloïdchemie

 prof. dr. G.J. Fleer
 persoonlijk hoogleraar bij de leer-
 stoelgroep Fysische Chemie en
 Kolloïdkunde

Samenstelling promotiecommissie:

prof. dr. J. Lyklema	(Wageningen Universiteit)
prof. dr. R. van der Linde	(Technische Universiteit Eindhoven)
prof. dr. G.J. Vancso	(Technische Universiteit Twente)
dr. E.M. Blokhuis	(Universiteit Leiden)

0000 0886 6275

Wetting of Brushes by Polymer Melts

Joost Maas

Proefschrift

ter verkrijging van de graad van doctor

op gezag van de rector magnificus

van Wageningen Universiteit,

prof. dr. ir. L. Speelman,

in het openbaar te verdedigen

op woensdag 20 juni 2001

des namiddags te half twee in de aula.



1615060

Joost Hubert Maas

Wetting of Brushes by Polymer Melts

Thesis Wageningen Universiteit

ISBN 90-5808-442-6

Subject headings: wetting / dewetting / thin films / polymers

Contents

Chapter	page
1. Introduction: Wetting, Powder Coatings and Pigments	1
2. Physically Adsorbed Brushes	15
3. Chemically Grafted Brushes	29
4. Wetting of Brushes by Polymer Melts	43
5. Wetting Transition in a Polymer Brush: Polymer droplet coexisting with two film thicknesses	73
6. Wetting of Dense Brushes: the role of entropy	85
7. Thin block copolymer films: corrugation under the AFM tip	99
8. Other Block copolymers as Wetting Agents	107
Summary	123
Samenvatting	127
Curriculum Vitae	131
Dankwoord	133

Chapter 1 Introduction: Wetting , Powder Coatings and Pigments

1. Wetting and dewetting

When a liquid drop is placed on a flat solid surface, it may show two types of equilibrium situations: partial wetting or complete wetting. Partial wetting refers to the situation where droplets with a finite contact angle are present on the surface, and at complete wetting the droplet spreads and there is, in equilibrium, a thin film of liquid present on the surface. A metastable film of a polymer liquid can be formed on a non-wettable surface by spin coating¹⁻³. At low temperatures, such a film is solid-like and therefore does not change. However, it will relax towards its equilibrium when annealed above the glass transition temperature (T_g) of the polymer. When partial wetting occurs, the initially flat film will eventually break up into droplets with a specific contact angle. The breakup process of metastable films has been studied extensively experimentally^{4,5-11} and theoretically¹²⁻¹⁵, and is reasonably well understood. This process is obviously very relevant to applications in paint, adhesives and biomedical devices.

We consider one example in more detail. Smooth polystyrene films of varying thickness can be deposited by spin coating on oxidised silicon wafers. In figure 1.1 we show some optical microscope images of the dewetting process observed for such films. First, circular holes are formed in the polystyrene film which are found to grow as a function of the annealing time. If two holes touch, the liquid between thins to a ribbon; when there are many holes, this leads to a polygon network of such ribbons. The ribbons are unstable and break up into droplets, so that one gets a polygonal structure of polymer droplets on the surface (figure 1.1)³.

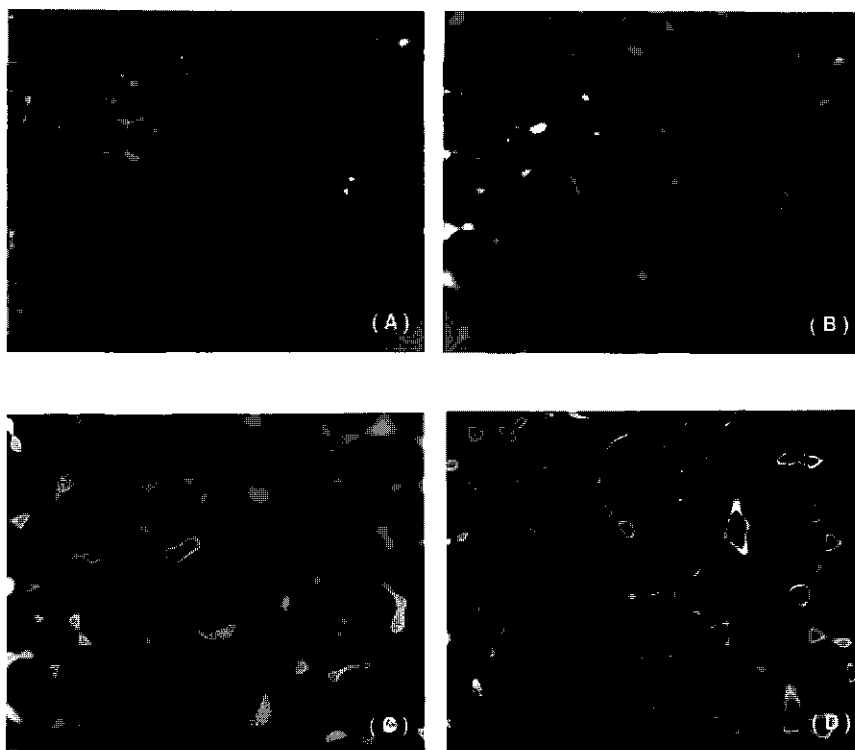


Figure 1.1. Optical micrographs of a polystyrene ($M_n=9000$ g/mole) film (12 nm) onto SiO_2 after annealing for 5 (A), 15 (B), 60 (C) and 210 (D) minutes at 170°C , some 70 degrees above T_g . The length of the images is 0.15 mm

A series of polystyrene samples with varying molecular weight was annealed at 170°C and the rate of hole growth was determined. A linear growth is observed in all cases, indicating a constant dewetting velocity. In figure 1.2, the average radii of the holes are plotted as a function of the annealing time. As expected, the dewetting velocity (given by the slope of the curves) is found to decrease with increasing molar mass, because of increasing viscosity.

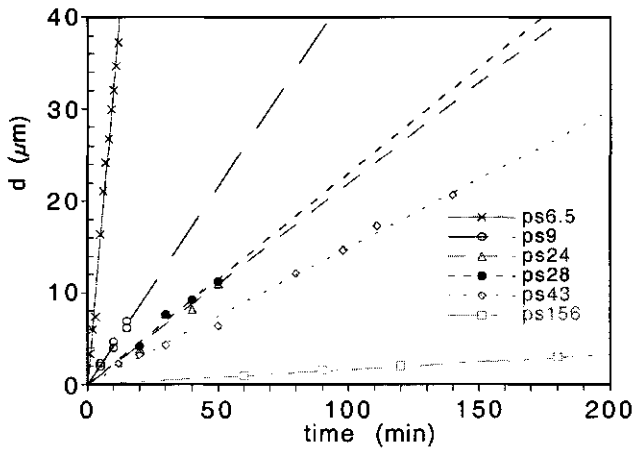


Figure 1.2. Radii of holes in a polystyrene film versus time annealed at 170 °C for various molecular weights. The numbers are given in kg/mole.

Theoretical descriptions of the dewetting process starts from a small fluctuation of the film thickness¹⁶⁻²¹. The stability is then controlled by the development of the structures. Unstable fluctuations (non wettable surface) develop into holes which grow in size. Stable fluctuations do not result in an amplification of the disturbance and the liquid film on the surface is stable. Polymer liquids can be more complicated than normal liquids due to the entanglements of the chains. The flow behaviour and the kinetics of hole growth can be different for both types of liquids. Entangled polymers can slip on smooth surfaces^{22,23}. The kinetics of hole formation is characterised by the radius d of the dry patch and increases in time (t) as a power law $d(t) \propto t^n$. For Poiseuille flow (normal liquids) the exponent $n = 1$ and for liquids with slip $n = 2/3$ ^{20,24}. The polymers used in figure 1.2 have no slip and $n = 1$.

The wetting behaviour of a polymer melt onto a surface can be modified by grafting suitable polymers to the substrate²⁵⁻²⁸. For example, it has been found that a partially

wettable surface can be made completely wettable by means of grafting a polymer that is compatible with the melt onto the surface. One would be tempted to conclude that grafting always leads to improved wetting. However, theoretical studies and experiments show that very densely grafted polymers (so-called brushes) may have the opposite effect^{26,27,29-32}. This may even happen if the free polymer melt and the brush are of identical chemical structure^{26,27,33-35}. This is referred to as 'autophobicity'. Apparently, the grafting density is a crucial variable. A systematic study of these effects is highly desirable.

2. Tethered chains: mushrooms and brushes

By attaching polymer chains on a solid surface at low grafting densities such that the distance between the grafted points is larger than the radius of gyration of the chain, one essentially obtain isolated coils without interaction. Such chains are now commonly called 'mushrooms' (fig. 1.3a). In a good solvent these mushrooms are swollen, whereas in a non-solvent they are collapsed. As the grafting density increases, the coils will interact and stretch. This situation is called a 'brush' (fig. 1.3b).

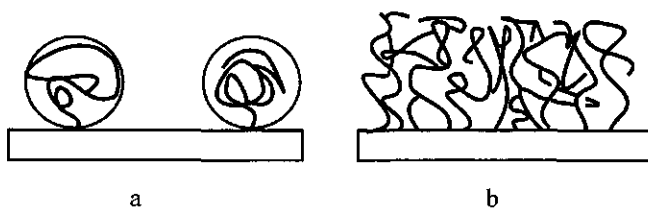


Figure 1.3. Surface covered with mushrooms (a) and brushes (b).

One way to prepare polymer brushes is by adsorption of block copolymers on a surface, where one block has a high affinity for the surface and the other block has no or a relatively low affinity for the surface. The block which adsorbs onto the surface is called the anchor block and the other block is called the buoy block of the polymer. The adsorbed amount of the block copolymer is a function of the composition of the block copolymer, solvent quality and the type of surface^{25,28,36}.

Another way to prepare polymer brushes is by chemical grafting from a surface with reaction initiators present on the surface and monomers present in solution is often used³⁷⁻³⁹. Another chemical grafting technique is grafting to the surface. Reactive (end) groups, which will react with surface groups are used to form a brush. In this way very dense monodisperse brushes can be prepared^{27,40}. Also used is spreading and compressing the surface area with a langmuir trough. Passing the sample through the interface will transfer the brush from the air/water interface onto the substrate⁷.

3. Powder Coatings

Coatings are thin (solid) films applied on substrates to protect or decorate the underlying material. Thin films are important in many cases, e.g., life employs thin films (e.g. in lungs for breathing and on feathers of water birds). Man-made coatings are usually based on polymeric systems which form a permanent network on the substrate. In order to process coatings, solvents can be used which evaporate during film formation. Organic solvents were used frequently in the past but nowadays environmental regulations require that coatings contain less of such solvents. Powder coatings are one kind of solvent-free coatings. Film formation in these materials occurs by annealing the substrate. Powder coatings are composed of pigment particles dispersed in a resin. The polymer resin is the actual film forming coating material, and the pigment particles serve to protect the substrate and provide colour. To coat a metal surface, the dry powder particles are first electrostatically deposited on the substrate. Upon heating (annealing above the glass transition temperature) the powder particles melt into droplets. The droplets coalesce and after some time a smooth and homogeneous film is formed. After cooling down, the coating has been established. Compared to solvent based liquid coatings, powder coatings are more environmentally friendly because their application does not lead to the release of polluting organic vapours into the air⁴¹.

In the ideal situation, the adhesion to the substrate is strong and the pigment particles are dispersed homogeneously throughout the film. In practice, the performance of powder coatings is not always so good. Sometimes, the adhesion of the coating to the

surface is too weak due to poor interaction between the coating and the surface. In other cases, the film may be inhomogeneous due to aggregation of the pigment particles or segregation of the particles to one of the interfaces. The work described in this thesis is motivated by these latter effects. We have investigated a method to improve the coating with regard to aggregation and surface segregation (figure 1.4), in other words, to stabilise the pigment particles.

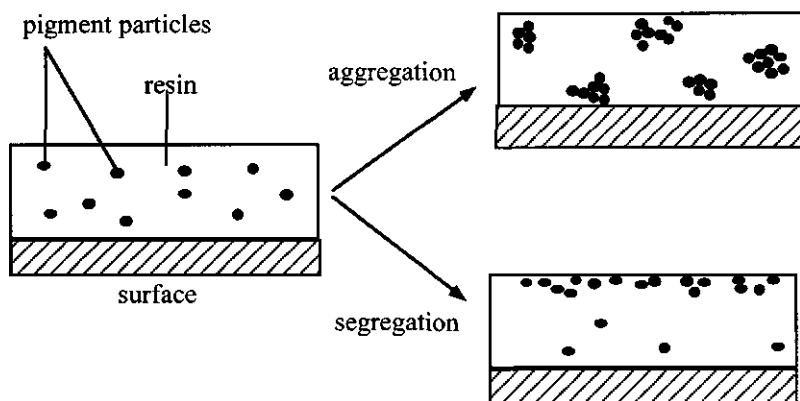


Figure 1.4. Aggregation and segregation of pigment particles in a resin.

4. Stabilisation of pigment particles

Between any pair of identical particles embedded in a medium, there is a Van der Waals interaction. This Van der Waals interaction is always attractive, irrespective of the matrix. In order to prevent aggregation, the short-range attraction must be counteracted by some repulsion.

Colloidal particles may be stabilised by electrostatic repulsion with a number of charges located at the interface. This can be positive or negative depending on the nature of the surface groups. These charges have to be compensated in the solution to maintain electroneutrality. Close to the surface there is a different concentration of counterions compared to the bulk concentration. The region close to the surface is called the electrical double layer and the thickness of this layer is a function of the electrolyte concentration and is characterised by the Debye length ($1/\kappa$) as can be seen in figure 1.5. κ is important in that it describes the fall-off of the potential with

distance. At low electrolyte concentrations this double layer is relatively large and at high electrolyte concentrations this double layer is small. These charges provide a long range repulsion and can overcome the attractive Van der Waals interactions.

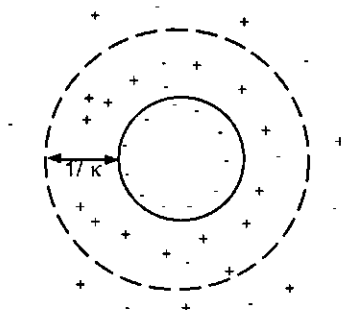


Figure 1.5. Schematic illustration of a negatively charged particle with a double layer.

Another way to introduce repulsion is by attaching to the particle polymers which are sufficiently long and dense to lead to an increase of the minimum distance between the particles⁴²⁻⁴⁸. The Van der Waals force at this distance of smallest approach will be smaller than that for bare particles (figure 1.6). If the increase of the distance is large enough, stabilisation of the particles is achieved. Analytical theories of steric stabilisation have been developed for low grafting densities^{49,50} and for high grafting densities and analysed as function of the solvent quality, stiffness of the chains, grafting density and the temperature⁵¹⁻⁵⁴.

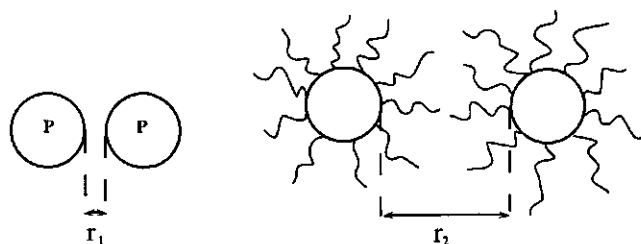


Figure 1.6. The minimum distance between two bare particles P (a) is smaller than steric stabilised particles (b). The Van der Waals forces are therefore smaller for the sterically stabilised particles.

The use of polymers as stabilisers can also improve the wettability of the pigment particles. If the wettability of the pigment is not complete, two things may happen: the particles may migrate to the resin/air surface and be exposed there (fig. 1.7 a,b), or small gass bubbles may stick to the particles (fig. 1.7c).

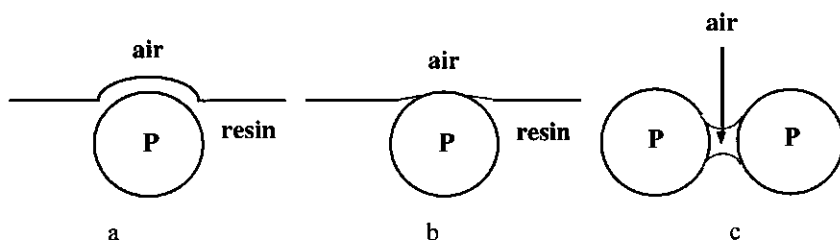


Figure 1.7. Pigment particle which is completely wetted by a liquid (a), a particle which is partially wetted (b), and a gass bubble between two particles (c).

5. Aim of the present investigation

The main issue of this thesis is to get a better understanding of how grafted chains influence the wetting behaviour of a polymer melt. In particular, the role of the length and the density of the grafted chains, as well as that of the length of the chains in the melt will be investigated. Eventually, this should help us to know how we can improve particles in a polymer matrix. A suitable approach is to study wetting and dewetting behaviour of thin films on substrates. As a model, we selected silicon (oxide) wafers modified by tethered polystyrene (PS) with free polystyrene as the liquid homopolymer.

6. Atomic Force Microscopy

Atomic Force Microscopy (AFM) is a versatile method for the characterisation of polymer surfaces and has developed into a technique suitable for scales ranging from microns to nanometers. The surface is scanned with a probe consisting of a sharp tip mounted on a cantilever. The bending of the cantilever is monitored with a laser and a photodetector. The laser beam is focused on the cantilever and the light is reflected into the detector. The sample is moved under the tip by a piezo in a horizontal plane

and the vertical motion is controlled by a feedback mechanism. In the contact mode this feedback mechanism moves the sample in the vertical direction in such a way that the deflection is at a constant value. The tip is in this mode constant in contact with the surface. For soft surfaces this can result in a modification of the surface by the tip. In the tapping mode the cantilever is oscillated. This oscillation changes when there is an interaction between the tip and the sample. The feedback mechanism adjusts the vertical motion the oscillation has against the set point value. In this mode the tip has no contact with the surface and this method is therefore very suitable for soft surfaces^{55,56}.

7. Outline of the thesis

The adsorption of PVP/PS block copolymers consisting of a poly-4-vinylpyridine anchor block and a polystyrene buoy block onto silicon oxide surfaces is discussed in chapter 2. The adsorption kinetics as well as the composition of the block copolymer is discussed and different adsorption methods are discussed and compared to theoretical scaling laws.

In chapter 3 we describe a chemical grafting technique for the preparation of brushes. We have used a polystyrene with a functional end group which can react both with hydrogen-terminated silicon and with silicon oxide.

The wetting behaviour of a PS film onto brushes is discussed in chapter 4. As a function of the grafting density, two wetting transitions were found: non-wetting to wetting at low coverage and wetting to non-wetting at a high brush density. Scaling laws for the two wetting transitions are derived and compared with the experimental results. The experimental data are also compared with numerical self-consistent-field calculations and a good agreement is found.

In chapter 5 we focus on the two special patterns which occur around the wetting transitions. These patterns occur in narrow bands and are present at both transitions.

We have experimentally measured a macroscopic droplet coexisting in equilibrium with *two* film thicknesses. The coexistence of these thicknesses in equilibrium suggest a double minimum in the free energy. Self consistent field calculations applied to this problem shows indeed a double minimum, confirming our experimental results.

The temperature dependence of a droplet on dense brushes is described in chapter 6. Using optical microscopy we investigated the wetting behaviour of a droplet on a brush as a function of the temperature and the grafting density of the brush. We also discuss in this chapter the wetting of PS layer on bimodal brushes, consisting of hairs of two different lengths.

The deformation of the adsorbed PVP/PS polymer surfaces by the low tip-to-sample forces from the AFM is described in chapter 7. The contact mode AFM experiments showed that the AFM tip produces rims oriented perpendicularly to the scanning direction. A wide range of molar masses of both blocks was investigated to check if there is a dependence of the rim distance of the block copolymers on the size of the PVP block copolymer.

In chapter 8 we present some observations using different systems. The first is a polystyrene layer on a brush of a poly-4-vinylpyridine-polystyrene- poly-4-vinylpyridine triblock copolymer. The second is the film formation and the wettability of PS onto a layer of dendrimer functionalised with PS. Finally, the adsorption of poly-2-vinylpyridine-polycaprolactone (PVP/PCL) block-copolymers onto silicon oxide surfaces is described, as well as the wettability of the homopolymer polycaprolactone onto such adsorbed layers.

References

1. G. Reiter, *Langmuir*, 1993, 1344-1351
2. G. Reiter, *Physical Review Letters*, 1992, 75-78
3. S. Walheim, M. Boltau, J. Mlynek, G. Krausch, U. Steiner, *Macromolecules*, 1997, 4995-5003
4. T.G. Stange, D.F. Evans, W.A. Hendrickson, *Langmuir*, 13, 1997, 4459-4465
5. I.W. Hamley, E.L. Hiscutt, Y. W. Yang, C. Booth, *Journal of Colloid and Interfacial Science*, 209, 1999, 255-260
6. T.G. Stange, D.F. Evans, *Langmuir*, 13, 1997, 4459-4465
7. O. Karthaus, L. Gråsjö, N. Maruyama, M. Shimomura, *Thin Solid Films*, 327-329, 1998, 829-832
8. M. Mertig, U. Thiele, J. Bradt, D. Klemm, W. Pompe, *Appl. Phys. A* 66., 1998, S565-S568
9. H.S. Khesghi, L.E. Scriven, *Chemical Engineering Science*, 46, 2, 1991, 519-526
10. P. Müller-Buschbaum, M. Stamm, *Macromolecules*, 31, 1998, 3686-3692
11. P. Müller-Buschbaum, M. Stamm, *Physica B*, 248, 1998, 229-237
12. T.Kerle, R. Yerushalmi-Rozen, J.Klein, L.J.Fetters, *Europhys. Lett.*, 44, 4, 1998, 484-490
13. H. Liu, A. Bhattacharya, A. Chakrabarti, *Journal of Chemical Physics*, 109, 19, 1998, 8607
14. C. Redon, F. Brochard-Wyart, F. Rondelez, *Phys. Rev. Lett.*, 66, 6, 1991, 715
15. F. Brochard-Wyart, G. Debregeas, R. Fondecave, P. Martin, *Macromolecules*, 30, 1997, 1211-1213
16. J.Singh, A. Sharma, *J.Adhesion Sci. Technol*, 14, 2, 2000, 145-166
17. A. Sharma, R. Khanna, *Phys. Rev. Lett.*, 81, 1998, 3463
18. A. Sharma, R. Khanna, *J. Chem. Phys*, 110, 1999, 4929
19. R. Khanna, A. Sharma, *J.Colloid interface Sci.*, 195, 1997, 42
20. H. Liu, A. Bhattacharya, A. Chakrabarti, *J. Chem. Phys.*, 109 (19), 1998, 8607
21. F. Brochard-Wyart, J. Daillant, *Can. J. Phys.*, 68, 1990, 1084

- 22 C. Redon, J.B. Brzoska, F. Brochard-Wyart, *Macromolecules*, 27, 1994, 468
- 23 F. Brochard-Wyart, P.G. de Gennes, H.Hervet, C. Redon, *Langmuir*, 10, 1994, 1566
- 24 K. Jacobs, R. Seemann, G. Schatz, S. Herminghaus, *Langmuir*, 14, 1998, 4961-4963
- 25 Reiter G., Sharma A., Casoli A., David M-O.Khanna R., Auroy P.,*Langmuir*, 1999, 15, 2551-2558
- 26 Y. Liu et al., *Phys. Rev. Let.*, 73, 3, 1994, 440-443
- 27 C. Gay, *Macromolecules*, 30, 19, 1997, 5939
- 28 Watanabe H, Tirrell M., *Macromolecules*, 1993, 26, 6455
- 29 T. Kerle, R. Yerushalmi-Rozen, J. Klein, *Macromolecules*, 1998, 31, 422-429
- 30 R. Yerushalmi-Rozen, J. Klein, *Langmuir*, 1995, 11, 2806-2814
- 31 G. Reiter, P. Auroy, L. Auvray, *Macromolecules*, 1996, 29, 2150-2157
- 32 R. Yerushalmi-Rozen, J. Klein, L.J. Fetters, *Science*, 263, 1994, 793
- 33 D. Long, A. Adjari, L. Leibler, *Langmuir*, 12, 1996, 1675
- 34 K.R. Shull, *Faraday Discuss.*, 1994, 203
- 35 T. Kerle, R. Yerushalmi-Rozen, J. Klein, *J. Europhys. Lett.*, 38, 1997 207
- 36 Tauton H.J., Toprakcioglu C., Fetters L.J., Klein J., *Macromolecules*, 1990, 23, 571
- 37 Prucker O., R  he J. *Macromolecules*, 1998, 31, 3, 592-601
- 38 Prucker O., R  he J. *Macromolecules*, 1998, 31, 3, 602-613
- 39 Prucker O., Naumann C.A., R  he J., Knoll W., Frank C.W., *J. Am. Chem. Soc.*, 1999; 121 (38), 8766-8770
40. J.H. Maas, M.A. Cohen Stuart, A.B. Sieval, H. Zuilhof, E.J.R. Sudh  lter, submitted to Thin Solid Films
- 41 T.A. Misev, Powder Coatings, Chemistry and Technology, John Wiley & Sons, Chichester, 1991
- 42 E.J. Verweij, J.H. de Boer, *Rec. Trav. Chim.*, 57, 1938, 383
- 43 R.H. Ottewill, *Ann. Rep. A*, 66, 1969, 183
- 44 Napper, D.H., Polymeric stabilization of colloidal dispersions, Academic press,

1983

- 45 B. Vincent, *Colloid Science*, Vol. I, The chemical Society London, 1973
- 46 R.H. Ottewill, *Colloid Polymer Sci.*, 67, 1980, 71
- 47 T.F. Tadros, *Adv. Colloid Interface Sci.*, 12, 1980, 141
- 48 T.F. Tadros, *The effects of polymers on dispersion properties*, Academic Press, London, 1980
- 49 P.R. Gerber, M.A. Moor, *Macromolecules*, 10, 1977, 476
- 50 A.K. Dolan, S.F. Edwards, *Proc. R. Soc. London Ser. A*, 377, 509, 1974
- 51 E.B. Zhulina, O. Borisov, V. Priamitsyn, *J. Colloid Interface Science*, 137(2), 1990, 495
- 52 S.T. Milner, T.A. Witten, M.E. Cates, *Europhys Lett.*, 5, 1988, 413
- 53 S.T. Milner, T.A. Witten, M.E. Cates, *Macromolecules*, 21, 1988, 2610
- 54 S.T. Milner, *Europhys Lett.*, 7, 1988, 695
- 55 S.N. Magonov, D.H. Reneker, *Ann. Rev. Mater. Sci.*, 27, 1997, 175-222
- 56 S.S. Sheiko, *Advances in Polymer Science*, 151, Springer-Verlag, Berlin, 2000, 61-190

Chapter 2 Physically adsorbed brushes

Abstract

The adsorption of PVP/PS block copolymers consisting of a poly-4-vinylpyridine anchor block and a polystyrene buoy block onto silicon oxide surfaces is described. We have studied the adsorption kinetics from dilute solutions on substrates as a function of the composition of the block copolymer using ellipsometry. Adsorption from solution is very fast. We have also studied adsorption from the melt. This method generates denser brushes due to the fact that the chains are less swollen in the melt than in a good solvent. Both preparation techniques are compared to theoretical scaling laws. A good agreement for both data sets is found indicating that both preparation methods lead to adsorbed amounts which are not too far from equilibrium.

1. Introduction

Mono- and multilayer systems of polymers have considerable technological potential as a novel class of materials with special properties. A polymer at a surface or an interface often shows a behaviour different from that in the bulk. For example, the adsorption of homopolymers can be used to stabilise colloidal particles¹ and to promote adhesion². One way to improve dispersion stability is to use block copolymers as stabilisers, where one block (the anchor) has a high affinity for the surface and the other block (the buoy) has no affinity to the surface and sticks into the matrix. The total adsorbed amount of block copolymer in a monolayer can be changed by varying the block size ratio and the molar mass of the polymer. When a block copolymer is adsorbed from a good solvent (non-selective solvent) one gets a swollen anchor layer; no micelles are formed. In a selective solvent, one block tends to self-associate so that the polymer forms micelles in the solution. If the solvent is selective for the anchor molecules, the anchor blocks will form a dense layer onto the surface. Scaling models for copolymer adsorption from a selective³ and from a non-selective solvent⁴ have been developed and used to explain experimentally observed results⁵.

2 Scaling theory for polymer adsorption

To express the asymmetry of a block copolymer, we use the characteristic asymmetry ratio β , defined as the ratio of the projected areas of both blocks. The ratio of both monomer sizes is assumed to be equal. For a good solvent for both blocks (i.e., non selective solvent) β may be defined as^{3,4}

$$\beta = \frac{R_{g,b}^2}{R_{g,a}^2} = \left(\frac{N_b}{N_a} \right)^{\frac{6}{5}} \quad (2.1)$$

Where R_g is the radius of gyration and N the number of monomeric units. The subscript a and b is used for respectively anchor and buoy. The block which has no affinity (or a relatively low affinity for the surface compared to the other block of the

block copolymer), is called the buoy block of the polymer. The block which has a relatively high affinity for the surface is called the anchor block and will preferentially adsorb to the surface. The cross-over regime between the anchor and buoy dominated regimes in the adsorbed layer occurs at $\beta \approx N_a$. Nearly all the polymers used in this chapter form layers in the anchor-dominated regime and therefore we will mainly focus on the scaling laws for this regime as formulated by Marques and Joanny (MJ)^{3,4}. For the adsorption from a non-selective solvent these authors derived expressions for the surface density σ in terms of the polymerization index of the anchor and buoy blocks. For the anchor regime ($\beta < N_a$) the surface density scales as

$$\sigma \sim N_a^{-1} \quad (2.2)$$

The thickness of the film is related to the surface density and the degree of polymerization of the adsorbed block. The non adsorbed blocks can have a stretched conformation in the direction normal to the surface forming a brush. For a layer of end-grafted chains with length N_b , the layer thickness d scales as^{6,7}

$$d \sim N_b \sigma^{1/3} \quad (2.3)$$

where N_b is the degree of polymerization of the buoy block. Combination of (2.2) and (2.3) gives the adsorbed layer thickness for a block copolymer in the anchor regime.

$$d \sim N_b N_a^{-1/3} \quad (2.4)$$

3. Experimental

Polystyrene-poly(4-vinylpyridine) (PS/PVP) polymers with different block lengths and a overall polydispersity index < 1.2 were purchased from Polymer Source Inc. and used without further purification. The characteristics of the samples used in this study are listed in table 2.1. The numbers in column 1 represent the molar mass of the blocks (in kg/mole) and will be used to refer to the various samples. The total number of

monomer units is denoted with N ($= N_S + N_{VP}$) and the given polydispersity is the overall polydispersity.

table 2.1. Characteristics of the PS/PVP block copolymers

polymer PS/PVP	N_S	N_{VP}	N	fraction VP	M_w/M_n
20/20	206	197	403	0.49	1.13
32/13	306	126	432	0.29	1.08
33/8	316	77	393	0.20	1.06
34/3	326	28	354	0.08	1.07
48/21	458	199	657	0.30	1.14
194/21	1865	204	2069	0.10	1.13
1.4/22	13	208	221	0.94	1.13

Silicon wafers with an oxide layer of approximately 80 nm, prepared by thermal oxidation, were used as substrate. Two different procedures for preparing thin PS/PVP layers were investigated: (i) adsorption from a polymer melt and (ii) adsorption from dilute solution (dip coating). Spin coating from solutions is widely used to prepare polymer monolayers onto different substrates⁸⁻¹⁰. We applied spin coating from concentrated solutions (10g/l) of PS/PVP into a thick film, followed by annealing at a temperature above the T_g of both blocks to adsorb the polymer onto the substrate. The adsorption takes place in the melt at elevated temperatures and spin coating a solution is only to form a thin polymeric layer. The concentration of the polymer and the spinning speed is therefore not important as long as the surface is fully covered with the polymer after spin coating. In order to obtain a single adsorbed layer, excess material was removed by washing with fresh solvent. For the second method (adsorption from dilute solution by dip coating) a piece of silica was dipped into a solution (100ppm). The substrate was kept in the solution for 30 min. Excess material was removed by washing with solvent. Finally, the samples were dried with nitrogen.

Three different solvents were tested: chloroform, tetrahydrofuran (THF) and toluene. The best results, in terms of homogeneity and the roughness of the polymer film, were obtained with the non-selective solvent chloroform. Dynamic light scattering experiments showed that no micelles are formed, as expected. THF and toluene are selective for one of the blocks (good solvents for PS). Hence, micelles are formed in solution. The thickness of the dry polymer layer was determined by computer-controlled null ellipsometry (Sentech SE-400). The refractive index for $\lambda = 632.8$ nm was taken as 1.58¹¹

Adsorption kinetics experiments were performed using a ellipsometer (Multiskop) and a home built liquid cell. The arms of the ellipsometer were fixed at 70° with respect to the normal. The solvent used in kinetic experiments is methylethylketon (MEK) and is a good solvent for both blocks of PS/PVP polymers. Concentrated solution of the polymer were added to the liquid cell so that the concentration of the polymer in the cell was approximately 100ppm.

The AFM measurements were performed with a Digital Instruments Nanoscope III AFM equipped with a scanner capable of scanning an area of $12\mu\text{m}^2$. All measurements were performed in air at room temperature and a relative humidity level of 50-60%. Commercially available Si_3N_4 tips were used on cantilevers with a spring constant of approximately 0.58 N/m.

4. Results and discussion

The results obtained from the kinetic experiments are plotted in figure 2.1. In this figure the thickness of the solvated brush is plotted as function of the adsorption time. The polymer was added in a very concentrated solution to the liquid cell at 60 sec. The concentration after injection of the concentrated solution was approximately 100ppm. As can be seen from the figure, an increase of the solvated brush with decreasing the PVP content in the PS/PVP block copolymer is observed at a constant total number of monomers. The adsorption of the polymer onto the surface is very fast and the surface is fully covered within one minute.

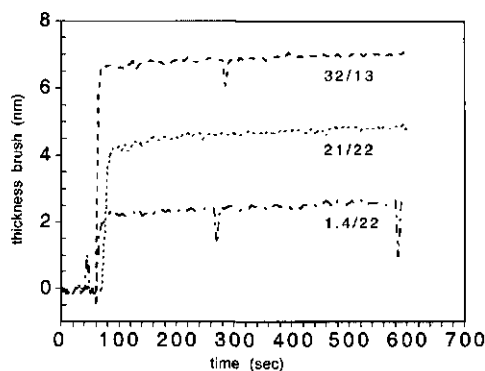


Figure 2.1. Adsorption kinetics of PS/PVP from a good solvent (methylethyl keton) onto a silicon oxide surface for three polymers. The numbers represent the molar mass of the blocks in kg/mole. The thickness of the brush is the solvated thickness as measured in the liquid cell of the ellipsometer.

Drying the adsorbed layers and measuring the thickness of the collapsed layer showed the same trend as can be seen in table 2.2.

Table 2.2. Thickness of three PS/PVP polymers in solution (MEK) and dried.

PS/PVP	thickness brush (solvated) nm	thickness brush (collapsed) nm
1.4/22	2.64	0.83
21/22	4.73	1.22
32/13	7.11	1.58

The kinetic experiments were performed in MEK due to the higher contrast between the different refractive indices of the solvated brush, the solution and the silicon oxide. When using chloroform the refractive indices of the solvated brush, the solution and the silicon oxide are respectively 1.47, 1.45 and 1.46. These values are so close that it is practically very difficult to obtain reliable data from the experiments.

The adsorption kinetics from chloroform and the layer thickness of the brushes in the dry state are comparable with the results obtained from the MEK experiments. This indicates that the kinetics in chloroform is also very fast.

The surface layer topography as captured by the first scan immediately after dip coating and solvent evaporation is shown in figure 2.2. These typical images show that the surface coverage is homogeneous and smooth for films prepared with chloroform (fig.2.2a). The (RMS) roughness of the polymer surface is $<0.5\text{nm}$. The surface roughness of films prepared by THF is higher, probably due to micelles adhering to the surface so that a less homogeneous film is obtained (fig. 2.2b). Films prepared from toluene show large patches where there is no polymer (fig. 2.2c). This may be due to traces of water in the solvent. The surface image of the polymer deposited by adsorption from a melt resulted in a homogeneous, smooth film with a surface roughness comparable to that of the chloroform dip-coating method.

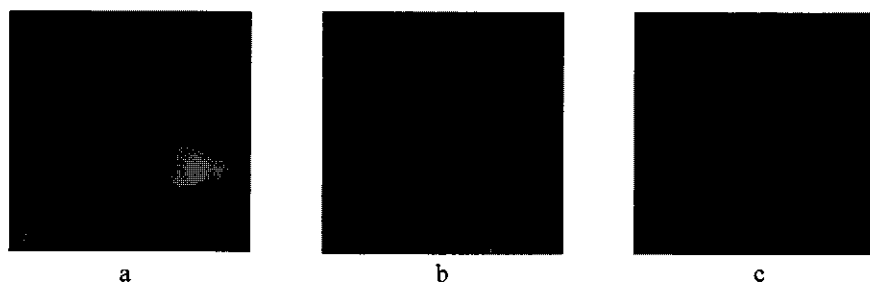


Figure 2.2. Surface image of dip-coated PS/PVP (20/20) using different solvents, as captured by the first scan. Image $10 \times 10 \mu\text{m}^2$. The height difference is the difference between the depressed dark regions and the bright elevated regions. (a) Chloroform, height 5 nm (b) THF, height 20 nm (c) Toluene, height 50 nm.

The coverages Γ (mg/m^2), determined by means of ellipsometry, are presented in figure 2.3. As can be seen from the figure, Γ has a maximum around 10% PVP. This behaviour is characteristic for selective adsorption of diblock copolymers^{5,12,13} and

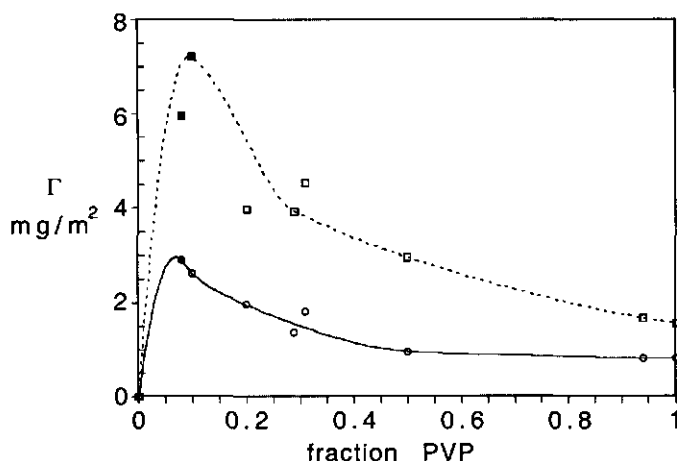


Figure 2.3. Surface coverage (Γ) as function of the fraction PVP. Squares refer to spin coating (10000 ppm, CHCl_3 , 3000 RPM, annealed for 24 hr. at 145 °C, circles to dip coating (100 ppm, CHCl_3 , 30 min.). Open symbols are for polymers in the anchor-dominated regime and filled symbols for polymers which are in the cross-over towards or in the buoy-dominated regime.

can be qualitatively understood as follows. If $N_{VP} \gg N_S$ the area covered by the PVP onto the surface is so large that it is not necessary for the polystyrene buoy blocks to stretch. The PS coils do not overlap and form a swollen chain with a thickness of the order of the radius of gyration. The adsorbed amount of the anchor blocks remains almost constant as long as the buoy blocks do not overlap. The opposite case, $N_{VP} \ll N_S$, results in a large overlap between the PS buoys forming highly stretched PS brushes and a surface that is not fully covered by the anchor blocks. The amount of adsorbed PVP is dictated by the stretched buoy blocks and increasing the size of the buoy block at constant N_{VP} will result in a decrease of the number of attached chains per unit area and an increase of the layer thickness. In between these two situations, the surface coverage is the result of a balance between the adsorption energy of the

PVP blocks and the loss of entropy of the PS when forced to stretch, as illustrated in figure 2.4.

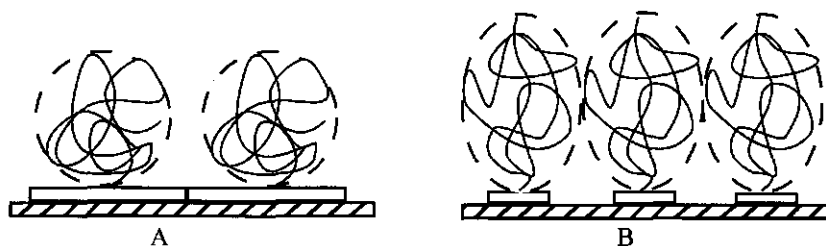


Figure 2.4. Illustration of the anchor (A)- and buoy dominated regime (B) for adsorbed PVP/PS in a non-selective solvent.

Comparison of our experimental results obtained from dip-coating and adsorption from a melt with self-consistent-field predictions¹³ for the adsorbed amount for diblock polymers shows that the qualitative agreement between theory and experiment is quite good.

The measured layer thickness of the adsorbed films is compared to the MJ scaling predictions for the anchor regime (eq. 2.4). These predictions for the adsorbed amounts are derived for adsorption from solution. The question must be asked whether it is justified to apply these laws for polymers in the dry state. The polymers are adsorbed onto the surface from solution or from a polymer melt (θ -solvent). The total amount of polymer adsorbed onto the surface will not change upon drying the samples. The difference between the thickness of adsorbed block copolymers in solution and in the dry state will then only vary in the pre factor. Hence, we try to check our experimental results with the MJ scaling law for adsorbed block copolymers by plotting d against $N_b N_a^{-1/3}$ according to equation 2.4. It can be seen from figure 2.5 that for both methods of preparation the thickness follows the MJ scaling model quite well; the points in the anchor regime lie on a straight line. Spin coating results in films which are thicker by a factor of two as compared to dip coating, about the same factor as for the adsorbed amount (fig. 2.3).

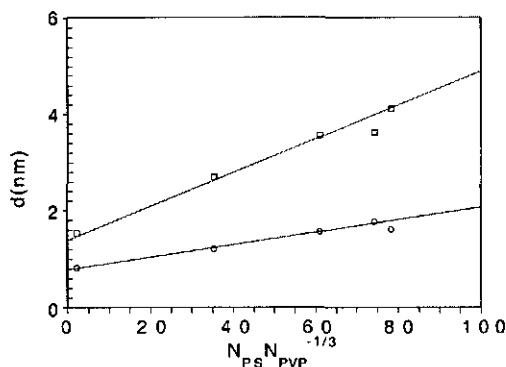


Figure 2.5. Layer thickness of dry films obtained after adsorption from chloroform or spincoating as a function of $N_b N_a^{-1/3}$, according to the MJ scaling predictions for the anchor regime. Squares refer to adsorption from a melt (annealing for 24 hr. at 145 °C, circles to dip coating (100 ppm, CHCl_3 , 30 min.).

The excellent agreement between experimental results and scaling predictions for both data sets is surprising, as the scaling prediction is based on thermodynamical equilibrium, where at fixed chain structure there can only be one Γ value. Since we find two different Γ values for the two preparation methods, at least one of those must correspond to non-equilibrium. We suggest that adsorption from dilute solutions is undersaturated and, hence, not in equilibrium because of the following reasons. The polymers following the MJ scaling predictions are all in the anchor-dominated regime, which means that the surface is almost fully covered by the anchor blocks. When the adsorption from solution has reached a steady state (i.e., when the adsorbed amounts no longer change in time) a PS/PVP chain cannot adsorb onto the surface unless another polymer chain leaves. Hence, a newly incoming polymer chain cannot adsorb because there is no available area on the surface. In addition, the adsorbed buoy blocks exert a steric repulsion on incoming chains. Hence, in this method Γ is kinetically trapped in a low value.

For the adsorption from a melt case the layer structure is different, with probably an excess of material which has not been fully removed in the rinsing step. After annealing above the T_g of both blocks the system acquire a domain structure dictated by the relative block lengths, it is likely that only parts of the anchor blocks are in contact with the surface.

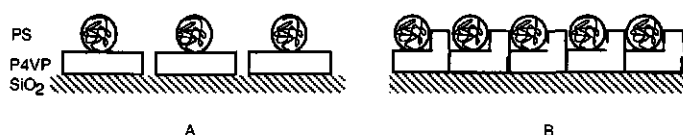


Figure 2.6. Schematic representation of adsorbed PS/PVP after washing with fresh solvent onto silica by (A) dip coating and (B) adsorption from a melt.

Washing with solvent will remove non-adsorbed and loosely attached material, but the high coverage of the anchors blocks is apparently preserved. Washing with solvent would give the possibility for stretched buoy blocks, if any, to decrease unfavourable overlap interactions. However, the polymers we have used are almost all in the anchor dominated regime and therefore the overlap between the buoy blocks will be negligible. We tentatively conclude that in the case of dip coating the adsorbed amount is probably below the equilibrium amount, whereas for the films prepared by spin coating it is above. A speculative and highly schematic representation of both preparation techniques after washing is shown in fig 2.6.

5. Conclusions

We have studied the adsorption of PS/PVP block copolymers from a non-selective solvent and from a polymer melt on a flat silica surface and examined the films with AFM. The adsorbed amounts in both preparation techniques (dip-coating and adsorption from a melt) were compared with scaling predictions. Qualitatively, there is good agreement for both data sets. However, the adsorbed amounts and the thicknesses obtained after adsorption from a melt is higher than after dip-coating by a factor of about two. Hence, at least one (and probably both) preparations techniques

produces non- equilibrium films. The fact that nevertheless the scaling laws apply is an indication that both data sets are not too far from equilibrium. The equilibrium adsorption is probably in between the situation obtained after dip-coating and adsorption from a polymer melt.

References

- 1 Napper, D.H., Polymeric stabilization of colloidal dispersions, Academic press, 1983
- 2 Lee, L.H., Adhesion and adsorption of polymers, plenum press, New York, 1980
- 3 Marques, C.M., Joanny, J.F., Leibler, L., Macromolecules, 1988, 21, 1051
- 4 Marques, C.M., Joanny, J.F., Macromolecules, 1989, 22, 1451
- 5 Guzonas, D., Hair, M.L., Cosgrove, T., Macromolecules, 1992, 25, 2777
- 6 Alexander, S., J. Phys (Paris), 1977, 38, 983
- 7 De Gennes, P.G., Macromolecules, 1980, 13, 1069
- 8 Reiter, G.; Langmuir, 1993, 1344-1351
- 9 Reiter, G.; Physical Review Letters, 1991, 75-78
- 10 Walheim, S; Boltau, M; Mlynek, J; Krausch, G; Steiner, U; Macromolecules, 1997, 4995-5003
- 11 Koneripalli, N.; Levicky, R.; Bates, F.; Matsen, M.W.; Satija, S.K.; Ankner, J.; Kaiser, H., Macromolecules, 1998, 31, 3498-3508
- 12 Evers, O.A., Scheutjens J.M.H.M., Fleer G.J., J. Chem. Soc. Faraday Trans., 86, 1990, 1333
- 13 Fleer, G.J.; Cohen Stuart, M.A.; Scheutjens, J.M.H.M.; Cosgrove, T.; Vincent, B.; Polymers at interfaces, Chapman & Hall, 1993

Chapter 3 Chemically grafted brushes

Abstract

We have grafted end-functionalised polystyrene through a covalent bond on hydrogen-terminated silicon and on silica surfaces. The reaction is carried out from a polymer melt. The grafting density of the brushes prepared from the melt is much higher than that obtained by reaction in solution. The reaction of the vinyl-terminated polystyrene takes place at the surface under very mild conditions. The preparation of brushes is a versatile 'one pot'-synthesis involving only the substrate and the vinyl-terminated polystyrene. The method also allows to prepare bimodal (mixed) brushes from a suitable mixture of precursors. A combined reaction of the polymers on a silica substrate which is partially hydrogen-terminated shows that patterns can be prepared in a polymer brush

1 Introduction

Modification of surfaces has strong academic and industrial interest because of its important role in modern technology. Many natural and technological materials such as milk and paint are stabilised by special molecules to prevent aggregation. Aggregation occurs due to the attractive forces that act between the particles in the absence of a stabilising mechanism. Stabilisation can be obtained by electrostatic means and by steric interactions or a combination of these effects. Modifying a surface by covering it with a polymer brush is often very effective to stabilise the surface in a matrix. These polymer brushes are interesting due to their effect on wetting and related phenomena¹⁻³. Highly functionalised materials can be prepared in this way, and the properties of the surface can be tuned to obtain the desired functionalities.

One method that is often used for the preparation of brushes is the adsorption of block copolymers onto surfaces from solution or polymer melts. If one block has a high affinity for the surface and the other block has no affinity for the surface, a brush may be formed both in solution and in a melt^{1,4-5}. Brushes prepared in this way using monodisperse block copolymers are monodisperse, and the adsorbed amount depends on the composition of the block copolymer⁶⁻⁷.

Chemical grafting is another way to prepare brushes. Two different grafting techniques are often used. The first is grafting from a surface with reaction initiators present on the surface and monomers present in solution. The brushes prepared in this way are polydisperse, and the chain length (distribution) and grafting density must be determined indirectly afterwards, e.g., by detaching the chains and determining the total brush mass. The thickness of the brushes obtained by this method may be very large (microns)⁸⁻¹⁰.

The other chemical grafting technique is grafting to the surface. The polymers used in this method have a reactive (end) group, which will react with surface groups. Since the chain length of the polymers can be well controlled, this provides a way to prepare uniform and monodisperse brushes¹. The purpose of this chapter is to present two new ways of brush preparation via the grafting to technique, namely one on oxide free,

hydrogen-terminated silicon and one on silica surfaces, using a vinyl group as the reactive end group in both cases. Grafting of 1-alkenes on hydrogen-terminated crystalline silicon surfaces results in the formation of densely packed monolayers that are covalently bound to the Si surface^{11,13-17}. We have investigated whether this reaction can also be used to prepare dense layers of end-attached polymers.

In this chapter we report the preparation of brushes by two different reactions: (1) between vinyl-terminated polymers (figure 3.1) and hydrogen-terminated silicon to form an alkyl (Si-CH₂) bond, and (2) vinyl-terminated polymers and silicon oxide to form an ether (Si-O-C) linkage. When low molecular weight alkenes are grafted, the reaction requires high reaction temperature (150-200 °C) and preferably a high concentration of the 1-alkene^{1,13-17}. Therefore the reaction is usually carried out in pure alkene or in very concentrated solutions, employing solvents with a high boiling point. Often this requires refluxing conditions. With polymers, the use of solutions is impractical because of the relatively large quantities of precious polymer needed. However, volatility is negligible, so that the reaction can be done directly in the melt. An important advantage of using polymer melts is also that one can get much denser brushes than when polymer brushes are prepared in solution.

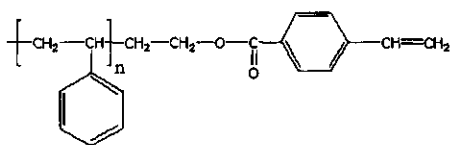


Figure 3.1. Vinyl-terminated polystyrene

2 Experimental method section

2.1 Materials

Vinyl-terminated polystyrene (PS) of two different molar masses and a polydispersity index <1.2 were purchased from Polymer Source Inc. and used without further purification. These polymers will be denoted as PS₂₀ and PS₂₀₀ (2 and 20 kg/mole, respectively). All solvents were degassed and free of water. The synthesis of the brushes was performed in an oxygen- and water-free atmosphere unless otherwise

stated. Solvent evaporation was performed under reduced pressure in a nitrogen atmosphere.

2.2 Grafting on hydrogen-terminated silicon

A piece of silicon was etched for 2 min in HF (2.5%) to remove the native oxide layer, blown dry with nitrogen and immediately covered with a solution of the vinyl-terminated PS in CHCl_3 (14 g/l). After evaporation of the solvent a film of the polymer remained on the surface. We perform the reaction in the melt at elevated temperatures and spin coating the chloroform solution is only to form a thin polymeric layer on the surface. The system was heated for 24 h at 145 °C in vacuo in order for the grafting reaction to occur. Non-grafted excess material was, subsequently removed thoroughly by washing three times with fresh solvent. Some samples were also prepared by immersing the silicon samples in a mesitylene solution of the reactive polymer under refluxing conditions, as described by Sieval et al.^{11,14}. A polymer concentration of 0.5 g/ml was used in these experiments.

2.3 Grafting on silicon oxide surfaces

Silicon wafers with an oxide layer of approximately 80 nm were used as substrate and covered, in an inert atmosphere, with a solution of the vinyl-terminated PS in CHCl_3 (14g/l). Again, the solution is only to handle the polymer more easily when covering the surface with polymeric material. After evaporation of the solvent, the system was annealed in vacuo for 24 h at 145 °C. Excess material was removed by washing with fresh solvent and the substrate was subsequently dried in a stream of nitrogen.

2.4 Bimodal brushes

A piece of silicon was etched for 2 min in HF (2.5%), blown dry with nitrogen and immediately covered with a solution containing a mixture of the two vinyl-terminated polystyrenes PS₂₀ and PS₂₀₀ in a specific ratio varying from 0 upto 100% PS₂₀₀ (w/w) in CHCl_3 . The total concentration of the mixture of polymers was 1mg/ml. After evaporation of the solvent a film of the polymer remained on the surface. The system

was annealed for 24 h at 145 °C in vacuo. After annealing, excess material was removed thoroughly by washing three times with fresh solvent.

2.5 Patterns in polymer brushes

A piece of silicon was etched for 2 min in HF (2.5%) and blown dry with nitrogen. A mask was placed on the hydrogen-terminated silicon and the system was exposed to UV-light for 5 sec in air. The blocked (non-exposed) areas are still hydrogen terminated but the exposed areas are oxidised to silica as shown in the upper part of figure 3.2. The substrate is then covered, in an inert atmosphere, with a solution of the vinyl-terminated PS in CHCl_3 (14g/l). After evaporation of the solvent, the system was annealed in vacuo for 24 h at 145 °C. Excess material was removed by washing with fresh solvent and subsequently the substrate was dried in a stream of nitrogen. The exposed areas were hydrolysed by placing the sample in boiling water for 30 min. After drying the sample can be covered again with a vinyl terminated polystyrene of different chain length. After annealing in vacuo for 24 h at 145 °C a brush was formed with the polymer and the hydroxyl groups of the silica. In this way patterns can be made in a polymer brush. Schematically this is shown in figure 3.2.

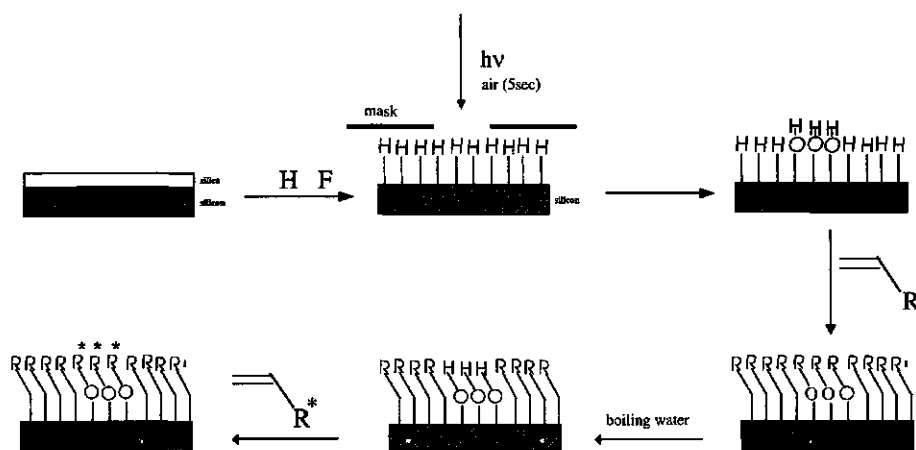


figure 3.2. Reaction schema of vinyl terminated polystyrene with the substrate

2.6 Ellipsometry

The thickness of the brush after washing was determined by computer-controlled null ellipsometry (Sentech SE-400) using a laser ($\lambda = 632.8$ nm) and an incident angle of 70° . The ellipsometry software from Sentech was used to calculate the film thicknesses. The refractive index for the polymer layer was taken as 1.58^{12} .

2.7 Atomic Force Microscopy

The AFM measurements were performed with a Digital Instruments Nanoscope III AFM equipped with a scanner capable of scanning an area of $100\ \mu\text{m}^2$. All AFM measurements were performed in air at room temperature and a relative humidity level of 50-60%. Commercially available tapping mode tips were used on cantilevers with a resonance frequency in the range of 350-400 kHz.

3 Results and discussion

By spin coating a highly concentrated solution of functionalised PS in chloroform we obtain a relatively thick layer (~ 70 nm) of end-functionalized PS onto the surface. This layer consist of non-reacted end-functionalized PS. It is important that the reaction takes place in an oxygen free atmosphere (because oxygen will lead to a variety of undesired reactions) and above the glass transition temperature of the polymer (in order to have sufficient mobility of the reactant). After annealing, the resulting layer consists of both covalently attached polymer directly bound to the surface, and physically adsorbed polymer on top of this.

The characteristics of the polymers used for the chemical grafting and the properties of the resulting grafted layers after removal of the physically adsorbed polymer are listed in table 3.1. The numbers (20 and 200) in column 1 represent the number of monomeric units in the polymer and will be used to refer to the various samples. Two surfaces were prepared in the melt ($145\ ^\circ\text{C}$), and two samples were prepared in solution (mesitylene, $0.5\ \text{g/ml}$, $165\ ^\circ\text{C}$)¹⁴.

table 3.1 characteristics of the vinyl-terminated PS layers on Si-H.

polymer	thickness brush (nm)	Γ mg/m ²	σ nm ⁻²
melt			
PS ₂₀ -vinyl	2.7	3.0	0.95
PS ₂₀₀ -vinyl	19.2	21.1	0.55
solution			
PS ₂₀ -vinyl	2.4	2.6	0.81
PS ₂₀₀ -vinyl	3.7	4.1	0.13

The grafting density (σ) of the PS₂₀ layer prepared in the melt is 0.95 nm⁻², which means that every chain has almost 1 nm² available on the surface. At this grafting density, the layer thickness equals 2.7 nm, which implies that every chain has on average an extension that is about 63 % of the extended all-trans conformation (assuming a tetrahedral angle of 109° and a bond length of 0.154 nm, PS₂₀ is 4.3 nm long.) For the PS₂₀₀ polymer the grafting density is 0.55 nm⁻², and the layer thickness equals 19.2 nm. These chains are stretched normal to the surface to about 42 % of the all-trans conformation, which is more than 2000 times the end-to-end distance in the random coil state.

3.1 Polystyrene brushes on silica

In the course of this study we found that vinyl-terminated PS also reacts with silica. The latter reaction is reversible, so the brushes can be removed by exposing them to boiling water or water of high pH. When exposed to boiling water or basic solutions the (mono)layer was indeed removed, which indicates that the ether linkage was hydrolysed to the alcohol and Si-OH groups. The fact that hydroxyl groups are involved in the reaction is supported by the following observation. When a Si-wafer was completely dehydroxylated by heating at 500 °C for 4 h, and then covered with the vinyl-terminated polystyrene, no reaction took place. After washing with fresh solvent no polymer film was present on the surface indicating that hydroxyl groups are needed for the reaction.

table 3.2 characteristics of the vinyl-terminated PS layers adsorbed from a polymer melt on silica

polymer	thickness brush (nm)	Γ mg/m ²	σ nm ⁻²
PS ₂₀ -vinyl	1.3	1.5	0.47
PS ₂₀₀ -vinyl	9.8	10.9	0.33

The characteristics of the grafted layers on silica are listed in table 3.2. The grafting density for the reaction of PS₂₀-vinyl and PS₂₀₀-vinyl on silica surfaces is 0.47 and 0.33 nm⁻², respectively, which is lower than that obtained in the case of hydrogen-terminated silicon.

The difference in grafting densities for the hydrogen-terminated substrate and the silica substrate is probably due to the difference in the number of reactive groups on the surface. The number of Si-H groups on Si-H (100) is larger than the number of Si-OH groups per unit area on silica¹⁸. The surface topography as measured by AFM shows that a PS₂₀ brush prepared by adsorption from a polymer melt is homogeneous and smooth (figure 3.3).

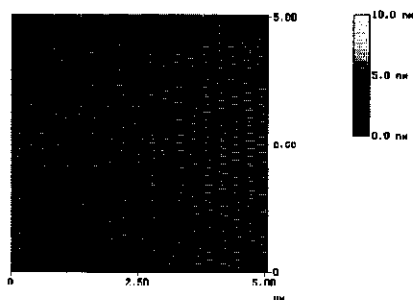


Figure 3.3. AFM image of a PS₂₀ brush prepared by adsorption from a polymer melt.

table 3.3. Bimodal Brushes.

PS ₂₀ (%)	PS ₂₀₀ (%)	Thickness (nm)
0	100	19.2
20	80	12.1
50	50	7.9
80	20	3.4
100	0	2.7

The characteristics of the bimodal grafted layers on hydrogen-terminated silicon are listed in table 3.3. The numbers in the first 2 columns represent the mol fraction (*100%) of the polymer. When a mixture of PS₂₀₀ and PS₂₀ in chloroform is used to cover the surface a bimodal brush can be made. After evaporation of the chloroform in an inert atmosphere the surface is fully covered with a polymeric layer in the glassy state. After annealing above the glass transition temperature it is likely to assume that the brush is formed with a ratio of the two polymers that is approximately equal to the ratio of the polymers in the initial chloroform solution. The ratio of the polymers near the surface will not change very much compared to the bulk concentration of the reactive end groups of both polymers. Increasing the number of grafted PS₂₀ chains gives a decrease of the layer thickness, as expected. As can be seen from the data, the thickness of the polymer film as function of the fraction PS₂₀₀ is not linear. This is largely due to two effects. First, stretching occurs mainly at high grafting densities, resulting in the observation that only 100% PS₂₀₀ the large thickness (19.2 nm) starts to approach the length of an all-trans polymer chain (42 nm). At lower percentages PS₂₀₀ there is relatively more free space available in the top of the layers which will yield more extensive disorder and tilting with larger percentages of the smaller PS₂₀. Second, the grafting densities decrease when the fraction of PS₂₀₀ increases. This suggests that at lower mole fractions of PS₂₀₀ relatively more PS₂₀ will be bound at the surface. When the reaction with the two different polymers is performed in solution the situation becomes even more pronounced. Small molecules can move much faster in a liquid, so if these react instantaneously there will be relatively more small

molecules on the surface. The layer thickness of a mixture (1:1) of both polymers performed in solution resulted in a film of 2.9 nm.

4 Patterns in polymer brushes

The reaction of vinyl-terminated PS with silica forms a chemical bond which can be removed by exposing the brush to boiling water or water of high pH. The reaction is reversible, so the brushes formed at the exposed areas can be removed and replaced by an other polymer by exposing them to boiling water or water of high pH followed by the reaction of the vinyl terminated polystyrene. Figure 3.4a is an AFM image of a depressed region in a PS₂₀ brush after placing a sample in boiling water. After the treatment with HF the sample was partially exposed to UV-light in air for 5 sec. The elevated (light) region is the polymeric brush with a thickness of 2.5 nm. The depressed (dark) region is silica and is the area which has been exposed to the UV-light. After covering the sample with a vinyl terminated polystyrene with a different molecular weight, the system was annealed in vacuo. After washing and drying the sample was examined with AFM. Figure 3.4b shows a elevated (light) region in a PS₂₀₀ brush consisting of PS₂₀₀ and is the area which has been exposed to the UV-light. The PS₂₀₀ is bound to the surface via an ether linkage whereas the PS₂₀ is bound to the surface via an Si-C bond. In this way patterns can be made in a polymer brush.

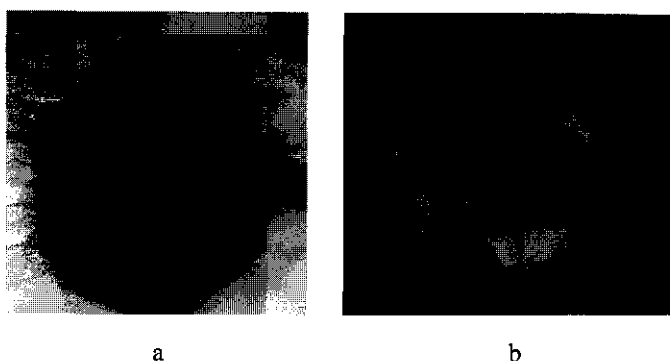


Figure 3.4. Pattern of silicon oxide in a PS₂₀ brush (a) and a PS₂₀₀ pattern in a PS₂₀ brush. Maximum height difference in figure 3.4a 10 nm and in figure 3.4b 30 nm. Dark regions are depressed and light areas are elevated.

5 Conclusions

We have grafted end-group functionalised polystyrene on hydrogen-terminated silicon and silica surfaces. Brushes prepared on hydrogen-terminated silicon and silica are attached via a Si-C bond, and brushes prepared on a silicon oxide surface are bound via an ether linkage. The grafting density of the brushes prepared in a polymer melt is much higher compared to those obtained by reaction in solution. The method also allows to prepare bimodal brushes from a suitable mixture of precursors. By exposing parts of the hydrogen terminated silicon to UV-light patterns of silica or other brushes can be made in a polymeric brush.

References

- 1 Reiter G., Sharma A., Casoli A., David M-O.Khanna R., Auroy P., *Langmuir*, **1999**, 15, 2551-2558
- 2 Y. Liu et al., *Phys. Rev. Let.*, 73, 3, **1994**, 440-443
- 3 C. Gay, *Macromolecules*, **30**, 19, **1997**, 5939
- 4 Watanabe H, Tirrell M., *Macromolecules*, **1993**, 26, 6455
- 5 Tauton H.J., Toprakcioglu C., Fetters L.J., Klein J., *Macromolecules*, **1990**, 23, 571
- 6 G.J. Fleer, M.A. Cohen Stuart, J.M.H.M. Scheutjens, T. Cosgrove, B. Vincent, *Polymers at interfaces* (Chapman & Hall, London, 1993)
- 7 J.H. Maas, M.A. Cohen Stuart, G.J. Fleer, *Thin Solid Films*, 358, **2000**, 234-240
- 8 Prucker O., Ruhe J. *Macromolecules*, 1998, 31, 3, 592-601
- 9 Prucker O., Ruhe J. *Macromolecules*, 1998, 31, 3, 602-613
- 10 Prucker O., Naumann C.A., Ruhe J., Knoll W., Frank C.W., *J. Am. Chem. Soc.*, **1999**; 121 (38), 8766-8770
- 11 Sieval A.B., Demirel A.L., Nissink J.W.M., Linford M.R., van der Maas J.H., de Jeu W.H., Zuilhof H., Sudhölter E.J.R. *Langmuir*, **1998**, 14 (7), 1759-1768
- 12 N. Koneripalli, R. Levicky, F. Bates, M.W. Matsen, S.K. Satija, J. Ankner, H. Kaiser, *Macromolecules*, 31 (1998), pp. 3498
- 13 Linford M.R., Fenter P., Eisenberger P.M., Chidsey C.E.D., *J. Am. Chem. Soc.*, **1995**; 117, 3145-3155
- 14 Sieval A.B., Vleeming V., Zuilhof H., Sudhölter E.J.R. *Langmuir*, **1999**, 15 (23), 8288-8291
- 15 Terry J., Linford M.R., Wigren C., Cao R.Y., Pianetta P., Chidsey C.E.D., *J. Appl. Phys.*, **1999**, 85 (1), 213-221
- 16 Buriak J.M., *Chem. Commun.*, **1999**, 1051-1060
- 17 Sieval A.B., Linke R., Zuilhof H., Sudhölter E.J.R., *Adv. Materials*, **2000**, 12,

1457-1460

18 see A.P. Legrand, *The surface properties of silicas* (John Wiley & Sons, Chichester, 1998) and references therein

19 R.K. Iler, *The colloid chemistry of silica and silicates* (Cornell University Press, Ithaca, New York, 1955)

Chapter 4 Wetting of brushes by polymer melts

Abstract

In this chapter the wetting behaviour of a PS melt on top of a chemically identical homodisperse brush is discussed. We report experimental results confirming the theoretically predicted surface patterns for thin films on a flat surface. Using a non-wettable bare surface modified by a polymer brush of varying grafting densities, two wetting/dewetting transitions can be found. At low grafting densities of the brush the non wettable surface is screened by the brush and the modified surface can be made wettable. The second wetting transition occurs at high grafting densities and is a result of the incompatibility of the grafted chains or adsorbed and the free chains. Scaling laws for both transitions are compared with the experimental results. Self-consistent-field calculations are carried out to calculate the contact angle of a polymer droplet on a chemically identical brush.

1 Introduction

Wetting phenomena control many processes, not only in technological applications such as painting, lubrication, flotation, but also in agricultural and biology (insecticide sprays, breathing.) In many of the technological applications the successful design of materials requires the modification of thermodynamic properties, such as the interfacial tension. A fundamental understanding of these thermodynamic properties is therefore required.

When a liquid is placed on a flat solid surface, it may show two types of equilibrium situations: partial wetting or complete wetting. In the case of complete wetting, the situation of lowest free energy is a continuous liquid film on the substrate, whereas partial wetting implies coexistence between droplets and an (almost) dry state. In the latter case, a continuous liquid film is unstable or metastable and will dewet when allowed to relax towards its thermodynamic equilibrium. The initially flat film will eventually break up into droplets with a specific contact angle. The break-up process of metastable films has been studied extensively and is now reasonably well understood¹⁻³. Experiments with polymeric liquids have shown that not only droplets can be formed but that a variety of surface patterns can appear, ranging from macroscopic droplets to holes in equilibrium with droplets⁴⁻⁹. Theoretical models describing how these morphologies and patterns develop during dewetting have recently become available¹⁰⁻¹³. These models, and the calculations based on them, provide a correlation between the interfacial interactions and the time evolution of local film thicknesses.

The wetting behaviour of a polymer melt onto a surface can be modified by a brush attached to the substrate^{5,14-15}. For example, a partially wet surface can be made completely wetting by means of a polymer brush that is compatible with the melt⁵. It is also possible, by an appropriate choice of the brush, to obtain the opposite effect, i.e., a transition from complete to partial wetting. In this chapter we discuss the special case where the brush and the melt are chemically identical, so that the relevant variables are the length of the chains and the number of attached chains per unit area, referred to as the grafting density.

The consequences of grafting chains on a solid surface were first discussed by Alexander and de Gennes^{16,17}. They used a scaling approach in which a constant density is assumed throughout the brush: all the brush chains are assumed to be equally stretched and to end at a distance from the substrate equal to the thickness of the brush. Such a treatment clearly neglects the entropy associated with the spatial distribution of chain ends. Some ten years later, a numerical self-consistent-field calculation was reported in which the density profile is no longer assumed to be a block profile and where the end points of the chains are distributed throughout the brush¹⁸. Analytical equations based on a similar model were developed by Milner et al. and by Zhulina et al.¹⁹⁻²¹. Since then, polymer brush models have been extended to many cases, e.g., polydisperse brushes^{20,22} and charged brushes²³⁻²⁵.

In this chapter, we report a complete set of experiments on the wetting behaviour of brush surfaces by a polymer melt and we compare the results with theoretical models. The brushes used in the experiments were prepared in two ways, either by adsorbing block copolymers onto the surface, or by chemical grafting of end-functionalised polystyrene on the surface. We focus on the effects of the chain length P of the polymer melt and the grafting density σ of the brush. We thus obtain a phase diagram in the (P, σ) plane. The remainder of this chapter is organised as follows. In section 2 we discuss theoretical results. We first develop some simple scaling relations for two wetting transitions, one from partial to complete wetting at low σ (section 2.1), and one from complete to partial wetting at higher σ (section 2.2). In section 2.3 we present numerical calculations obtained with an SCF-model. After a short experimental part (section 3), we present in section 4 the results, which are interpreted in the light of the theoretical predictions.

2. Theory

2.1 Scaling law for the first wetting transition

We consider the situation of a substrate that is initially partially wetted by the polymer melt. By attaching chains that can mix with the melt, the wettability is

improved and at some grafting density σ^* complete wetting is obtained. The non-wetting region bounded by $\sigma = 0$ and $\sigma = \sigma^*$ will be denoted as the *allophobic* regime: the melt does not like the chemically different surface. In order to develop an expression for σ^* , we first consider the bare surface ($\sigma = 0$).

The spreading coefficient S is a parameter used to characterise the wettability of a surface. It is defined as the difference of the surface tensions of the initial and final situation as depicted in figure 4.1. This liquid film may be unstable or metastable and can dewet.

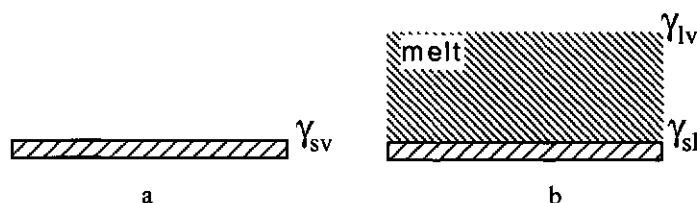


Figure 4.1. Schematic representation of the relevant surface tensions in the case of (a) a solid-vapour (sv) interface and (b) a macroscopic layer on the surface, with solid-liquid (sl) and liquid-vapour (lv) interfaces.

Generally, S is defined by

$$S = \gamma_{lv} - (\gamma_{sl} + \gamma_{sv}) \quad (4.1)$$

where γ_{lv} is the liquid-vapour surface tension, γ_{sl} the liquid-solid interfacial tension and γ_{sv} the solid-vapour surface tension. Complete wetting of the liquid on the substrate occurs if $S > 0$ and dewetting (partial wetting) implies if $S < 0$. In our case S is negative for a bare surface, it increases with σ , and it reaches $S = 0$ at the critical grafting density σ^* . At this critical grafting density the surface is transformed from a non-wettable to a wettable surface. In partial wetting situations a macroscopic equilibrium contact angle δ of the droplets can be measured. The spreading coefficient in this partial wetting situation can be expressed in terms of γ_{lv} and the contact angle δ , which obeys Young's law $\gamma_{lv} \cos \delta = \gamma_{sv} - \gamma_{sl}$.

$$S = \gamma_{lv} (\cos \delta - 1) \quad (4.2)$$

We will denote S for a bare surface as S_0 , and the corresponding contact angle as δ_0 . Grafting chains on such a surface will increase the wettability, i.e. increase S . At sufficiently high adsorbed amounts or grafting densities, the sv surface is fully covered with collapsed coils (see figure 4.2a). Immersing the substrate in a chemically identical polymer melt, the chain dissolves and gains conformational entropy (figure 4.2b).

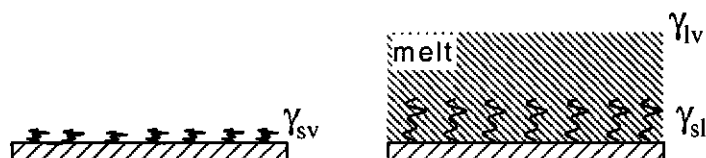


Figure 4.2. Schematic representation of modified surfaces and the interfacial tensions of (a) collapsed brush-vapour interface and (b) brush immersed in a melt.

The total free energy change ΔF due to the attached polymers has two contributions: one from the mixing of the attached chains with the free chains (ΔF^{mix}), and one from the swelling of the (initially collapsed) attached chain to an attached random coil (ΔF^{conf}). The mixing entropy gain of one free and single chain in a polymer melt can be calculated using the Flory-Huggins theory²⁶.

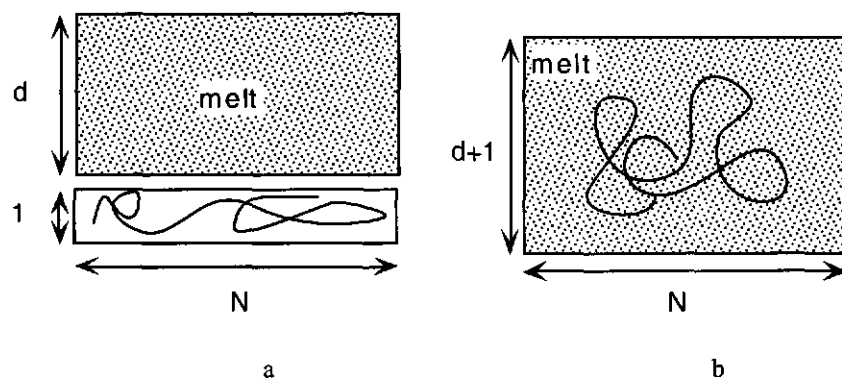


Figure 4.3. Schematic representation of the entropy of mixing for a free chain. (a) is before mixing and (b) is after mixing.

Consider a single, free and collapsed chain with thickness 1 and length N (in units of the monomer length a) as depicted in figure 4.3. Immersing this chain in a polymer melt with thickness d , containing Nd sites and Nd/P melt chains, we can express the mixing free energy as

$$\frac{\Delta F^{free}}{kT} = \ln \frac{1}{d+1} + \frac{Nd}{P} \ln \frac{d}{d+1} \quad (4.3)$$

Here, P is the length of the polymer chains in the melt (in monomeric units). The mixing entropy of the chain according to equation 4.3 is an overestimate, due to the fact that we did not take into account that the polymer is grafted onto the surface, both in the reference state and in the final situation. The mixing entropy of a *grafted* chain in a polymer melt is found after correcting:

$$\Delta F^{mix} = \Delta F^{free} + (\Delta F_{brush} - \Delta F_{ref}) \quad (4.4)$$

Here, ΔF_{brush} is the correction due to grafting in the mixed state (figure 4.3 b) and ΔF_{ref} the analogous correction for the reference state (figure 4.3 a); both corrections are positive.

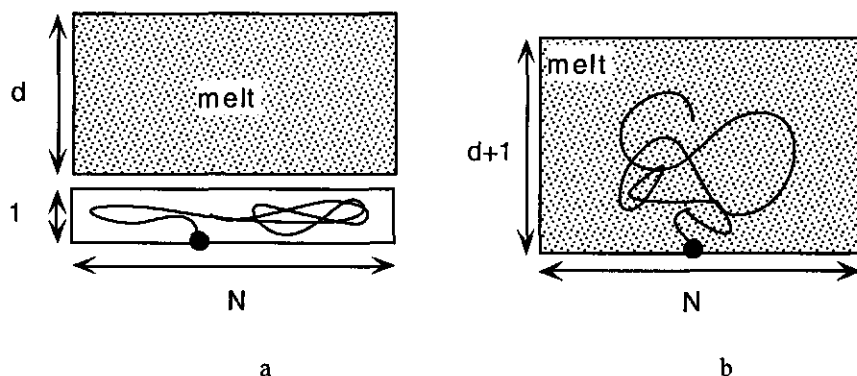


Figure 4.4. Schematic representation of the entropy of mixing for a attached chain. (a) is before mixing and (b) is after mixing.

These corrections are simply related to the relative reduction in available space for the end point, and we find $\Delta F_{ref} = kT \ln N$ and $\Delta F_{brush} = kT \ln[N(d+1)]$, respectively, so

that the term in brackets in equation (4.4) equals $kT \ln(d+1)$. Hence, the first term in equation (4.3) cancels:

$$\frac{\Delta F^{mix}}{kT} = \frac{Nd}{P} \ln \frac{d}{d+1} \quad (4.5)$$

When a collapsed chain is immersed in a polymer melt, the chain can swell depending on the solvent quality. In our case the attached chain and the polymer melt are identical and a chain becomes a Gaussian coil with a radius of gyration of $R = N^{1/2}a$. The radius of gyration of a coil in the collapsed reference state is $R_0 = N^{1/3}a$. Hence, the swelling coefficient α (with respect to the random coil state) is given by²⁷

$$\alpha^2 = \frac{R^2}{R_0^2} = \frac{(N^{1/3}a)^2}{(N^{1/2}a)^2} = \frac{1}{N^{1/3}} \quad (4.6)$$

and the associated free energy for $\alpha \ll 1$ equals²⁷

$$\frac{\Delta F^{conf}}{kT} \approx -\frac{1}{\alpha^2} = -N^{1/3} \quad (4.7)$$

Combining equation (4.5) and (4.7), we arrive at

$$\frac{\Delta F}{kT} = \frac{\Delta F^{mix} + \Delta F^{conf}}{kT} = \frac{Nd}{P} \ln \frac{d}{d+1} - N^{1/3} \quad (4.8)$$

Equation (4.8) for $1/d \ll 1$ may be simplified by expanding the logarithmic term up to first order in $1/d$. The result is

$$\frac{\Delta F}{kT} = -\left(\frac{N}{P} + N^{1/3}\right) \quad (4.9)$$

Attaching σ chains per unit area onto the surface will increase the difference $\gamma_{sl} - \gamma_{sv}$ in equation (4.1) by a (negative) amount $\sigma \Delta F$, decreasing S by the same amount, lead to an free energy gain (of entropic origin) per unit area of $\sigma \Delta F^{mix}$. The critical grafting density (σ^*) at which $S = 0$ transforms the non-wettable surface to a wettable surface.

The wetting criterion $S = 0$ at $\sigma = \sigma^*$ is thus

$$S = S_0 - \sigma^* \Delta F = 0 \quad (4.10)$$

Substituting equation 4.2 and 4.9 in equation 4.10 we obtain for the critical grafting density

$$\sigma^* = \frac{-\gamma_{lv}(\cos \delta_0 - 1)}{kT \left(\frac{N}{P} + N^{1/3} \right)} \quad (4.11)$$

The surface tension γ_{lv} generally increases with increasing molar mass (i.e., with P). However, the variation of this surface tension as function of the molecular weight is no more than a few percent and therefore not taken into account in the present scaling approach.

2.2 Scaling law for the second wetting transition

At high σ , a second transition may occur due to the expulsion of free chains from a dense brush. We therefore consider the free energy of a chain in a brush^{17,28}

$$\frac{F}{kT} \cong \frac{H^2}{a^2 N} + \frac{a^3 N^2 \sigma}{PH} \quad (4.12)$$

Again, N is the number of monomeric units in the brush, a the length of a monomer, P the degree of polymerization of the polymer melt and σ the grafting density (nm^{-2}). The parameter H is the thickness of the brush. The first term in equation 4.12 represents the elastic contribution, and the second term describes the mixing of the free melt with the brush. Minimalisation of the free energy with respect to H gives for the brush height

$$H \cong a^{5/3} NP^{-1/3} \sigma^{1/3} \quad (4.13)$$

Increasing the grafting density (creating a denser brush) leads to an increase in brush height. Decreasing the length P of the polymer melt facilitates the interpenetration and results in increased swelling of the brush and a concomitant increase of the brush height.

The average brush density $\langle \phi \rangle$ of the brush can be written as

$$\langle \varphi \rangle = \frac{N\sigma a^3}{H} \quad (4.14)$$

where $N\sigma a^3$ is the collapsed volume of one chain. When the brush in contact with the melt is fully collapsed (no penetration of the melt chains into the brush, $\langle \varphi \rangle = 1$), this volume equals $H\sigma^{-1}$ where σ^{-1} is the area per chain. When penetration of the melt chains takes place, $\langle \varphi \rangle$ is smaller than unity and H is correspondingly higher due to the swelling accompanying the interpenetration. Inserting H from eq. (4.13) into (4.14) we find

$$\langle \varphi \rangle = (\sigma a^2)^{2/3} P^{1/3} \quad (4.15)$$

Note that $\langle \varphi \rangle$ does not depend on N .

We now consider the wetting behaviour. We may expect that, for wetting to occur, some interpenetration is necessary. Non-wetting corresponds to a fully collapsed brush with $\langle \varphi \rangle = 1$ and no interpenetration.

We denote the grafting density at the second (autophobic) wetting transition as σ^{**} . The name expresses the dislike of free melt chains for chemically identical brush chains, for entropic reasons. A reasonable estimate for σ^{**} is obtained by assuming $\langle \varphi \rangle = 1$ at $\sigma = \sigma^{**}$. This condition gives

$$\sigma^{**} \sim \sqrt{\frac{1}{P}} \quad (4.16)$$

We thus find that the grafting density of the brush at the autophobic wetting transition should scale as the square root of $1/P$. We finally note that, for large P our equations (4.11) and (4.16) would imply that σ^* and σ^{**} should eventually cross at $P^* \approx (\sigma^* a^2)^{-2}$. Hence, for sufficiently large P (at fixed N), the complete wetting regime may eventually disappear.

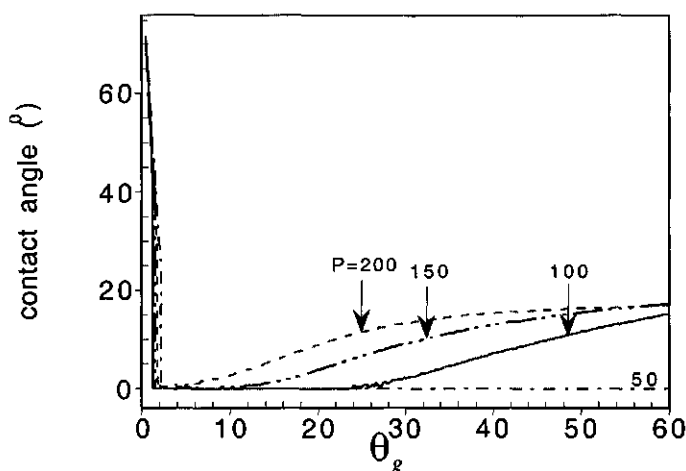


Figure 4.9. Calculated contact angle for different lengths P of the polymer melt as function of the grafting density, on a brush with $N = 200$.

Contact angles of a free polymer melt on surfaces with terminally grafted chains were calculated using formula 4.17. Figure 4.9 shows some results for a polymer droplet on a brush with $N = 200$. At low grafting density (allophobic region) the contact angle is high and essentially independent of the molar mass of the melt. Increasing the grafting density to approximately $\theta_g^* \approx 2$ results in complete wetting. At higher grafting densities of the brush, a non-zero contact angle reappears at θ_g^{**} and then starts to increase due to the expulsion of the free melt out of the brush. This is the autophobic region. With decreasing chain length of the free polymer, the interval $(\theta_g^*, \theta_g^{**})$ where there is complete wetting increases. Beyond θ_g^{**} , the contact angle increases with increasing grafting density upto a plateau value of $\approx 18^\circ$ for all molecular weights. A polymer melt with $P = 50$ does not reach the autophobic region in the range of figure 4.9 but the autophobic wetting transition should occur at high grafting densities ($\theta_g > 60$).

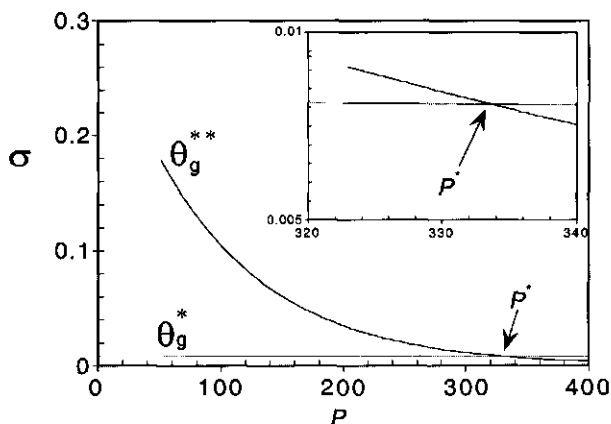


Figure 4.10. Calculated wetting/dewetting diagram for a polymer brush with $N = 100$. The inset shows more detail around $P = P^*$.

From plots like figure 4.9 the values of $\theta_g^*(= \sigma^*N)$ and $\theta_g^{**}(= \sigma^{**}N)$ can be found for any value of P . In this way we can obtain a theoretical phase diagram as shown in figure 4.10. As can be seen from the figure, the two wetting transitions intersect ($\theta_g^* = \theta_g^{**}$). In this case ($N = 100$) this intersection is at $P^* = 333$. Beyond P^* , the substrate will dewet for all grafting densities of the brush. For $P < P^*$ the contact angle is finite at low σ , it is zero for $\sigma^* < \sigma < \sigma^{**}$, and it increases again for $\sigma > \sigma^{**}$. For $P > P^*$ there is no complete wetting window anymore, and $\delta(\sigma)$ shows a minimum, but remains finite. This confirms our earlier conclusion based on scaling approach (see the discussion below equation 4.16).

3. Experimental

3.1 Materials

As substrates, we used either silicon wafers with an oxide layer of approximately 80 nm (prepared by thermal oxidation) or hydrogen terminated silicon wafers, depending on the technique used to prepare brushes. PS does not wet oxidised silicon wafers, whereas hydrogenated (passivated) Si seems to be completely wetted by PS.

3.2 Preparation of brushes

Brushes with relatively low grafting density were prepared by adsorbing poly-4-vinylpyridine-polystyrene (PVP/PS) block copolymers on oxidized silicon. The adsorption was carried out using either dipcoating in a dilute solution (using a non-selective solvent) or adsorption from the melt, depending on the desired density of the brush. A detailed description is given elsewhere³⁴.

In order to obtain dense brushes, we applied chemical grafting of vinyl-terminated PS (figure 4.11) on hydrogen-terminated silicon to form an alkyl (Si-CH₂-) bond. The reaction can be done either from solution or directly from the melt. An important advantage of using polymer melts for this reaction is that one can get much denser brushes than with grafting from solution. We used two PS samples with a different degree of polymerization (20 and 200, respectively). The polymers are referred to as PS with a subscript indicating the number of monomeric units. The highest grafting density (σ) of the PS₂₀ layer is 0.95 nm⁻², (i.e., every chain has 1.05 nm² available on the surface) and the thickness is 3.0 nm. For PS₂₀₀ this was 0.55 nm⁻², with a layer thickness of 19.2 nm. A detailed description of the chemical grafting method is given in chapter 3³⁵.

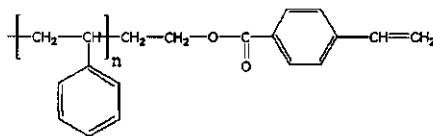


Figure 4.11. Vinyl terminated polystyrene

3.3 Overlayers

PS overlayers on the brushes were made by spincoating the polymer from CHCl_3 at 3000 rpm, using appropriate concentrations (1-5 mg/ml). The thickness of the dry polymer layer was determined by computer-controlled null ellipsometry (Sentech SE-400). The refractive index for $\lambda = 632.8$ nm was taken as 1.58³⁶. The AFM measurements were performed with a Digital Instruments Nanoscope III AFM equipped with a scanner, capable of scanning an area of 100 μm^2 . All AFM measurements were performed in air at room temperature and a relative humidity of 50-60%. Commercially available tapping-mode tips were used on cantilevers with a resonance frequency in the range of 350 - 400 kHz. The sample surfaces were stored in vacuo at a temperature (145°C), well beyond the T_g of PS ($\sim 100^\circ\text{C}$). After 12 days the samples were quenched to room temperature and the surface topography of the top films was investigated by means of AFM.

4. Results & discussion

4.1 PS layer on a chemical identical brush

Our brush preparation methods give the possibility to make a whole variety of PS brushes, ranging from very dilute to very dense. We will now focus on the wetting behaviour of a PS overlayer on these PS brushes. Previous studies considered the effect of the brush length N and the free chain length P on wetting, but disregarded the grafting density σ ¹⁴. From these studies, it was concluded that the wetting-dewetting transition is only a function of the ratio N/P . In this chapter we do not only vary P but also the grafting density σ of the brush and the film thickness d of the melt.

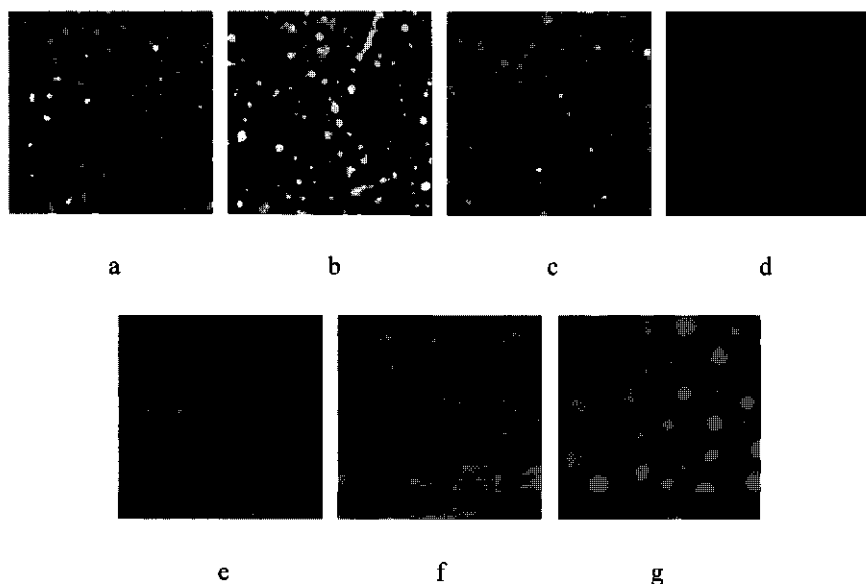


Figure 4.11. AFM images of a PS melt ($M_n = 183$ kg/mole) onto a PS brush. Image $10 \times 10 \mu\text{m}^2$, maximum height difference between the dark depressed regions and the elevated bright patches 30 nm. (a) dewetting, (b) 'holes + hills', (c) 'hills', (d) wetting, (e) 'hills', (f) 'holes + hills', (g) dewetting. From left to right σ increases: $\sigma = 0.09$ (a), 0.19 (b), 0.21 (c), 0.35 (d), 0.50 (e), 0.52 (f), 0.95 nm^{-2} .

Figure 4.11 shows seven representative AFM images (a-g) obtained for PS films with $M_n = 183$ kg/mole on brushes with an increasing grafting density of the PS brush. The bright areas are elevated, and the darker patches depressed regions. A very dilute brush is seen in figure 4.11 a: σ is low (0.09 nm^{-2}), the PS film is unstable and dewets. We observe a surface covered with small polymeric droplets. The contact angle can be estimated to be about 20° . Complete wetting is found for a brush with $\sigma = 0.35 \text{ nm}^{-2}$ (figure 4.11 d). At very high amounts of grafted PS onto the surface ($\sigma = 0.95 \text{ nm}^{-2}$, figure 4.11 g), the free PS film is unstable and dewets.

The cross-over between these three major regimes is characterised by two narrow intermediate regimes around the transition from partial to complete wetting. These two regimes are present on both wetting (figure 4.11b,c) dewetting (figure 4.11e,f)

transitions. In cases b ($\sigma = 0.19 \text{ nm}^{-2}$) and f ($\sigma = 0.52 \text{ nm}^{-2}$) the film has developed a large number of both droplets on top of the film and depressions below it. We refer to this situation as 'holes and hills'. In cases c ($\sigma = 0.21 \text{ nm}^{-2}$) and e ($\sigma = 0.50 \text{ nm}^{-2}$) droplets ('hills') have appeared on top of a smooth film of free PS but there are no depressions. The development of these intermediate surface patterns in thin films on a flat surface will be discussed in section 4.2.

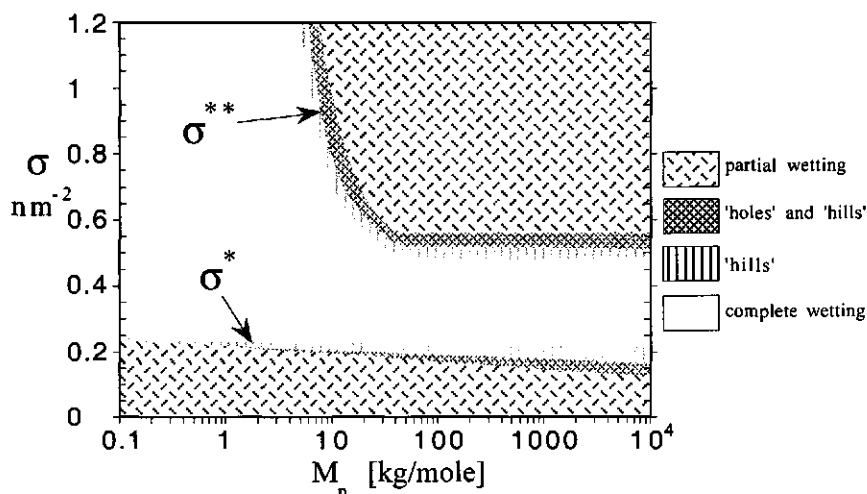


Figure 4.12. Wetting phase diagram of a PS melt of varying M_n onto a PS brush of varying grafting density σ after annealing 12 days at 145°C under reduced pressure. The initial film thickness in all experiments is $5 \text{ nm} \pm 0.1 \text{ nm}$.

We repeated the experiments with PS of different M_n , spanning a range of 1 - 10^4 kg/mole . The results are summarized in the (σ, P) phase diagram given in figure 4.12. Regions of complete wetting, partial wetting and the intermediate regimes are indicated. The two intermediate regimes occur in narrow bands, both at the first transition ($\sigma \approx 0.19 \text{ nm}^{-2}$), and at the second transition ($\sigma \approx 0.55 \text{ nm}^{-2}$ for high M_n).

For the first wetting transition (σ^*), the molar mass of the free PS has hardly an effect, which agrees with eq. (4.11) for large P . This may suggest that kinetic factors are not relevant and that the system is probably close to thermodynamic equilibrium.

We now compare the experimental data for the wetting transitions with the scaling predictions (equation (4.11) and (4.16)). Experimentally, the wetting transition at low σ occurs at a grafting density around 0.15 chains/nm². Equation (4.11) predicts a value of ~ 0.08 chains/nm² (for large P). Taking into account that this scaling law was derived from very simple arguments for very diluted brushes, it describes the first wetting transition from the allophobic region to complete wetting remarkably well (figure 4.13).

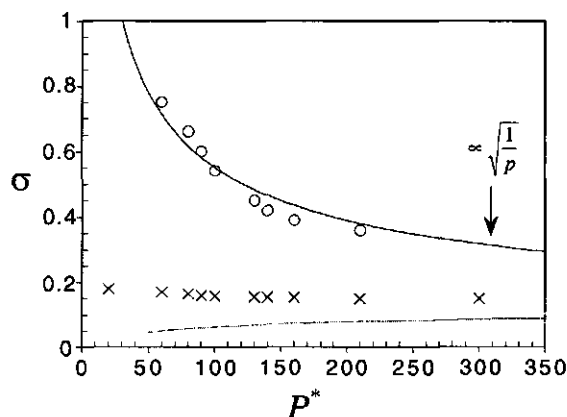


Figure 4.13. Comparison of experimental and theoretical wetting phase diagram. Experimental results are obtained from figure 4.12. The molar mass of P^* is converted to the number of monomeric units of the brush. The solid curves are the theoretical predictions.

In figure 4.13 we have also plotted the experimental data of σ^{**} (figure 4.12) and the scaling result (equation 4.16). This latter scaling law is derived for dense brushes and

describes the second wetting transition towards autophobic dewetting very well. We conclude that there is good agreement between experiment and theory within the experimental window. From theory we would expect to lose the complete wetting regime when the two curves in figure 4.13 cross at very high P . We have no experimental data, however, to check this prediction.

In figure 4.14 the influence of the initial film thickness d of the free PS as function of σ is shown. As can be seen, both wetting transitions depend slightly on d , but with opposite trends. For example, at $\sigma = 0.14 \text{ nm}^{-2}$ and $d = 2 \text{ nm}$ there is complete wetting; increasing d to 9 nm leads to partial wetting (see the arrow $a \rightarrow b$ in figure 4.14). The autophobic transition from dewetting to wetting shifts at increasing film thickness to higher σ . In contrast, the autophobic transition shifts to lower σ with increasing d . Upon passing through the transition, the typical patterns as discussed in figure 4.11 are seen again. Apparently, the 'wetting window' in σ becomes narrower as the film becomes thicker.

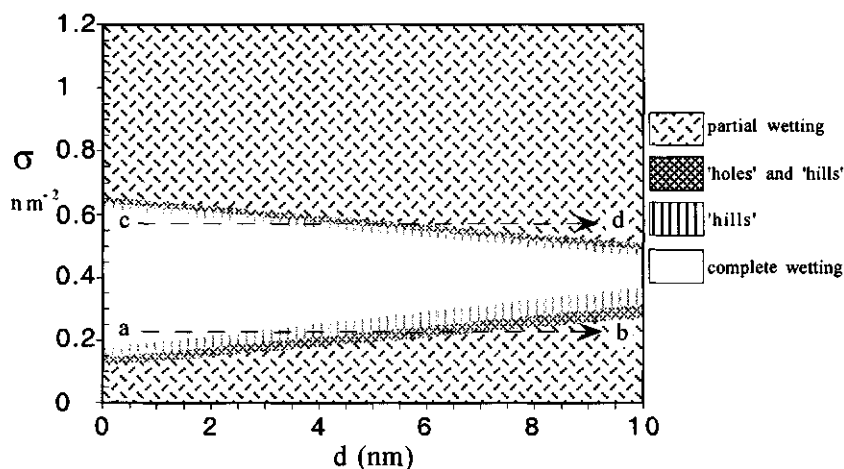


Figure 4.14. Wetting behaviour as a function of the initial film thickness of the free PS, for $M_n = 183 \text{ kg/mole}$.

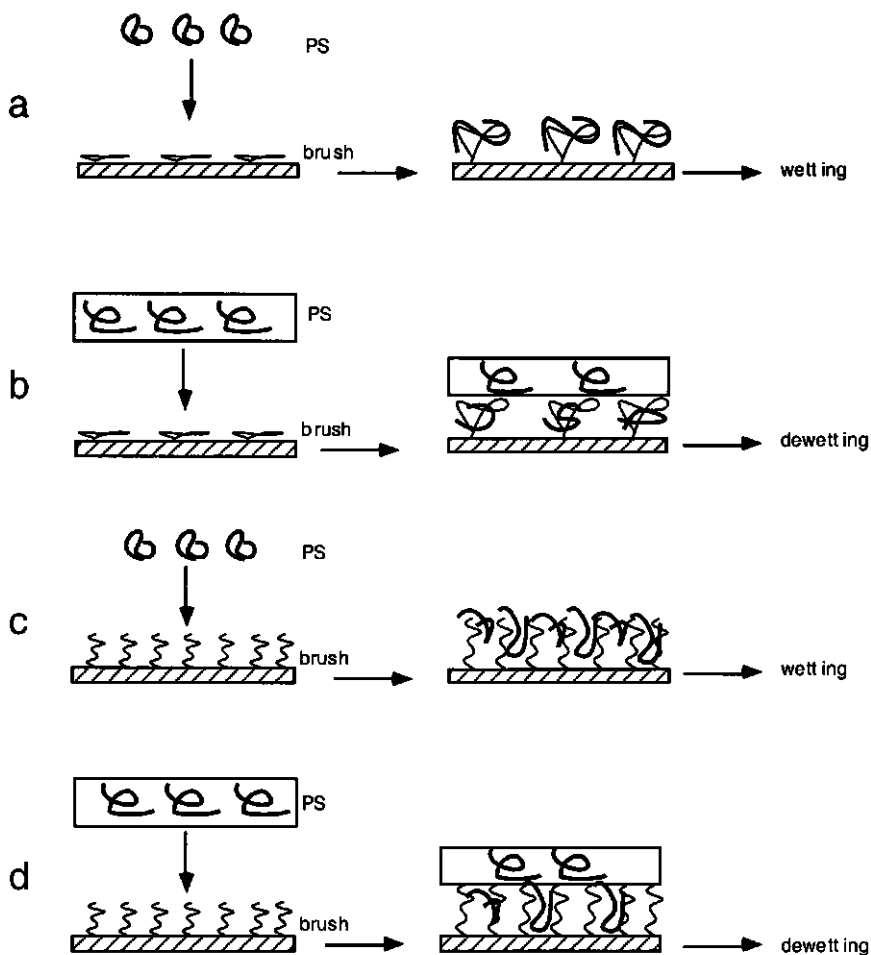


Figure 4.15. Schematic representation of a polymer brush covered with a polymer melt. (a) Dilute brush covered with a very thin layer of free chains. All these chains can make contact with the attached chains. (b) Dilute brush covered with a thick layer of free chains. The surface will dewet due to the non-wettable surface. (c) Dense brush covered with a very thin layer of free chains. All these chains can penetrate into the brush, leading to a wettable surface. (d) Dense brush covered with a thick layer of free chains. The surface will dewet due to the entropic difference between the free and grafted chains.

The following scenario for this film thickness dependence seems plausible. Starting with a very dilute brush and a very thin overlayer (point a in figure 4.14), the whole overlayer can be used to swell the attached chains on the surface. The result is that the intrinsic non-wettable surface shows wetting behaviour. Basically, there is not enough free polymer available to form droplets. Schematically this is shown in figure 4.15a. Increasing the thickness of the overlayer to point b in figure 4.14 results in a dewetting behaviour. In this case part of the overlayer is used to swell the brush and the excess of the layer experiences a non-wettable surface, eventually resulting in dewetting of the surface (figure 4.15b). Starting with a dense brush and a very thin overlayer (point c in figure 4.14), all the chains of the free melt can penetrate into the brush and the brush swells (see figure 4.15c). Increasing the thickness of the overlayer to point d in figure 4.14 results again in a dewetting behaviour (figure 4.15d). In this case a small fraction of the overlayer can penetrate into the brush and the excess material displays autophobic behaviour.

4.2 Pattern formation around wetting transition

We have observed in our experiments that both the allophobic and the autophobic wetting transition are characterised by two intermediate regimes (figure 4.11). The first intermediate regime corresponds to coexistence of two thicknesses: a thin polymer film on top of the brush and droplets of bulk liquid. In the second regime three thicknesses occur simultaneously: macroscopic droplets, nearly dry surface and a mesoscopic thin polymeric film. Similar patterns have been observed for films in a electrical field and are very likely a consequence of the way instabilities in the film develop³⁷. Simulations of instabilities in dewetting films have recently become available¹⁰⁻¹³. In these calculations the predictions of the surface patterns in thin films on a flat surface are based on linear stability analysis, leading to an equation for the evolution of a thin film. This equation is derived from the Navier-Stokes equation applied to the growth of instabilities of the thin film with the surface tension and the

disjoining pressure of the film as driving forces. For the special case where there was a double minimum in the free energy curve as a function of the thickness, the calculations gave the following results¹⁰. Thick films become rough and disproportionated by creating cylindrical holes. With increasing annealing time the holes grow in size until they touch, leading to a polygonal network of liquid ribbons. Eventually these ribbons decay into droplets due to the well known instabilities of a ridge. Films thinner than those corresponding to spinodal minimum decay into droplets via a spinodal dewetting mechanism. Films of intermediate thickness show a variety of structures on the substrate. These structures can be modified not only by changing the film thickness but also by changing the free energy curve. Our experiments shows structures very similar to those obtained by this stability analysis, indicating that the pattern formation may well be due to a double minimum in the free energy. Indeed, such a double minimum in the free energy was found in our self-consistent-field calculations⁵, thus supporting this explanation.

5 Conclusions

We have studied the wetting behaviour of a polymer film on a surface carrying a polymer brush of the same material, as function of the brush grafting density and chain length of the free polymer. From a simple scaling analysis we find that if the bare surface is partially wet (i.e., has a finite contact angle), a brush may cause two wetting transitions: one from partial to complete wetting at low grafting density, and one back from complete to partial wetting at high grafting density. The region of partial wetting at low grafting density we call the allophobic regime, the second region of partial wetting at high grafting density is the autophobic regime. The lower transition (allophobic to complete) occurs at a nearly constant grafting density, independent of the molar mass P of the free chains. In contrast, the grafting density at the upper transition (complete to autophobic) varies as $P^{-1/2}$. As a consequence, we predict an intersection point of the two transitions at high P , where the complete wetting regime thus ends. All these scaling predictions are confirmed by numerical self-consistent-field calculations.

We have experimentally investigated films of PS on PS brushes. These brushes were prepared either by adsorption of poly-4-vinyl-pyridine-polystyrene block copolymers or by chemical reaction of end-functionalised polystyrene. The experiments fully confirmed the existence of the two wetting transitions, separating an allophobic, a complete wetting and an autophobic regime. The dependences of the transitions on the grafting density and the molar mass P was as expected. However, in the experiments the end of the complete wetting regime at high P was not reached. A weak dependence of the transitions on the film thickness d was observed for which no quantitative theory is available, but which could be qualitatively explained.

Around the wetting transitions, peculiar patterns are formed which were concluded to be signatures of the destabilisation process which is driven by the disjoining pressure in the film. In line with recent calculations reported in literature, the occurrence of droplets in equilibrium with depressed regions was described to the presence of two minima in the free energy as function of the film thickness. Such a double minimum was indeed found in self-consistent-field calculations, thus supporting this conclusion.

This work was supported Financially from the Dutch National Research School Polymeren-PTN. Discussions with prof. A. Skvortsov (St. Petersburg) are gratefully acknowledged.

References

1. G. Reiter, *Langmuir*, 9,5 (1993), 1344-1351
2. G. Reiter, *Phys. Rev. Let.*, 68, 1 (1992), 75-78
3. T.G. Stange , D.F. Evans, *Langmuir*, 13 (1997), 4459-4465
4. G. Reiter, A. Sharma, R. Khanna, A. Casoli, M.O.David, *J.Colloid interface Sci.*, 214, (1999), 126-128
5. J.H. Maas, M.A. Cohen Stuart, F.A.M. Leermakers, N.A.M. Besseling, *Langmuir*, 16, 2000, 3478- 3481
6. G. Reiter, A. Sharma, R. Khanna, A. Casoli, M.O.David, *Europhys. Lett.*, 46, (1999), 512-518
7. U. Thiele, M.Mertig, W. Pompe, *Phys. Rev. Lett.*,80, (1998), 2869
8. S. Hemminghaus, K.Jacobs, K.Mecke, J.Bischoff, A.Ferry, *Science*, 282, (1998), 916
9. G. Reiter, A. Sharma, A. Casoli, M.O. David, P. Auroy, *Langmuir*, 15, (1999), 2551-2558
- 10 J.Singh, A. Sharma, *J.Adhesion Sci. Technol*, 14, 2, (2000), 145-166
- 11 A. Sharma, R. Khanna, *Phys. Rev. Lett.*,81, (1998), 3463
- 12 A. Sharma, R. Khanna, *J. Chem. Phys*, 110, (1999), 4929
- 13 R. Khanna, A. Sharma, *J.Colloid interface Sci.*, 195, (1997), 42
- 14 Y. Liu et al., *Phys. Rev. Let.*, 73, 3 (1994), 440-443
- 15 R. Yerushalmi-Rozen, J. Klein, L.J. Fetters, *Science*, 263 (1994), 793-795
- 16 S. Alexander, *J. de Phys. Fr.*,38, (1977), 983
- 17 P.G. de Gennes, *Macromolecules*, 13, (1980), 1069
- 18 T. Cosgrove, T. Heath, B. van Lent, F. Leermakers, J.M.H.M. Scheutjens, *Macromolecules*, 20, (1987), 1692
- 19 S.T. Milner, T.A. Witten, M.E. Cates, *Europhys. Lett*, 5, (1988), 413
- 20 S.T. Milner, T.A. Witten, M.E. Cates, *Macromolecules*, 21, (1988), 2610
- 21 E.B. Zhulina, O.V. Borisov, V.A. Priamitsyn, *J.Colloid interface Sci.*, 137, (1990), 495

- 22 T.M. Birshtein, Y.V. Liatskaya, E.B. Zhulina, *Polymer*, 31, (1990), 2185
- 23 O.V. Borisov, T.M. Birshtein, E.B. Zhulina, *Macromolecules*, 27, (1994), 4795
- 24 O.V. Borisov, T.M. Birshtein, E.B. Zhulina, *J. Phys. II Fr.*, 1, (1991), 521
- 25 E.B. Zhulina, T.M. Birshtein, O.V. Borisov, *Macromolecules*, 28, (1995), 1491
- 26 P.J. Flory, *Principles of Polymer Chemistry*, Cornell University Press, Ithaca (1953)
- 27 A. Y. Grosberg, A.R. Khokhlov, *Giant Molecules*, Academic Press, San Diego (1997)
- 28 M. Aubouy, G.H. Frederickson, P.Pincus, E. Raphaël, *Macromolecules*, 28, (1995), 2979
- 29 K.R. Shull, *Faraday Discuss.*, 98, 22 (1994)
- 30 L.I. Klushin, T.M. Birshtein, A.M. Mercurieva, *Macromol. Theory Simul.*, 7, 483-495 (1998)
- 31 E.P.K. Currie, M. Wagemaker, M.A. Cohen Stuart, G.J. Fleer, *Macromolecules*, 32, 9041 (1999)
- 32 C.M. Wijmans, J.M.H.M. Scheutjens, E.B. Zhulina, *Macromolecules*, 25, 1992, 2657
- 33 G.J. Fleer, M.A. Cohen Stuart, J.M.H.M. Scheutjens, T. Cosgrove, B. Vincent, *Polymers at interfaces*, Chapman & Hall, London, 1993
- 34 J.H. Maas, M.A. Cohen Stuart, G.J. Fleer, *Thin Solid Films*, 358, 2000, 234-240
- 35 J.H. Maas, submitted to *Thin Solid Films*
- 36 N. Koneripalli, R. Levicky, F. Bates, M.W. Matsen, S.K. Satija, J. Ankner, H. Kaiser, *Macromolecules*, 31 (1998), 3498
- 37 U. Steiner, *private communication*

Chapter 5 Wetting transition in a polymer brush: Polymer droplet coexisting with two film thicknesses

Abstract

We have systematic experimental observations that just below the wetting transition of a polystyrene (PS) melt onto a substrate covered by a poly-4-vinylpyridine-PS (PVP/PS) di-block copolymer there can be a macroscopic droplet and two coexisting layer thicknesses of PS. In addition to the usual macroscopic droplet and a microscopically thin film at the substrate (typical for partial wetting), a second mesoscopically thick film is selected. This film is a polymer 'brush' of order 10 nm thick swollen with free PS chains. The presence of this extra mesoscopically thick film proves that the wetting behaviour near the wetting transition is richer than predicted by the classical wetting theory. The disjoining potential profile must be a function with two local minima near the surface instead of just one. We have seen the selection of this mesoscopic film thickness in the dewetting behaviour of an unstable spin-coated film of PS on the brushed interface. The self consistent field theory applied to this problem shows that a mesoscopically thick film may indeed be trapped in a brush: there is a prewetting transition in combination with partial wetting.

1 Introduction

Recently it was found for the wetting of pentane on water that a macroscopic droplet in equilibrium with a microscopically thin film transforms by way of a first-order transition to a macroscopic thick droplet in equilibrium with a mesoscopic film¹. At the transition temperature three states coexist: a macroscopic droplet, a mesoscopically and a microscopically thin film. These observations have been explained by the hypothesis that there are substrate interactions on two separate length scales. At the first-order transition the short-ranged forces indicate wetting, whereas at that point the longer ranged Van der Waals forces are such that the vapour-pentane and pentane-water interfaces are attractive. These attractive Van der Waals forces prevent the unbounded growth of the wetting film (partial wetting). The wetting transition occurred at some higher temperature when the Van der Waals forces changed sign. The wetting transition was shown to be of the second-order type. The temperature dependence of the Van der Waals forces is of course highly specific and one can not systematically vary parameters in this system in order to play with the coexistence of the three phases nor with the wetting transition. We discuss a system which resembles the pentane-water system in some respects. In the alkane-water system, recent studies have shown that varying the salt concentration in the water has allowed one to shift the thin-thick transition and the critical wetting². We propose that a polymer brush may introduce a new length scale to an interfacial system, by means of the brush height H . This new length scale may similarly to the pentane-water case trigger equally interesting wetting behaviour: there are short-ranged interactions of a wetting component with the underlaying substrate, and effectively longer ranged interactions of a wetting component with a polymer brush. As a result we find that two film thicknesses can coexist with a macroscopic droplet in the system at a temperature below the wetting transition. The main advantage of the brush over the pentane-water system is that in the brush system there are a number of experimentally accessible parameters to systematically investigate this highly unusual phenomenon. We have found wetting transitions, but more precise experiments are needed to point to the order of them. In our discussion we will focus on the partially wet cases and in particular to the region where there are three coexisting phases at the surface.

2 Experimental

Silicon wafers with an oxide layer of approximately 80 nm, prepared by thermal oxidation, were used as substrate. Brushes were prepared by spin coating from concentrated solutions in a volatile, non-selective solvent (chloroform, 3000 RPM 10g/l) of PS/PVP, followed by annealing for 24 hours at 145 °C in vacuo. In order to obtain a single adsorbed layer, excess material was removed by washing with fresh solvent. Finally, samples were dried with nitrogen. Films of PS of varying molar mass were spincoated from CHCl₃ (1 mg/ml, 3000 RPM) over the treated surfaces, the thickness of the dry polymer layer was determined by computer-controlled null ellipsometry (Sentech SE-400). The refractive index for $\lambda = 632.8$ nm was taken as 1.58³ and subsequently stored at 145 °C in vacuo. After 12 days, the samples were quenched to room temperature and the surface topography of the top films, which are on average 5 nm thick, was investigated by means of AFM. The AFM measurements were performed with a Digital Instruments Nanoscope III AFM equipped with a scanner capable of scanning an area of 100 μm^2 . All measurements were performed in air at room temperature and a relative humidity level of 50-60%. Commercially available tapping mode tips were used on cantilevers with a resonance frequency in the range of 350 -400 kHz.

3 Results and discussion

A PS melt on inorganic substrates shows partial wetting. In an attempt to prepare stable films of PS onto such substrates, we have used a set of diblock copolymers of (PVP/PS) of varying block lengths to modify the surface of oxidised silicon wafers. The PVP block serves as the 'anchor' block, because it firmly adheres to the substrate; the PS block stands away from the substrate and is usually denoted as buoy. Hence, polyvinyl pyridine films are obtained with a varying density of end-attached polystyrene chains on top. For a surface treated with poly-4-vinylpyridine (PVP) only, ordinary dewetting occurs. That is, the usual pattern is observed of nucleation of holes in the film surrounded by a rim⁴⁻⁶. The holes grow according to a well-established rate law, until the rims touch, forming a kind of tessellation pattern. Finally the rims break up into droplets just like a liquid jet breaks up due to the Rayleigh instability.

One expects that the end-attached polystyrene introduced by replacing polyvinylpyridine by the diblock copolymer will promote the wetting of the treated surface by polystyrene so that, with increasing surface density of these chains, a transition from partial to complete wetting occurs. Of course, this transition is driven by the tendency of the grafted and the free chains to mix. Theoretical considerations have shown that a very dense packing of grafted chains hampers the favourable mixing of free and end-attached chains because it largely suppresses conformational degrees of freedom^{7,8}. Therefore, one expects that at very high grafting density there is a second transition towards a non-wetting system⁷.

Some years ago, experiments were reported that confirmed the stabilizing action of end-attached chains on a wetting film^{9,10}. Unstable films at high grafting density were then not observed. We have now revised the system of refs. 9 and 10 paying particular attention to the first wetting transition, and it turns out that new and unexpected phenomena occur around that transition.

The amounts of copolymer adsorbed onto a silica wafer are presented in figure 2.1 in chapter 2 (dashed line) as a function of the block length ratio v . A characteristic pattern is obtained^{11,12,13} with a pronounced maximum around $v \sim 0.1$ where long PS blocks are anchored by short PVP blocks, giving a dense brush with a substantial adsorbed amount. To the right of this maximum the PS blocks become shorter and the PVP blocks longer, with the effect that the total amount of polymer, and the amount of PS per unit area decrease. To the left the PVP blocks become too short to keep many molecules firmly anchored; therefore Γ decreases at $v = 0$: (for pure PS) no adsorption occurs. The pattern described here is precisely as found by theoretical treatments^{13,14,15}. In the terminology of Joanny and Marques the maximum separates two regimes, the 'buoy dominated' (low v) and the 'anchor dominated' (high v) regime. (We note in passing that adsorbed layers can also be prepared by an alternative route of adsorption from dilute (non-micellar) solution by dipcoating. This leads to lower adsorbed masses than for the spin-coating/annealing/rinsing procedure, but with a similar v -dependence, see figure 2.1 chapter 2).

Figure 5.1 shows four representative images (a-d) obtained for PS films with $M_n = 183$ kg/mole and 4 different block copolymer sublayers, with increasing amounts Γ_{PS}

of grafted PS per unit area. The bright areas are elevated, and the darker patches depressed regions.

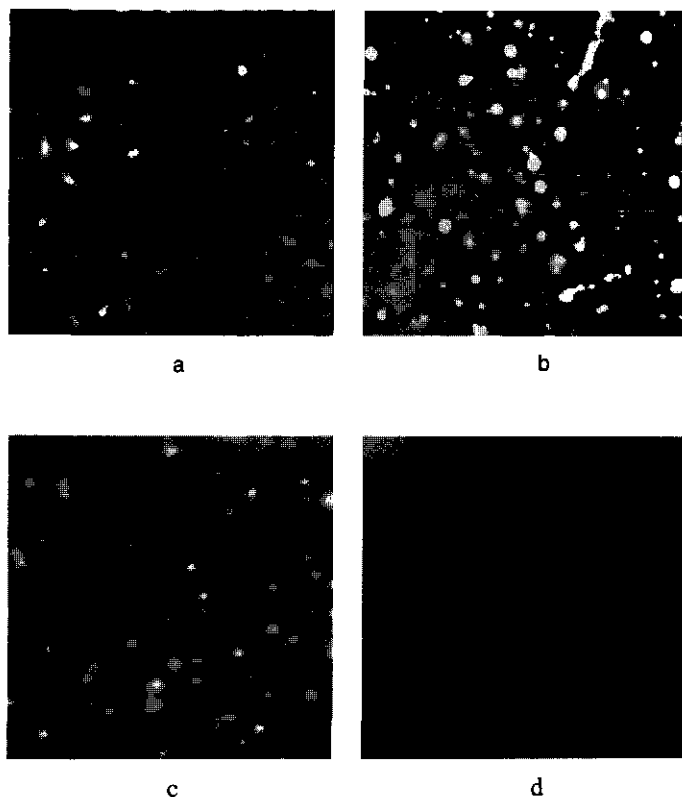


Figure 5.1. AFM images of PS (183 kg/mole) onto a PVP/PS brush after annealing for 12 days at 145°C; The numbers after PVP/PS represent the molecular weight of the blocks (in units of kg/mole) (a) dewetting PVP/PS (20/20) Γ_{PS} is 1.8 mg/m², (b) 'holes +hills' PVP/PS (13/32) Γ_{PS} 4.0 mg/m², (c) 'hills' PVP/PS (21/48) Γ_{PS} is 4.3 mg/m², (d) wetting PVP/PS (21/194) Γ_{PS} is 7.3 mg/m². Images 25*25μm², height 30nm.

Case a is as expected: Γ_{PS} is low (1.8 mg/m²), the film is unstable and dewets. We observe a surface covered with many small droplets separated by 'dry' PVP surface; the contact angle can be estimated to be about 20°, about the same as PS on glass⁴. A characteristic cross-section height profile is given in figure 5.2a. Case d, the other

extreme, is also straightforward: Γ_{PS} is high and a stable, featureless film is found: complete wetting.

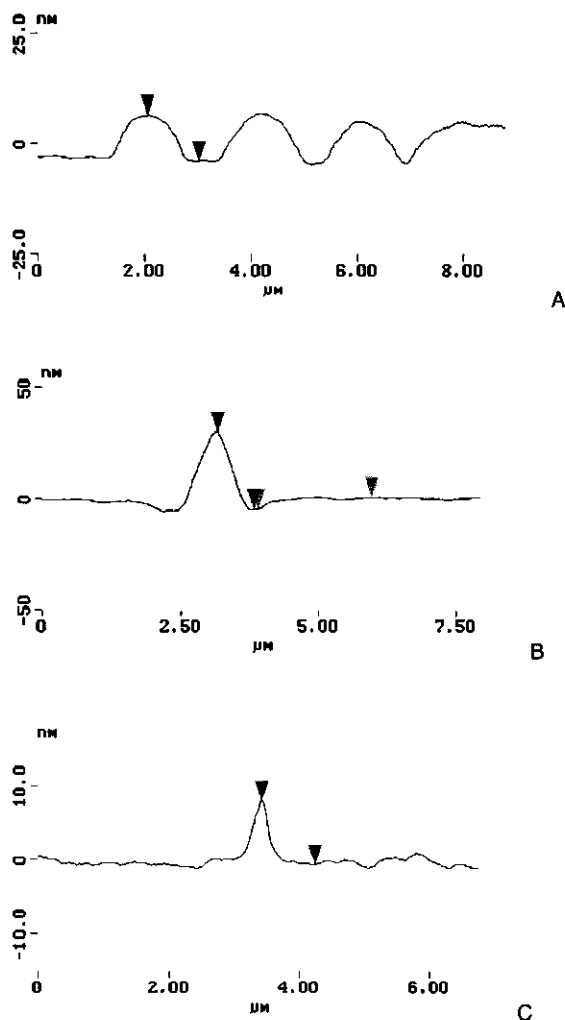


Figure 5.2. Cross-sections, showing height profiles. (a) dewetting, (b) 'holes + hills' and (c) 'hills'.

The surprises are in cases b and c. In b ($\Gamma_{PS} = 4.0 \text{ mg/m}^2$), the originally smooth film has developed a number of circular droplets surrounded by a depression. It seems as if there has been nucleation of droplets which then accumulated some polymer from

their immediate surroundings. A cross-section, showing this unusual height profile, is given in figure 5.2b. In case c (at $\Gamma_{PS} = 4.3 \text{ mg/m}^2$, i.e. only slightly higher) the depressions have disappeared altogether, but randomly distributed droplets have appeared on top of a smooth film of PS. An example of a droplet height profile is shown in figure 5.2c.

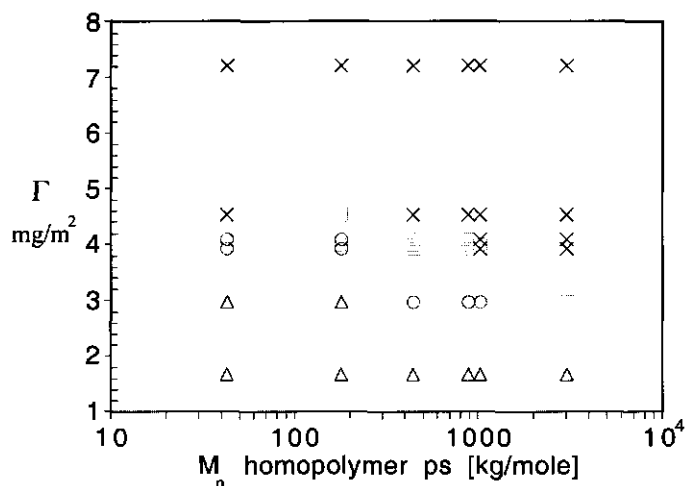


Figure 5.3. Experimental data of a PS film on top of a PVP/PS brush annealed for 12 days at 145 °C. Dewetting was observed for triangles, 'holes + hills' correspond to circles, squares refer to 'hills' and crosses correspond to wetting.

What causes these striking phenomena? First, one may wonder whether the structures observed are controlled by thermodynamic or by kinetic factors. We therefore repeated the experiments with PS of different M_n , spanning a range of 10-10⁴ kg/mole. All results are summarized in figure 5.3 where we indicate each experiment as a point characterized by its Γ_{PS} (grafted) and its M_{PS} (free). This is a magnification of the wetting dewetting transition of figure 4.12 in chapter 4. Regions of stable (complete wetting) films (x) corresponding to case d of figure. 5.1, 'hills' (◻), 'hills + holes' (○) and 'holes' (Δ) are indicated. It is readily seen that the two new 'regimes' occur in narrow bands between the common unstable and stable regimes, in roughly the same

Γ_{ps} ranges, irrespective of M_{ps} . Thermodynamic considerations gives us a line where three states are simultaneously in equilibrium. However, near this line each of the three states is at least locally stable and therefore these states are observable simultaneously in narrow bands.

The rates at which the patterns appear, however, vary greatly, from an hour at low M_n to many days at high M_n . This suggests that kinetic factors are not relevant for the final outcome, and that equilibrium thermodynamics govern these phenomena.

Apparently, we see, in case c, coexistence between a mesoscopic film (4 nm) and macroscopic (bulk) liquid, whereas in case b we have *three* regions: (i) bulk liquid (droplets), (ii) dry surface (around the droplets) and (iii) a mesoscopic film. The three distinct states (micro- and mesoscopic film and the macroscopic droplet) as found experimentally may admittedly be there just transiently: it seems unlikely that the exact temperature that all three states are stable is selected. However, near the wetting transition each of the three states is locally stable and therefore the three phases are observable simultaneously.

The coexistence of dry surface with a mesoscopic film suggests a special shape for the disjoining potential function, namely with a double minimum, one (primary) located at the surface, and one at the distance corresponding to the thickness of the mesoscopic film. This double minimum has also been found for the alkane-water system¹⁵. For the case of ordinary dewetting this function has a single minimum at the surface; the depth and width of this minimum is related to the contact angle¹⁶. The occurrence of this second length scale is most likely connected to the extension of the grafted chains. In order to check this conjecture, we have carried out self-consistent field calculations for the system at hand. In these calculations the brush and the free melt are modelled as flexible, linear chains. A polymer i is considered as a series of N_i segments numbered $s=1\dots N_i$. All components (brush, free melt and surface sites) are placed in a lattice of M layers parallel to the surface and numbered from $z=0$ (surface sites) to $z=M$. In each layer all segments of the polymer experiences a potential $u(z)$ composed of entropic and energetic interactions. A first order Markov approach is used to evaluate the probabilities of all possible conformations of the polymer. The equilibrium volume fractions $\rho_i(z)$ are calculated based on the potential and the probabilities. Once

$u(z)$ and $\rho(z)$ are determined other thermodynamic properties of the system can be derived. A detailed description of self-consistent field calculations have been extensively explained elsewhere¹⁸. We obtain both equilibrium density profiles for grafted and for free chains, as well as thermodynamic properties such as the free energy corresponding to an (imposed) thickness. By repeating the calculation for various thicknesses we can construct the entire free energy curve. Figure 5.4 shows a disjoining potential curve for various values of the thickness (d) of the free melt onto a brush.

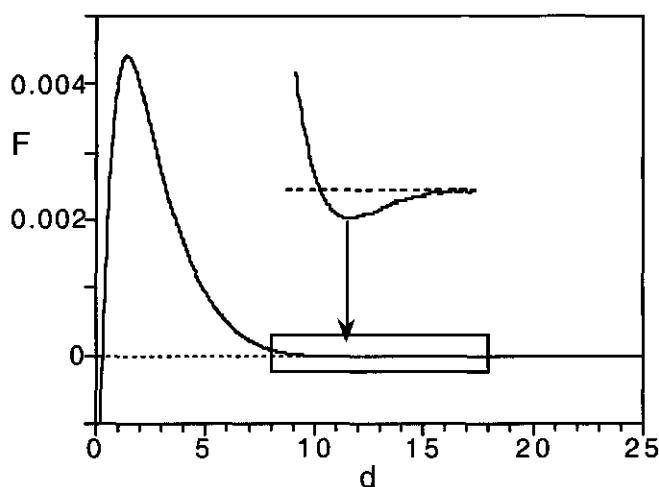


Figure 5.4 Disjoining potential calculations of a polymer melt (polymerization index 100) onto a brush (100 monomeric units, $\theta_{\text{graft}}=1.8$) as function of the thickness (d).

The disjoining potential and the thickness are both in arbitrary units. The pattern that emerges is quite remarkable: at low d , there is a deep primary minimum close to the surface, caused by the unfavourable contacts between free polymer and the substrate. The disjoining potential will go to infinity when d goes to 0 (not shown in figure 5.4).

When d is increased, the primary minimum becomes less deep, but at the same time, a shallow secondary minimum around $d=11$ develops, precisely as anticipated. With increasing grafting density, the primary minimum eventually vanishes, together with the secondary minimum; a monotonically decaying curve remains, corresponding to a stable macroscopic film (complete wetting).

How does the disjoining potential influence the patterns that develop on the surface? Consider a thermal height fluctuation on the surface (figure 5.5). Two possibilities are shown: a small dimple surrounded by a rim (a), or the reverse, a small elevation surrounded by a circular depression (b). If $F(d)$ is monotonically decreasing when d decreases, the dimple will grow and eventually form a hole. This is what happens in ordinary dewetting.

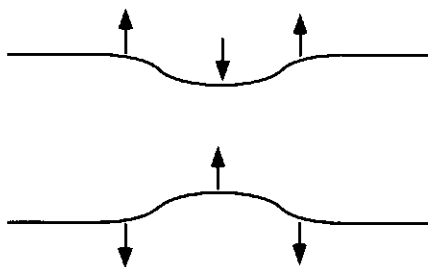


Figure 5.5 (a) ordinary dewetting and (b) secondary minimum

If, however, $F(d)$ decreases upon *thickening* of the film, a dimple (case b) will grow and a 'hill' forms, at the expense of the thickness of the remaining film. The 'hole + hill' structure seen in between these cases suggest that growth in both directions can occur, which implies that d lies initially in between the two minima.

4 Conclusions

In summary, we have experimentally measured a macroscopic droplet at equilibrium with two film thicknesses. In addition to the partial wetting (macroscopic droplet and thin film), a mesoscopic thick film is selected. When the prewetting step occurs at coexistence, there can indeed be a macroscopic droplet and two stable film thicknesses at equilibrium. We have seen this mesoscopic film in the dewetting behaviour of an PS film on top of a PS brush. The coexistence of the mesoscopic thickness suggests a double minimum in the disjoining potential. Self consistent field

calculations applied to this problem shows indeed a double minimum for the disjoining potential function.

References:

1. K. Ragil , J. Meunier, D. Broseta, J.O. Indekeu, D. Bonn, *Phys. Rev. Let.*, 77, 8 (1996), pp. 1532-1535
2. N. Shahidzadeh, D. Bonn, K. Ragil , D. Broseta, J. Meunier, *Phys. Rev. Let.*, 80, 18 (1998), pp. 3992-3995
3. N. Koneripalli, R. Levicky, F. Bates, M.W. Matsen, S.K. Satija, J. Ankner, H. Kaiser, *Macromolecules* , 31 (1998), pp. 3498
4. G. Reiter, *Langmuir*, 9,5 (1993), pp. 1344-1351
5. G. Reiter, *Phys. Rev. Let.*, 68, 1 (1992), pp. 75-78
6. T.G. Stange , D.F. Evans, *Langmuir*, 13 (1997), pp. 4459-4465
7. P.G. Ferreira, A. Ajdari, L. Leibler, *Macromolecules*, 31, 12 (1998), pp. 3994-4003
8. C. Gay, *Macromolecules*, 30, 19 (1997), pp. 5939
9. R. Yerushalmi-Rozen, J. Klein, L.J. Fetters, *Science*, 263 (1994), pp. 793-795
10. Y. Liu et al., *Phys. Rev. Let.*, 73, 3 (1994), pp. 440-443
11. O.A. Evers, Thesis, University of Wageningen (1990)
12. J.H. Maas, M.A. Cohen stuart, G.J. Fleer, submitted to thin solid films
13. O.A. Evers, J.M.H.M. Scheutjens, G.J. Fleer, *J. Chem. Soc. Faraday Trans*, 86 (1990), 1333-1341
14. C.M. Marques, J.F. Joanny, *Macromolecules*, 22 (1989), pp. 1454-1458
15. D. Guzonas, M.L. Hair, T. Cosgrove, *Macromolecules*, 25 (1992), pp. 2777-2779
16. J.O. Indekeu, K. Ragil , D. Bonn, D. Broseta, J. Meunier, *Journal of statistical physics*, 95, 5-6 (1999), pp. 1009-1043
17. K.R. Shull, *Faraday Discuss.*, 98 (1994)
18. G.J. Fleer, M.A. Cohen Stuart, J.M.H.M. Scheutjens, T. Cosgrove, B. Vincent, *Polymers at interfaces* (Chapman & Hall, London, 1993)

Chapter 6 Wetting of Dense Brushes: the role of entropy

abstract

A droplet of a polymer melt, placed on a chemically identical brush, has been studied experimentally. Upon Increasing the temperature, a brush of moderate grafting density ('soft' surface, $\sigma = 0.55\text{nm}^{-2}$) showed an increase of the contact angle of the polymer droplet. A very dense brush ('hard' surface, $\sigma = 0.95\text{nm}^{-2}$) showed no effect on the contact angle when the temperature was changed. The wetting behaviour of a polymeric melt on a brush can also be tuned by using a bimodal brush, i.e., a brush with chains of two different lengths, long (200 monomers) and short (20 monomers). Grafting a small fraction of long chains in a brush consisting of short majority chains increases wetting. At higher grafting densities of the long chains, the brush exhibit autophobic behaviour and the contact angle starts to increase due to the expulsion of the free melt out of the brush.

1. Introduction

When a (polymer) liquid is placed on a substrate, two different equilibrium situations can be found. These thermodynamic equilibrium states are denoted as partial and complete wetting. Complete wetting refers to the situation when the substrate is wetted by the liquid and the contact angle is zero. In partial wetting the (polymer) liquid only partially covers the surface, and droplets of liquid remain on the substrate with a finite contact angle. The larger the contact angle, the stronger the partial wetting behaviour. The contact angle is determined by three interfacial tensions: the liquid-vapour surface tension (γ_{lv}), the liquid-solid interfacial tension (γ_{sl}) and the solid-vapour interfacial tension (γ_{sv}). According to the Young-Dupré equation, the contact angle δ is given by:

$$\cos \delta = \frac{\gamma_{sv} - \gamma_{sl}}{\gamma_{lv}} \quad (6.1)$$

Surfaces with low γ_{sv} values have in general a high contact angle and therefore a poor wettability. On surfaces with high γ_{sv} , the contact angle is small. Liquids with low γ_{lv} values have a tendency to spread over the surface whereas liquids with a high γ_{lv} do not spread.

A special but interesting case is the wetting of a surface carrying densely grafted chains (a brush) by a melt liquid of chemically identical. If the brush is dense enough, the only contact between liquid and substrate is between equal polymer moieties. Hence, the energy does not affect the wettability, and the behaviour is governed by the entropy. In order to study these entropic effects we focus two influences on the wettability: (i) the effect of the temperature on the contact angle of a melt droplet on a dense brush and (ii) the effect of the length distribution of the grafted polymer.

2. Brush preparation

Various methods can be used for the preparation of a polymer brush. One method that is often used is the adsorption of block copolymers onto surfaces from solution or from polymer melts¹⁻³. The use of monodisperse block copolymers will result in a

brush which is monodisperse, with an adsorbed amount which depends on the composition of the block copolymer³⁻⁵.

Chemical grafting is another way to prepare brushes. Two different grafting techniques are often used. The first is grafting *from* a surface with reaction initiators covalently attached to the surface and reactive monomers present in solution. The brushes prepared in this way are not monodisperse, but the thickness of the brushes that can be obtained by this method is very large (of the order of microns)⁶⁻⁸.

The second chemical grafting technique is grafting *to* the surface. In this method one employs a polymer with a reactive (end) group, which react with a complementary group on the surface. Using monodisperse polymers one obtains uniform and monodisperse brushes⁹.

In the present study we have used the latter method for the preparation of monodisperse polystyrene brushes. The polymers used are two vinyl terminated polystyrene (PS₂₀ and PS₂₀₀). The subscript denotes the number of monomers in the polymer chains.

The maximum grafting density (σ) of the PS₂₀ layer which can be reached is 0.95 nm⁻² and for the PS₂₀₀ polymer 0.55 nm⁻². A detailed experimental report is given in chapter 3⁹. The procedure of chemical grafting using a polymer melt always resulted in homogeneous and reproducible brushes, as determined by AFM and water contact angle measurements. These PS brushes were used as substrate for a PS droplet.

3. Temperature effect

In general, the surface tensions of liquids vary nearly linearly with the temperature far below the critical temperature T_c . For polymers, the critical temperature is typically 600-900 °C. The surface tension decreases with increasing temperature. For most liquids on simple surfaces, the contact angle of a droplet is also a decreasing function of the temperature.

To investigate the temperature dependence of the contact angle of a droplet of a polymer melt onto a polymer brush we start with the Young-Dupré relation. Differentiating of equation (6.1) with respect to T gives

$$\frac{d \cos \delta}{dT} = \frac{1}{\gamma_{lv}} \left\{ \frac{d\gamma_{sv}}{dT} - \frac{d\gamma_{sl}}{dT} - \cos \delta \frac{d\gamma_{lv}}{dT} \right\} \quad (6.2)$$

According to classical thermodynamics $d\gamma/dT$ can be related to the excess interfacial entropy S^σ :

$$-\frac{d\gamma_{sv}}{dT} = S_{sv}^\sigma \quad -\frac{d\gamma_{sl}}{dT} = S_{sl}^\sigma \quad -\frac{d\gamma_{lv}}{dT} = S_{lv}^\sigma \quad (6.3)$$

Equations 6.2 and 6.3 can be combined to an expression for the temperature dependence of the contact angle as function of the temperature in terms of excess entropies:

$$\gamma_{lv} \frac{d \cos \delta}{dT} = -S_{sv}^\sigma + S_{sl}^\sigma + S_{lv}^\sigma \cos \delta \quad (6.4)$$

3.1. Experimental

3.2. Brush preparation

Pieces of a silicon wafer were etched for 2 min in HF (2.5%) to remove the native oxide layer, blown dry with nitrogen, and immediately covered with a solution of the vinyl-terminated PS in CHCl_3 (14 g/l). In this study we use two polymers of different length, denoted as PS₂₀ and PS₂₀₀ (2 and 20 kg/mole, respectively). After evaporation of the solvent a film of the polymer remained on the surface. The samples were heated for 24 h at 145 °C in vacuo in order for the grafting reaction to occur. All non-grafted excess material was subsequently removed by washing three times with fresh solvent. A detailed experimental account is given in chapter 3⁹.

3.3. Sample preparation

A grain of low molar mass PS (M_n 6000 g/mole) was placed on the brush and from above observed with a optical microscope (Olympus BX60). For heating the sample, we used a specially designed covered hot stage so that the sample could be kept in an oxygen-free atmosphere. The system was annealed at elevated temperatures until equilibrium was reached. The change in the shape of the droplet after a temperature change was followed using a CCD camera (Sony DXC 151AP) and a video printer. Image analysis was performed on a Macintosh computer using the public domain NIH Image program¹⁴. It is important that the relaxation towards equilibrium takes place in

a oxygen free atmosphere, because at elevated temperatures oxygen will lead to a variety of undesired reactions.

Figure 6.1a shows an optical microscopy image of a droplet in an inert atmosphere. As can be seen the droplet is almost circular and the contact line with the brush is sharp. The same experiment done in air resulted in an image as shown in figure 6.1b. The shape of the contact line is not sharp and fingering instabilities can be observed. In this case the moving contact line is clearly unstable.



Figure 6.1. Optical microscopy images of a PS droplet ($M_n = 6000$ g/mole) on a PS_{200} brush measured in (a) an inert atmosphere and (b) in air. Image size 15×11 mm².

3.4. Results and discussion

Figure 6.2 shows the diameter of a drop of PS as a function of time in an inert atmosphere. The temperature was initially set to 120 °C, then increased to 200 °C (after 90 hr), and finally (after 150 hr) decreased back to 120 °C. As can be seen, the diameter of the droplet on a PS_{200} brush increases gradually until it reaches a (thermodynamic) equilibrium situation at 120 °C (≈ 90 h). Changing the temperature to 200 °C causes a decrease in the diameter of the droplet, as show in more detail in the bottom graph of figure 6.2.

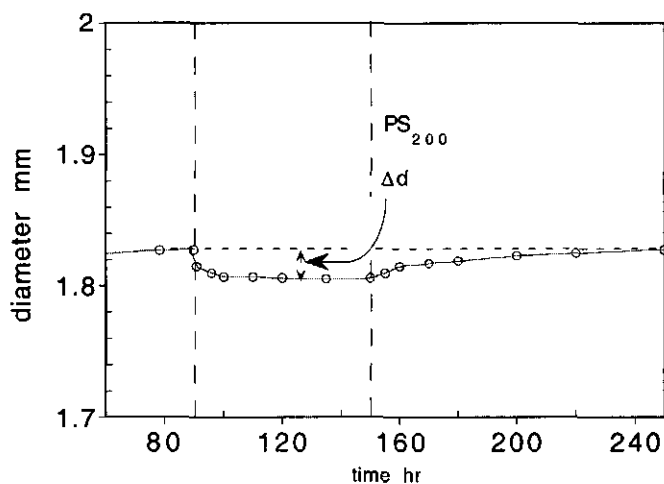
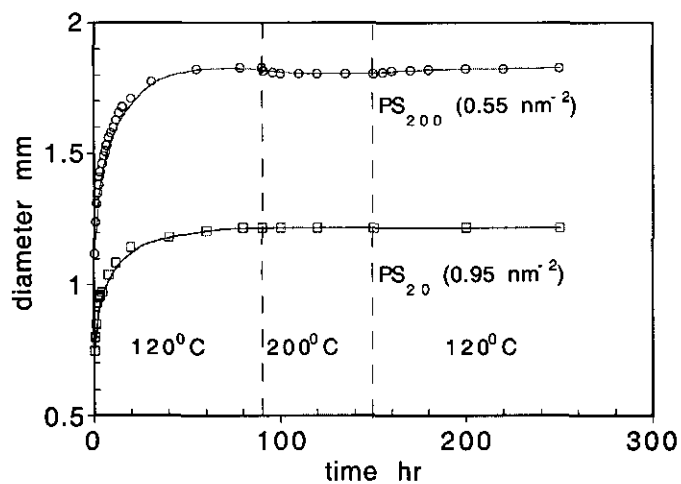


Figure 6.2. Diameter of a PS droplet ($M_n = 6000$) on a PS₂₀₀ brush and PS₂₀ brush as function of temperature and time (top figure). The vertical lines separate temperature regions, as indicated. The bottom figure is a magnification of the PS₂₀₀ graph.

This corresponds to an increase of the contact angle. Upon decreasing the temperature back to the initial value, one sees again an increase in the diameter of the droplet back to the original size. Hence, it seems that the wettability of a polymer droplet on this brush is reversible, and probably thermodynamically controlled. The same experiment was performed for a polymer droplet on a PS₂₀ brush. Again, the diameter increased gradually until it reaches the equilibrium state at 120 °C after approximately 90 h. However, upon heating the sample upto 200 °C there was no change in the diameter of the droplet. Cooling down from 200 °C to 120 °C did not produce any difference in diameter either.

From the change $dR/dT \approx \Delta R/\Delta T$ of the radius R with temperature, it is possible to find $d \cos \delta / dT$ using geometrical arguments (see figure 6.3).

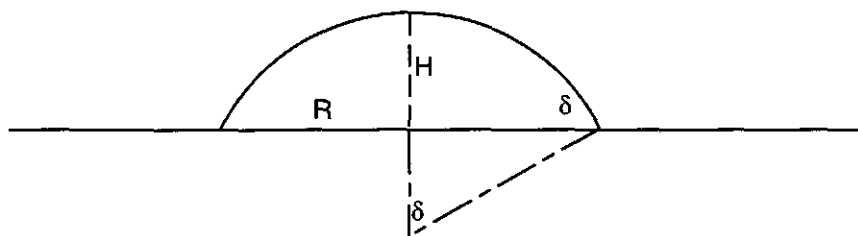


Figure 6.3. Geometry of a drop.

We consider the drop as a section of a sphere of radius r . When the drop height is H , the drop volume V is given by $\pi H^2(r - H/2)$. Using $R = r \sin \delta$ and $H = r(1 - \cos \delta)$, this may be written in terms of R and δ only:

$$V = \pi R^3 \frac{(1 - \cos \delta)^2 \sin \delta - \frac{1}{3}(1 - \cos \delta)^3}{\sin^3 \delta} \approx \frac{\pi R^3 \delta^2}{4} \quad (6.5)$$

The last version is the expansion for low δ . If we neglect thermal expansion of the drop, $dV/dT = 0$ or $2Rd\delta/dT = -3\delta dR/dT$. With $d\cos\delta = -\sin\delta d\delta \approx \delta d\delta$, we arrive at

$$\frac{d\cos\delta}{dT} = \frac{3}{2R} \frac{dR}{dT} \quad (6.6)$$

The values of $\gamma_{lv} (= 32.1 \cdot 10^{-3} \text{ Nm}^{-1})$ and $d\gamma_{lv}/dT (= -6.5 \cdot 10^{-5} \text{ Nm}^{-1}\text{K}^{-1})$ were taken from published data¹⁵. In this way we obtain $\gamma_{lv} d\cos\delta/dT = 6.6 \cdot 10^{-6} \text{ Nm}^{-1}\text{K}^{-1}$ and $S_{lv}^{\sigma} \cos\delta \approx S_{lv}^{\sigma} = -d\gamma_{lv}/dT = 6.5 \cdot 10^{-5} \text{ Nm}^{-1}\text{K}^{-1}$. From equation (6.4) we get for S_{sv}^{σ} - $S_{sl}^{\sigma} = 5.8 \cdot 10^{-5} \text{ Nm}^{-1}\text{K}^{-1}$. This result shows that the difference in excess interfacial entropy between the brush-vapour and the brush-melt is nearly equal to that of the free surface of the melt. Probably, S_{sv}^{σ} is comparable to S_{lv}^{σ} , so that S_{sl}^{σ} must be very small. In fact, it is likely that S_{sv}^{σ} is smaller than S_{lv}^{σ} (because the brush is constrained). This leads to the conclusion that S_{sl}^{σ} must be negative. Nevertheless, this small excess entropy is probably the reason that we experimentally observe a decrease of the contact area of the droplet at increasing temperature. Increasing the grafting density results in an even smaller difference in excess interfacial entropy between the brush-vapour and the brush-melt; at sufficiently high grafting densities no effect is visible anymore (see the curve for PS₂₀ in figure 6.2). We interpret this as follows. For the surface with a grafting density of 0.55 nm^{-2} the surface is 'soft' and free polymer chains can partially mix with the brush. Increasing the temperature results in an expulsion of the free polymer out of the brush leading to an increase of the sl interfacial tension. For the PS₂₀ brush, the interface between the brush and melt is already sharp and the surface is 'hard'. No free polymer is present in the brush. Increasing the temperature will in this case not result in a expulsion of the free chains from the brush. Our experiments prove that, at increased temperature, the contraction of a droplet on a brush only takes place at 'soft' brushes where some interpenetration occurs (at low T).

The number of chains per unit area of a PS₂₀ brush ($1.0 \text{ nm}^2/\text{chain}$) is 1.8 times the number of chains of a PS₂₀₀ brush ($1.8 \text{ nm}^2/\text{chain}$). The PS₂₀ brush is very dense and the free polymer melt does not mix with the brush chains. The contact angle of the PS

on the PS₂₀ brush is 23°, much higher than the 4° for PS₂₀₀ and comparable with the contact angle of a PS droplet on glass¹⁶.

Recently the temperature dependence of the contact angle of a melt of free on attached chains of polydimethylsiloxane was reported¹⁷. In this report the authors assume that the melt and the brush have about the same surface tension, and they also find a negative excess entropy for the brush/melt surface, which is attributed to the thermal expansion. This is not very likely. There must be a difference between the two surface tensions of the melt and the brush for reasons of conformational freedom: the free chains are Gaussian and the attached chains are stretched. Unfortunately, the fact that the substrate is a solid prohibits the direct measurements of the tensions and excess entropies of the sv and sl interfaces. Yet, it seems likely that the sl interface has a negative excess entropy, which is a rather unusual situation. Density gradients, which are responsible for a higher entropy at lv interfaces, plays no role here. The negative entropy at the brush/melt interface is probably related to the demixing of brush and melt chains.

4. Bimodal brushes

4.1. Preparation of bimodal brushes

A silicon wafer was etched for 2 min in HF (2.5%), blown dry with nitrogen and immediately covered with a solution containing two different vinyl-terminated polystyrenes in a specific ratio varying from 0 upto 100% PS₂₀₀ in CHCl₃. The total concentration of the mixture of polymers (PS₂₀ + PS₂₀₀) was 1mg/ml. The system was annealed for 24 h at 145 °C in vacuo. Excess material was removed thoroughly by washing three times with fresh solvent. A detailed experimental report is published elsewhere⁹.

4.2 Overlayer on bimodal brushes

The overlayers on the brushes were spin-coated from chloroform at 3000 rpm and different concentrations (1-5 mg/ml), depending on the desired thickness of the overlayer. The thickness of the dry polymer layer was determined by computer-

controlled null ellipsometry (Sentech SE-400). The refractive index for $\lambda = 632.8$ nm was taken as 1.58¹³. The AFM measurements were performed with a Digital Instruments Nanoscope III AFM equipped with a scanner capable of scanning an area of 100 μm^2 . All AFM measurements were performed in air at room temperature and a relative humidity level of 50-60%. Commercially available tapping mode tips were used on cantilevers with a resonance frequency in the range of 350 -400 kHz. The treated surfaces were stored at 145 °C in vacuo.

4.3 Wetting of bimodal brushes

A system with a combination of small chains and long chains grafted onto a solid surface can be considered as a system with two interfaces. One interface is at a distance from the surface equal to the thickness of the small chains and the other interface is the brush-vapour interface (see figure 6.4). The grafting density of the small chains is high so that, in the absence of long chains, autophobic behaviour occurs. Since contacts other than those between like chains do not occur, wetting experiments on these bimodal brushes are again entirely dictated by entropic effects.



Figure 6.4. Schematic representation of a bimodal brush onto a solid surface. The location of the new interface is indicated with an arrow.

Using the chemical grafting method we can make dense brushes with an autophobic behaviour, where the chains molecules are not compatible and will not mix, despite the fact that they consist of identical segments¹⁸⁻²³. Since there is no direct way to determine the long/short composition of the grafted layer, we assume that a ratio of the two polymers in the brush is the same as that in the initial chloroform solution from which the brush was made. In the melt the ratio of reactive end groups near the surface will probably not change very much compared to that in the bulk. When the

reaction is performed in solution the situation is totally different. Small molecules can move much faster in a liquid so there will be relatively more small molecules available at the surface.

The question is now whether we can improve the wettability of a PS film on a very dense brush by using a bimodal length distribution. Figure 6.5 shows 3 representative images (a-c) obtained for PS films with $M_n = 183$ kg/mole on brushes with an increasing ratio of PS_{200} / PS_{20} . In figure 6.5a, only 2 % of the grafted chains consist of PS_{200} , the rest is PS_{20} . The overlayer of 5 nm PS dewets the surface. Increasing the amount of PS_{200} to 5 % free PS wets the surface (figure 6.5b). The few PS_{200} chains in the brush are responsible for a fluffy interface and an increased tendency of the grafted and free chains to mix. At 60 % of PS_{200} the free PS dewets the surface again, but now due to the expulsion of the PS from the grafted layer (figure 6.5c). These results demonstrate that the complete wetting window in the phase diagram can be considerably increased by using a bimodal brush. The same result can probably be obtained by using a bimodal mixture for the free polymer or with a combination of a polydisperse brush and a polydisperse melt, but we do have no data to illustrate this.

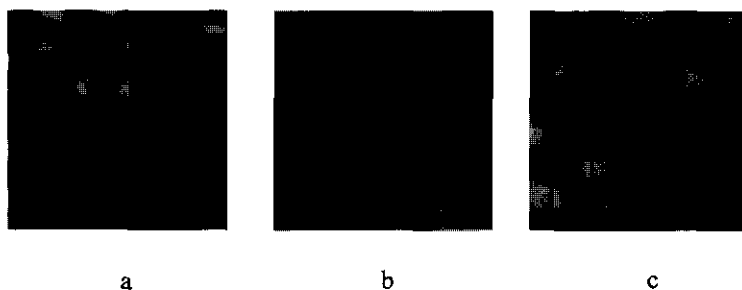


Figure 6.5. Wetting behaviour of a PS film (5nm) on a brush consisting of PS_{20} and (a) 2% $(PS)_{200}$, (b) 5% $(PS)_{200}$, and (c) 60% $(PS)_{200}$.

5. Conclusions

We have investigated droplets of polystyrene on a polystyrene brush to determine the temperature dependence of the wetting. At high grafting densities ($\approx 1 \text{ chain/nm}^2$) of relatively short chains the brush can be considered as a 'hard', impenetrable solid surface. A film of PS will dewet under formation of droplets with a specific contact angle when annealed above the T_g of the polymer. For a 'hard' surface, the contact angle is virtually independent of the temperature. A 'soft' surface is obtained with longer brush chains at a lower grafting density ($\approx 0.5 \text{ chain/nm}^2$). With such a substrate, increasing the temperature of a droplet of PS gives an *increase* of the contact angle. Finally, experiments with bimodal brushes show that a few percent of long chains added to a surface covered with small brush hairs strongly promotes the wettability of the brush.

references

1. Reiter G., Sharma A., Casoli A., David M-O.Khanna R., Auroy P., *Langmuir*, 15, 1999, 2551-2558
2. Watanabe H, Tirrell M., *Macromolecules*, 26, 1993, 6455
3. J.H. Maas, M.A. Cohen Stuart, G.J. Fleer, *Thin Solid Films*, 358, 2000, 234-240
4. Tauton H.J., Toprakcioglu C., Fetters L.J., Klein J., *Macromolecules*, 23, 1990, 571
5. Marques, C.M., Joanny, J.F., Leibler, I., *Macromolecules*, 21, 1988, 1051
6. Prucker O., R  he J. *Macromolecules*, 31, 3, 1998, 592-601
7. Prucker O., R  he J. *Macromolecules*, 31, 3, 1998, 602-613
8. Prucker O., Naumann C.A., R  he J., Knoll W., Frank C.W., *J. Am. Chem. Soc.*, 121, 38, 1999; 8766-8770
9. J.H. Maas, M.A. Cohen Stuart, A.B. Sieval, H. Zuilhof, E.J.R. Sudh  lter, submitted to thin solid films
10. P.G. de Gennes, *Macromolecules*, 13, 1980, 1069
11. M. Aubouy, G.H. Frederickson, P. Pincus, E. Rapha  l, *Macromolecules*, 28, 1995, 2979
12. G. Reiter, R. Khanna, *Langmuir*, 16, 2000, 6351
13. N. Koneripalli, R. Levicky, F. Bates, M.W. Matsen, S.K. Satija, J. Ankner, H. Kaiser, *Macromolecules*, 31, 1998, 3498
14. developed at the U.S. National Institutes of Health and available on the Internet at <http://rsb.info.nih.gov/nih-image/>.
15. S. Wu, *Polymer Interface and Adhesion*, Marcel Dekker, New York, 1982
16. G. Reiter, *Langmuir*, 9, 5, 1993, 1344-1351
17. G. Reiter, R. Khanna, *Phys. Rev. Lett.*, 85, 26, 2000, 5599
18. P.G. Ferreira, A. Ajdari, L. Leibler, *Macromolecules*, 31, 12, 1998, 3994-4003
19. C. Gay, *Macromolecules*, 30, 19, 1997, 5939
20. R. Yerushalmi-Rozen, J. Klein, L.J. Fetters, *Science*, 263, 1994, 793-795
21. Y. Liu et al., *Phys. Rev. Lett.*, 73, 3, 1994, 440-443

22. T. Kerle, R. Yerushalmi-Rozen, J. Klein, L.J. Fetters, *Macromolecules*, 31, 1998, 422-429
23. G. Reiter, P. Auroy, L. Auvray, *Macromolecules*, 29, 1996, 2150-2157

Chapter 7 Thin block copolymers films: corrugation under the AFM tip

Abstract

The tip of an atomic force microscope was used to induce nanoscale ordering in thin films of polystyrene-poly(4-vinyl pyridine) block copolymers under low force. The AFM tip produces rims on a mesoscopic scale oriented perpendicularly to the scanning direction. A wide range of molecular weights of both blocks was investigated and it was found that after two scans and at constant polymer length there is a linear relationship between the fraction polystyrene in the polymer and the average separation between two successive rims. Scanning the area in between two rims showed that there is no polymer left on the surface. This is an indication that the mobility of the poly(4-vinylpyridine) anchor blocks is high during sliding of the tip.

1. Introduction

Atomic force microscopy (AFM) has evolved during the last decade to probe surface properties at a nanometer scale. AFM can be used to probe hard materials¹ and soft materials such as proteins² and polymer surfaces^{1,3-7}. Since the AFM tip, in the contact mode, is in contact with the surface, the tip will have an interaction with the surface. The tip-sample interaction can provide deformation of the sample. It can also cause movement of material, accumulations or dragging it around, which results in an image of low quality. This tip-sample interaction can also be used to manipulate the surface. By scanning the surface repeatedly, structures are sometimes formed that are oriented perpendicularly to the scanning direction of the tip. Tip-induced ordering of polymer surfaces forming structures perpendicular to the scanning direction have been reported for polystyrene⁸, poly(methyl methacrylate)⁹, poly(phenylene oxide)⁹ and proteins²

In this chapter we specifically investigate polystyrene-poly(4-vinylpyridine) (PS/PVP) copolymer films made by adsorption onto flat silica surfaces. Two preparation procedures are tested, namely adsorption from solution and adsorption from a polymer melt. We investigate how the films behave when the AFM tip is used to scan the surface of the adsorbed block copolymers. The effect of the molecular weight and the fraction PVP on the periodicity of the rims were investigated.

2 Experimental

Polystyrene-poly(4-vinylpyridine) (PS/PVP) polymers with different block lengths and a polydispersity index < 1.2 were adsorbed on silica wafers from solution or from a polymer melt. The AFM measurements were performed with a Digital Instruments Nanoscope III AFM equipped with a scanner capable of scanning an area of $12\mu\text{m}^2$. All measurements were performed in air at room temperature and a relative humidity level of 50-60%. Commercially available Si_3N_4 tips were used on cantilevers with a spring constant of approximately 0.58 N/m. A detailed experimental section is described in chapter 2¹⁰.

3 Results and discussion

The various adsorbed layers were subjected to repeated scanning with AFM tips (contact mode), fixing the load force at 10^{-9} N. After the second scan, we observed the formation of distinct rims oriented perpendicularly to the scanning direction. Rotating the scan direction after rim formation resulted also in the rotation of the rims. Both preparation methods gave the same results. Figure 7.1 shows a set of images captured in the second scan for two samples of the polymer. In the height image, the sample surface is seen as pattern with alternating bright and dark regions. The bright bands can be assigned to the polymer rims and the darker patches are depressed regions. The difference in height between the bright and dark areas is 10 nm. It is obvious that there is a huge difference in the average rim distance between samples 48/21 and 193/21.

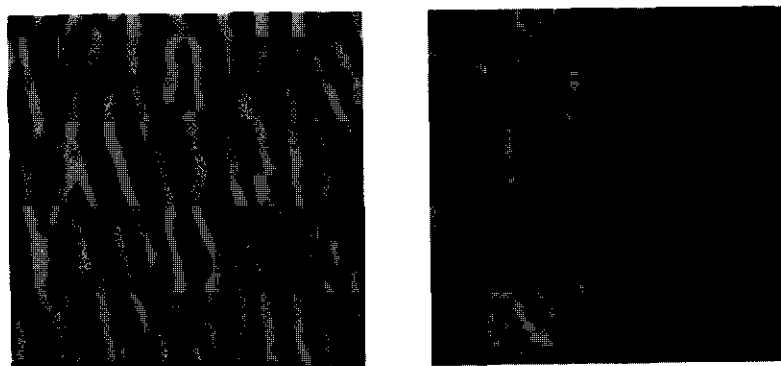


Figure 7.1. Surface images of dip-coated PS/PVP (from 100 ppm in chloroform) onto silica, captured after the second scan, for PS/PVP 48/21 (left) and 194/21 (right). Area $3 \times 3 \mu\text{m}^2$, height distance 10 nm.

The average distance between the rims is not only a function of the fraction PS in the polymer but depends also on the total length of the polymer. The development of the surface structures upon scanning is irreversible: they do not relax even over several months.

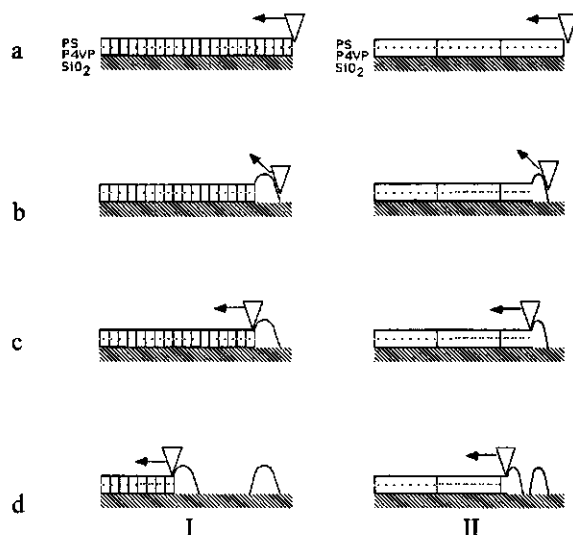


Figure 7.2. Schematic representation of block copolymer films onto silica scanned by AFM in the contact mode. The left side hand (I) refers to block copolymers with a small anchor block, the right hand side (II) to a large anchor block. From top to bottom: (a) the tip starts collecting material, (b) the stress at the tip increases and the tip jumps over, (c) the process starts again, (d) the tip has jumped over the second rim.

The following scenario for the rim formation seems plausible. While scanning over the polymer surface, the cantilever tip exerts a frictional force on individual molecules. The adhesion of the polymer onto the tip combined with the applied force results in an accumulation of material in front of the tip. The total amount of polymer will increase until the tip-polymer adhesion reaches a critical level. As the tip collects more polymer, more and more adsorbed blocks are dragged over the substrate. Hence, the frictional force between the PVP anchor blocks and the surface increases, and as the tip provides a limited area for adhesion, the stress at the tip will go up. At a certain critical stress, the adhesive contact between the tip and the accumulated polymer breaks and the tip jumps forward, leaving the collected polymer behind (figure 7.2a-d).

This process is then repeated, leading to the periodic structure that we observe. As the anchors become shorter, the friction is less, and more polymer can be accumulated before the tip detaches. Hence, the distance between rims increases as the anchor block becomes shorter.

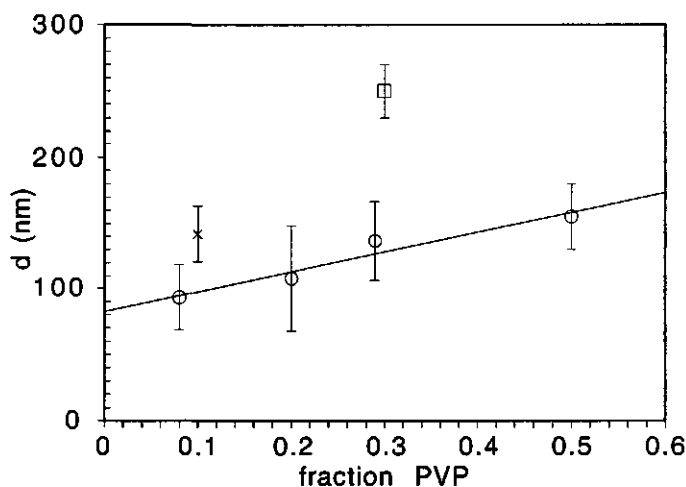


Figure 7.3. Average rim distance as function of the fraction PS after two scans. Circles: $M_n \approx 40$ kg/mole, square $M_n = 69$ kg/mole, cross $M_n = 216$ kg/mole.

Scratching the corrugated film and scanning the scratch in the tapping mode shows that there is no PVP left in the regions between two rims. This is an indication that the entire film is pulled off from the surface by the AFM tip. The effect of the anchor block size at given molar mass ($M_n \approx 40$ kg/mole) and of the total chain length is shown in figure 7.3. Comparing polymers with the same fraction PS and different total length shows an increase of the average rim distance with molar mass. Plotting the average rim distance as function of PVP fraction at constant length of the polymer gives a linear relationship. The points and error bars in figure 7.3 were comparable for both the spin coating and the dip treatment and are obtained by averaging nine profiles

from various samples. Scanning the block copolymer with a very high fraction PVP (0.94) showed no rim formation during the first scans due to the relatively hard PVP.

Films stored at room temperature for over three months before scanning exhibited the same structures as freshly prepared samples, but the number of scans needed to get the same average rim distance had to be increased. To rule out the possibility of residual solvent effects in the film, films were stored in vacuo before AFM imaging. These samples gave the same results after AFM imaging. The aging effect mentioned above thus indicates some relaxation in the polymer film over a long period. The rim formation in freshly prepared films continues when the number of scans is increased, forming less and larger rims. Figure 7.4 shows a small region in the centre which was scanned for 30 min; few and very large rims can be seen. A larger area was then scanned twice; here distinct oriented rims were formed. Finally, the overall picture was captured by a single scan, which gives a featureless homogeneous film.

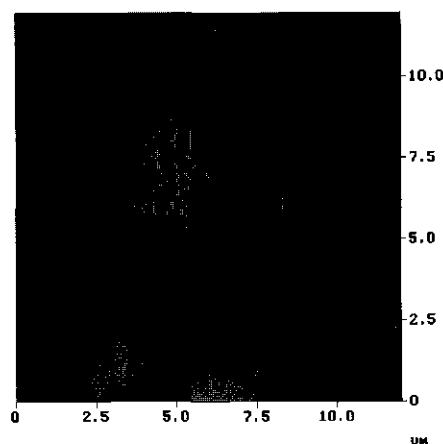


Figure 7.4. Image of PS/PVP (48/21) A small region of $3 \times 3 \mu\text{m}^2$ in the centre was scanned for 30 min. A larger area of $6 \times 6 \mu\text{m}^2$ was scanned twice and finally, an area of $12 \times 12 \mu\text{m}^2$ was scanned just once. Thickness of the film 1.9 nm, height difference 10 nm and the scanning direction is from left to right.

Scratching the film with the AFM tip with high force and high frequency showed once more that between two rims no polymer was left. This observation suggests that the adsorbed PVP blocks can be dragged over the surface fairly easily, even though hydrogen bonds are expected to contribute to the adhesion. These experiments conclusively show that adsorbed polymer can be swept into rims over a silica surface. Even when no solvent is present, the polymer chains are to some extent mobile, despite the strong adhesion of the anchor block onto the surface.

4 Conclusions

We have studied the adsorption of PS/PVP block copolymers from a non-selective solvent and from a polymer melt on a flat silica surface and examined the films with AFM. We have shown that films of PS/PVP are swept into rims of aggregates oriented perpendicularly to the scanning direction of the AFM tip. The average rim distance, as observed after the second scan, shows a linear dependence on the fraction PVP (at constant total polymer length). In between the rims, there is no PVP left on the surface. Our data suggest that the AFM tip can be used to manipulate polymer molecules and other soft surfaces, so that designed patterns could be obtained.

References

- 1 M.C. Goh, *Advances in chemical physics*, vol. XCI, 1995
- 2 A.S. Lea, A. Pungor, V. Hlady, J.D. Andrade, J.N. Herron, E.W. Voss, *Langmuir*, 8, 1992, 68.
- 3 S.S. Sheiko, *Advances in polymer science*, vol. 151, 2000
- 4 T. Bouhacina, J.P. Aime, S. Gauthier, D. Michel, *Physical Review B*, 56, 12, 1997
- 5 J.P. Peng, G.T. Barnes, *Thin Solid Films*, 284-285, 1996, 444-449
- 6 R. Kaneko, E. Hamada, *Wear*, 162-164, 1993, 370-377
- 7 A. Wawkuszewski, H.J. Cantow, S.N. Magonov, *Advanced Materials*, 6(6), 1994
- 8 O.M. Leung, M.C. Goh, *Science*, 255, 1992, 64.
- 9 J.C. Brumfield, C.A. Goss, E.A. Irene, R.W. Murray, *Langmuir*, 8, 1992, 2810
- 10 J.H. Maas, M.A. Cohen Stuart, G.J. Fleer, *Thin Solid Films*, 358, 2000, 234-240

Chapter 8 Other Block Copolymers as Wetting Agents

Abstract

In this chapter we describe experimental observations obtained with block copolymers and the wetting behaviour of polymer overlayers. The chapter is divided in three sections. The first section deals with triblock copolymers as wettability modifiers for the silicon oxide surface and the wetting properties of these brushes. In the second section, the adsorption and wetting behaviour of a diblock copolymer consisting of a polystyrene block and a poly(propylene imine) dendrimer is described. The last section deals with polycaprolacton (PCL) layers on polycaprolactone-poly-2-vinylpyridine (PCL/PVP) polymers. PCL is compatible with polyesters used in commercial powder coatings and therefore of interest for the stabilisation of pigment particles.

Section 1.

1.1 Experimental

A PVP/PS/PVP triblock copolymer was used in which each end group consisted of 80 4-vinylpyridine units and which had a middle block of 500 styrene monomers. Thick layers (~50 nm) of this triblock copolymer were spin-cast from solution (chloroform, 10g/l) onto silica wafers. The samples were after spin-coating treated in two different ways: (i) the samples were immediately washed with chloroform and used for the experiments or (ii) stored overnight at 145 °C in vacuo, then cooled down to room temperature, after which the non-attached material was removed by washing with chloroform. The thickness of the triblock layer obtained by both methods was 3.5 nm. PVP or PS of varying molar mass was spincoated from chloroform (1 mg/ml, 3000 rpm) over the block copolymer films and subsequently stored at 145 °C in vacuo. After 12 days the surface topography of the top films, which are on average 5 nm thick, was investigated by means of AFM.

1.2 Wetting behaviour of a PVP/PS/PVP triblock copolymer

The wetting behaviour of the techniques (i) and (ii) is totally different, as can be seen from figure 8.1.

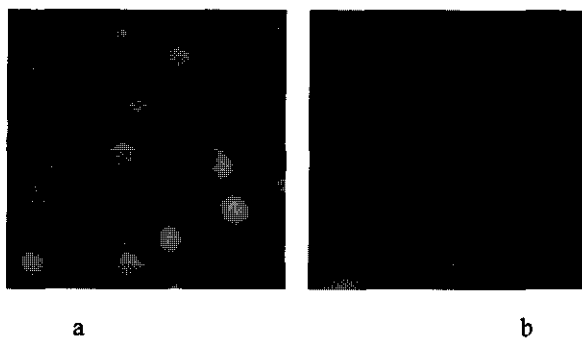


Figure 8.1. Wetting behaviour of a ps film on a PS/PVP/PS triblok copolymer after annealing for 12 days at 145 °C. In diagram (a) the triblock polymer was prepared by method (I) and in diagram (b) the triblock copolymer was prepared by method (ii). brush not annealed. Image size 10*10 μm , bright areas are elevated and dark patches are depressed regions.

The annealed Brush (ii) shows complete wetting, whereas that on the non-annealed triblock copolymer (i) shows dewetting of the PS film in the form of small droplets. The most outstanding feature in figure 8.1a are the needle like structures which can be seen in between the droplets of PS. These needles are 3 nm in height and several μm in length. A remarkable observation was made when using different molar masses of the free PS. With low molar mass PS the needles are very long and sometimes branched. Increasing the molar mass showed a decrease in the number of needles per unit area and a decrease in the length of the needles (see figure 8.2). At higher molar mass the needles were first isolated and upon increasing the molar mass even further, the needles eventually disappeared altogether.

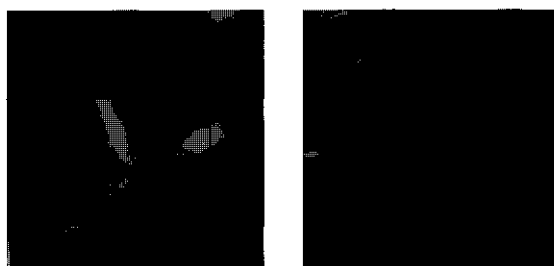


Figure 8.2. Images of PVP/PS/PVP spincast from solution (method (i)) and immediately covered with (left) PS 6 kg/mole and (right) PS 10^3 kg/mole, after annealing at elevated temperatures. Image size $2 \times 2 \mu\text{m}$, the bright areas are elevated and dark patches are depressed regions.

In order to investigate whether the needles consist of PS or PVP, the samples were probed with scanning electron microscopy (SEM). These experiments were performed after the samples were exposed to iodide vapour for 10 min. Iodide reacts with VP and in this way it may help to distinguish between VP and PS. Unfortunately, the resolution of the SEM was not high enough to see the contrast.

The difference in wetting behaviour is probably due to the fact that during the spin-coating process polymers adsorb onto the surface in a random fashion. Using a

triblock copolymer with two adsorbing blocks it is likely that most chains are only adsorbed by one end block rather than by two, as depicted in figure 8.3a.

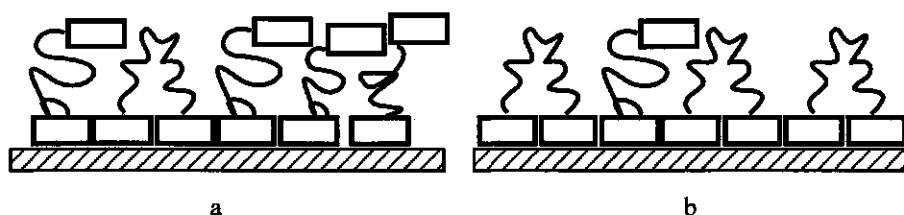


Figure 8.3 Schematically representation of PVP/PS/PVP onto the substrate without (a) annealing and after annealing (b).

During the annealing treatment of the sample, the non adsorbed PVP blocks are mobile and can adopt a conformation onto the surface, such that both ends are adsorbed and loops of PS are formed (figure 8.3b). The layer which has not been annealed must thus have PVP surface properties. This is confirmed by the following test. Spincoating a 5 nm thick film of PVP on the adsorbed layer (method (i)) and annealing shows patches which are wetted and areas where dewetting has occurred, as can be seen in figure 8.4a. The same experiment done for a brush which has been annealed showed ordinary dewetting (figure 8.4b).

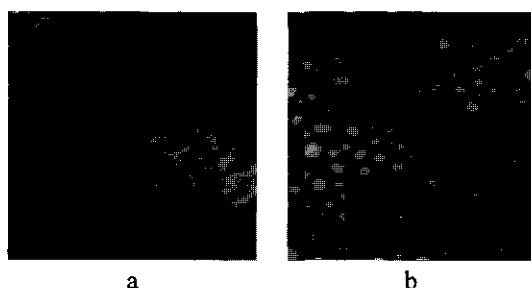


Figure 8.4. As figure 8.1 but now with a PVP layer ($M_n = 240$ kg/mole).

It is tempting to conclude that the unannealed triblock layer covered with PS somehow organises upon treatment at 145 °C such that it develops linear strips where PS loops

swollen with short PS chains occur. Why these strips are so surprisingly straight is presently unexplained.

Another interesting observation was a triblock copolymer overlayer on a PS₂₀ brush (see chapter 3) as the substrate. Spincoating a 5 nm thick PVP/PS/PVP layer on this brush shows a homogeneous flat film. After annealing the system, the film properties changed. Figure 8.5 shows an image of a PVP/PS/PVP layer after annealing and quenching to room temperature before imaging. As can be seen, circular structures are formed with a height of 15 nm or multiple thereof. The origin of these structures is unknown, and could be understood only after systematic investigations, which were not carried out.

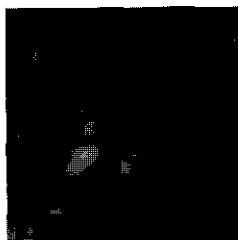


Figure 8.5. AFM image of a initial 5 nm PVP/PS/PVP layer on a PS₂₀ layer after annealing at 145 °C. Image size 2*2 μm .

Section 2

2.1 PS₃₀-dendrimer films

Dendrimers are well-defined branched molecules that emanate from a central core molecule. Poly(propylene imine) dendrimers have been synthesised in a stepwise method at the Department of Macromolecular and Organic Chemistry at Eindhoven University of Technology¹⁻³. The PS functionalised dendrimer used in this study is a PS₃₀-dendrimer-(NH₂)₁₆ as shown in figure 8.6.

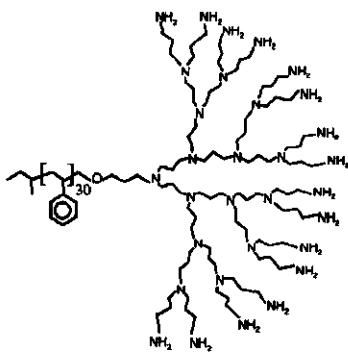


Figure 8.6. PS₃₀-poly(propylene imine) dendrimer with 16 NH₂ end groups (picture taken from ref 4).

PS₃₀-dendrimer films were prepared by dip coating from diluted tetrahydrofuran (THF) solutions (100ppm, 30 min). Non-adsorbed and loosely attached material was removed by washing with THF and the samples were subsequently dried with nitrogen. PS was spincoated from chloroform (1 mg/ml, 3000 RPM) over the surfaces, and the samples were subsequently stored at 145 °C in vacuo. After 12 days the surface topography of the top films, which are on average 5 nm thick, was investigated by means of AFM.

2.3 Wetting behaviour of a PS₃₀-dendrimer-(NH₂)₃₂ film.

The surface topography of dendrimer films after dip coating and solvent evaporation is shown in figure 8.7. The thickness of the PS₃₀-dendrimer-(NH₂)₃₂ layer is 2.5 nm as measured by ellipsometry in the dry state, using a refractive index of 1.53. This value was estimated from multiple angle measurements on films of the dendrimer. As can be seen from the figure, the surface coverage is homogeneous and smooth.



Figure 8.7. AFM image of a PS₃₀-dendrimer-(NH₂)₁₆ layer (2.5nm) onto silicon oxide after dipcoating from THF (100ppm) and washing. Image size 10*10 μm .

The wetting of PS homopolymer layers on was studied for a variety of molecular weights of PS, ranging from 1 to 10⁴ kg/mole. Dewetting of the PS layer was observed for all chain lengths of the PS. The rates at which the droplets appear, however, vary greatly, from one hour at low M_n to many days at high M_n . The contact angle of the droplets is about 20°, about the same as PS on glass⁵. It seems that adsorption of the PS₃₀-dendrimer-(NH₂)₁₆ onto the substrate results in a film where the PS tails are isolated coils that do not overlap. The lengths and grafting density of the end-attached PS chains is not sufficient to bring the spreading coefficient from a negative value to zero. The free PS film on this substrate is thus unstable and dewets and we have another case of allophobic behaviour. We observe a surface fully covered with small polymeric droplets (figure 8.8).

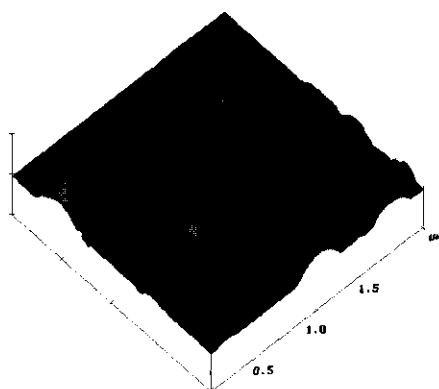


Figure 8.8. PS ($M_n \approx 10$ kg/mole) layer of 5 nm thickness on a PS_{30} -dendrimer- $(NH_2)_{16}$ underlayer after annealing for 2 days at $145^\circ C$. Image size $2 \times 2 \mu m$, and the bright areas are elevated and dark patches are depressed regions. Maximum height difference 10 nm.

Section 3

Polycaprolactone-poly-2-vinylpyridine (PCL/PVP) block copolymers

Polycaprolactone-poly(2-vinylpyridine) (PCL/PVP) polymers with different block lengths and a overall polydispersity index ~ 1.7 were synthesized at the Laboratory of Coating Technology of the Eindhoven University of Technology and used without further purification⁶⁻⁷. The structural formula is given in figure 8.9. The characteristics of the PCL/PVP samples used in this study are listed in table 8.1. The numbers in column 1 represent the number of monomeric units in both blocks and will be used to refer to the various samples.

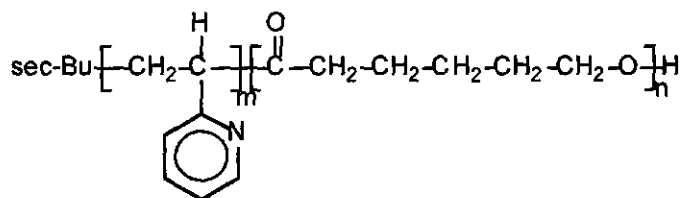


Figure 8.9. Polycaprolactone-poly-2-vinylpyridine

table 8.1. Characteristics of the PCL/PVP block copolymers

polymer PCL/PVP	M _n PCL (kg/mole)	M _n PVP (kg/mole)	N	fraction VP	M _w /M _n
10/13	1.0	1.3	23	0.56	-
9/18	0.9	1.8	27	0.67	1.5
13/13	1.3	1.3	26	0.50	1.5
13/22	1.3	2.2	35	0.63	1.6
55/50	5.5	5.0	105	0.48	1.5
39/9	3.9	0.9	48	0.19	1.7
58/15	5.8	1.5	73	0.21	1.8
39/10	3.9	1.0	49	0.20	1.7
63/35	6.3	3.5	98	0.36	-
126/41	12.6	4.1	167	0.25	-

3.1 PCL/PVP films

Brushes of these block copolymers were prepared by dip coating silicon oxide wafers into dilute solutions of PCL/PVP in a volatile, non-selective solvent (2-butanon, 100 ppm). The surface topography of the diblock copolymer layers, after dip coating and solvent evaporation is shown in figure 8.10. These typical images show that the surface coverage is homogeneous and smooth for films prepared from 2-butanon (figure 8.10a). The root mean square roughness of the polymer surface is less than 1 nm. The surface roughness of films prepared by chloroform (a selective solvent) is higher, probably due to polymer lumps adhering to the surface so that a less homogeneous film is obtained (figure 8.10b). PCL can crystallise; it seems that in chloroform part of the PCL is present in crystalites thereby forming larger clusters.

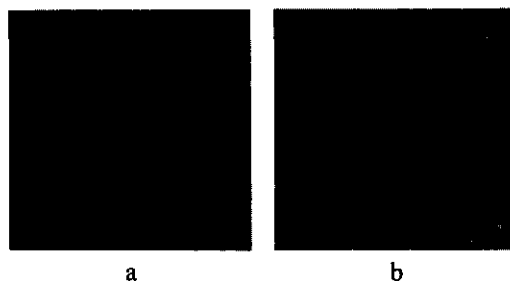


Figure 8.10. Films of PCL/PVP (39/9) prepared by adsorption from (a) 2-butanon and (b) chloroform.

3.3 Overlayers on PCL/PVP

PCL homopolymer or the resin Uralac (P3400, DSM Resins, The Netherlands) of varying molar mass were used as overlayers. The structure of these polymers is given in figure 8.11. These polymers were spincoated from 2-butanon (PCL) or chloroform (Uralac) (1 mg/ml, 3000 rpm) over the PCL/PVP treated surfaces and subsequently stored at 145 °C in vacuo. After 12 days the surface topography of the top films, which are on average 5 nm thick, was investigated by means of AFM.

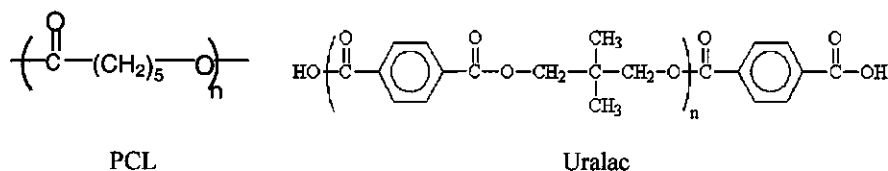


Figure 8.11. Homopolymer polycaprolactone and the polyester powder coating resin Uralac (P3400) a commercial carboxylic acid functional resin.

3.3 Wetting of PCL/PVP layers

The wetting of PCL homopolymer layers on PCL/PVP was studied for all PCL/PVP polymers listed in table 1 and three PCL polymers: two homopolymers (M_n 10 or 80 kg/mole) and one ester of PCL with trimethylolpropane ('PCL-triol, M_n 900 g/mole, see figure 8.12a) layers (5 nm thick) of these polymers were applied to the PCL/PVP

surfaces by spincoating. After annealing the samples for 2 days in vacuo at 145°C they were quenched to room temperature and investigated by AFM.

A typical AFM image of an overlayer of PCL-triol overlayer is shown in figure 8.12b. As can be seen from the figure, crystals and terraces of ~11 nm in height are formed and this occurs independent of the PCL/PVP block copolymer used for the underlayer.

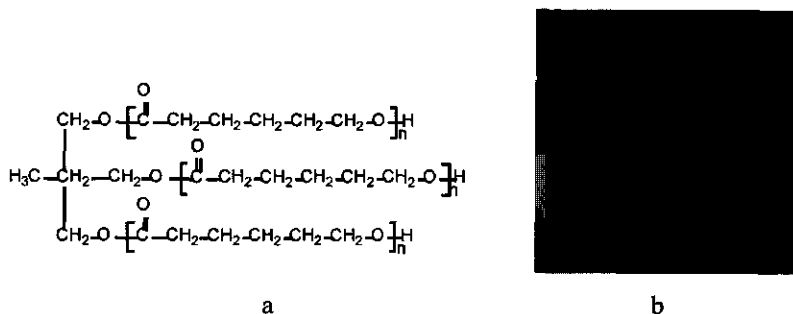


Figure 8.12. (a) tri-ester of PCL with 2-ethylglycerol ('PCL-triol' polymer). (b) AFM image of a PCL-triol layer of 5 nm on PCL/PVP 39/9 after annealing at 145°C for 2 days and cooling down to room temperature. Image size 2*2 μm, bright areas are elevated and dark patches are depressed regions. The terraces are 11nm in height.

Linear PCL-10 on a PCL brush shows wormlike structures, again independent of the type of underlayer, as can be seen in figure 8.13. The PCL film breaks up into stable wormlike structures of 20 nm height. Films annealed at 145°C for over two weeks exhibited the same wormlike structures as samples annealed for a few hours.



Figure 8.13. PCL-10 layer (5 nm) on a underlayer of PCL/PVP layer 39/9 after annealing for 2 weeks at 145°C. Image size 10*10 μm, the bright areas are elevated and dark patches are depressed regions. Maximum height difference 25 nm.

Upon increasing the molar mass of the PCL to 80 kg/mole one observes after annealing droplets of PCL and terraces of ~ 11 nm height. The droplets are 20 nm in height and are situated on top of the terraces, as shown in figure 8.14.

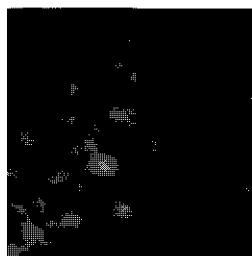


Figure 8.14. AFM image of a PCL-80 layer (5 nm) on a PCL/PVP layer (39/9) after annealing for 2 weeks at 145°C . Image size $10 \times 10 \mu\text{m}$, the bright areas are elevated and dark patches are depressed regions

Nearly all block copolymers/PCL combinations showed similar dewetting/crystallisation behaviour. The only brush/homopolymer PCL combinations with a deviation from this trend are underlayers formed by the symmetric PCL/PVP (55/50) and by PCL/PVP 58/15 brushes with a PCL-80 overlayer. As shown in figure 8.15, dendritic like structures of 10 nm in height are formed in this case. It looks as if PCL crystallises into 'spherulites' from a PCL crystal nucleus visible in the centre of the spherulites.



Figure 8.15. PCL-80 layer (5 nm) on an underlayer of PCL/PVP (58/15) after annealing for 2 weeks at 145°C . Image size $10 \times 10 \mu\text{m}$ and the bright areas are elevated and dark patches are depressed regions.

Experiments with very well controlled cooling and heating rates, as well as AFM experiments at elevated temperatures, would be needed to get more insight in the combination of dewetting and crystallisation. The crystallisation of PCL on bare substrates into spherulites has been studied⁸ and also the combination of dewetting and crystallisation of PCL onto glass substrates⁹. Film break up of these systems are ruled by competition of dewetting and crystallisation.

3.4 Wetting of PCL/PVP layers by Uralac P3400

The commercially used Uralac P3400 resin onto a bare silica surface forms smooth layers when spin cast from a chloroform solution (1 mg/ml). Annealing these surfaces at elevated temperature shows a roughening of the surface as can be seen in figure 8.16a. Overlayers of Uralac P3400 on top of all PCL/PVP layers showed complete wetting of the Uralac P3400 resin, independent of the underlying surface. Even for films stored at elevated temperatures in an inert atmosphere over several months no roughening was observed. A typical image is shown in figure 8.16b, it shows that the surface is homogeneous and smooth.



Figure 8.16. AFM image of Uralac (5 nm) on silicon oxide annealed for 24 hours (a), and Uralac (5nm) on PCL/PVP (39/9) after annealing for 1 month at 145°C. Image size 10*10 μm .

For the wetting of pigment particles in paint this means that Uralac is a stable matrix for the pigment particles covered with PCL/PVP block copolymers due to the mixing of the PCL homopolymer with the brush. We have shown in our model studies that, for wetting to occur, some interpenetration is necessary¹⁰⁻¹¹. Non-wetting corresponds

to a collapsed brush and no interpenetration. As shown in chapter 4 and 6, the degree of penetration depends on the length of the melt chains. Small chains can penetrate more easily because their translational entropy gain is relatively large. Long chains do not penetrate because they force the brush to stretch without gaining much translational entropy. Uralac P3400 has a relatively low molar mass and is polydisperse so there are always sufficiently low molar mass components in the melt which can penetrate into the PCL/PVP layer, giving rise to wetting in all cases.

4. Conclusions

Adsorbed PVP/PS/PVP triblock underlayers show complete wetting of a PS overlayer when the triblock copolymer is annealed after adsorbing the polymer onto the substrate, but dewetting occurs when the triblock polymer is not annealed after adsorption. During the annealing process, the triblock copolymer probably forms loops of PS resulting in an autophobic wetting behaviour. Increasing the number of loops shifts the wetting behaviour from dewetting to complete wetting. Needle-like structures are seen when the block copolymer layer is prepared without annealing. The origin of these structures is not known. A layer of PVP/PS/PVP on a very dense PS brush showed, after annealing, circular structures of 15 nm in diameter. The triblock copolymer forms these structures during the annealing process onto the surface.

Dewetting was observed for PS on PS₃₀-dendrimer-(NH₂)₁₆ underlayers. Adsorption of PS₃₀-dendrimer-(NH₂)₁₆ results in isolated PS chains, the number of coils is not enough to stabilise a PS overlayer.

Adsorption of a PCL/PVP block copolymer leads to a homogeneous layer when 2-butanone is used as the solvent. The behaviour of these underlayers with a thin overlayer of free PCL is governed by a compromise between crystallisation and dewetting. The PCL triol overlayers form crystals and terraces of ~11, whatever the underlying surface. Short chains of PCL-10 on a PCL/PVP underlayer produce wormlike structures of 20 nm in height. Dendritic structures are observed on 55/50 and 58/15 PCL/PVP underlayers. With a longer PCL-80 homopolymer layer, Uralac layer

on bare silicon oxide showed roughening of the surface after annealing. However, for Uralac on PCL/PVP underlayers, complete wetting was observed irrespective of the type PCL/PVP used.

References

1. J.C.M. van Hest, M.W.P.L. Baars, D.A.P. Delnoye, M.H.P. van Genderen, E.W. Meijer, *Science*, 268, 1995, 1592
2. J.C.M. van Hest, M.W.P.L. Baars, C. Elissen-Roman, M.H.P. van Genderen, E.W. Meijer, *Macromolecules*, 28, 1995, 6689
3. J.C.M. van Hest, thesis University of Technology Eindhoven, 1996
4. C. Elissen-Roman, thesis University of Technology Eindhoven, 1999
5. G. Reiter, *Langmuir*, 9, 5, 1993, 1344-1351
6. F.L. Duivenvoorde J.J.G.S. Van Es, C.F. Van Nostrum, R. Van Der Linde, *Macromol. Chem. Phys.*, 2000, 201, 656
7. F.L. Duivenvoorde, thesis University of Technology Eindhoven, 2000
8. J. Kressler, C. Wang, *Langmuir*, 13, 1997, 4407
9. B. Wunderlich, *Macromolecular Physics*, Academic Press, New York, 1973
10. Gay C, *Macromolecules*, 30, 1997, 5939
11. J.H. Maas, M.A. Cohen Stuart, F.A.M. Leermakers, N.A.M. Besseling, *Langmuir*, 16, 2000, 3478- 3481

Summary

The scientific and practical importance of thin polymer films is evident and in many applications polymer films are required. Hence, studying properties of polymer films is relevant. Adsorption of polymer at liquid/solid interfaces can stabilise particles in a matrix. Homopolymers are often used for steric stabilisation of particles although these polymers can also destabilise the system by bridging. Diblock copolymers with one adsorbing (anchor) block and one non-adsorbing (buoy) block are a much better choice when appropriate choices are made for the composition of the polymer. Bridging between particles is then avoided because the protruding buoy blocks do not adsorb on the opposite surface. The use of polymers as stabilisers can also improve the wettability of the pigment particles. The wetting behaviour of a liquid onto a surface can be modified by grafting suitable polymers to the substrate. However, grafting polymers very densely onto a surface may have the opposite effect. This thesis deals with the wetting behaviour of brushes by polymer melts. These brushes are obtained either by adsorbing block copolymers or by a chemical grafting procedure.

In chapter 2 we describe the adsorption of PVP/PS block copolymers consisting of a poly-4-vinylpyridine anchor block and a polystyrene buoy block onto silicon oxide surfaces. We investigated the adsorption kinetics and the adsorbed amounts as function of the composition of the block copolymer. Adsorption from solution is very fast and the surface is covered with the polymer within ten seconds. Adsorption from the melt generates denser brushes due to the fact that the chains are less swollen in the melt than in a good solvent. The properties of brushes obtained by both preparation techniques are compared to theoretical scaling laws. Good agreement for both data sets is found, indicating that with both preparation methods brushes are formed which are not too far from equilibrium.

Chemical grafting of brushes is described in chapter 3. We used a polystyrene with a vinyl end group which can react both with hydrogen-terminated silicon and with silicon oxide. Grafting performed directly from the melt results in very dense brushes. Reaction of the vinyl-terminated polystyrene with passivated silicon forms a silicon-carbon bond, whereas reaction of the same polymer with a silicon oxide surface gives a silicon-oxygen-carbon bond. The latter bond can be hydrolysed by boiling water or basic solutions. The chemical grafting technique allows us to prepare mixed brushes. Also, a reaction of functionalised polymer with a hydrogen-terminated silicon surface which is oxidised selectively at UV-illuminated patches (thus giving silicon oxide patches) can be performed. After hydrolysis, a brush pattern remains on the silicon parts, whereas the silicon oxide parts are free of polymer. Repeating the reaction with a polymer with a different chain length enables patterns long and short chains in a polymeric brush to be prepared.

Chapter 4 describes the wetting behaviour of a polystyrene melt on a polystyrene brush as a function of the grafting density and the chain length of the brush and the melt. Dewetting was observed for low grafting densities (allophobic region). Increasing the grafting density resulted in complete wetting. For high molar mass of the melt dewetting was again observed at very high grafting densities (autophobic regime). Low molar mass polymers showed complete wetting at high grafting densities. Numerical self-consistent-field calculations applied to this system shows that wetting can be controlled by changing the grafting density or by changing the length of the polymer melt. These calculations support our experimental observations.

The wetting and dewetting transitions are characterised by two intermediate regimes present at both the allophobic and the autophobic transition. In chapter 5 we focus on these intermediate regimes. The first intermediate regime consist of droplets in equilibrium with a mesoscopic thin film and a nearly dry surface. This

equilibrium situation can occur if the free energy curve as function of the film thickness has a special shape with a double minimum. This was confirmed by numerical self-consistent-field calculations. The second intermediate regime is polymer droplets in equilibrium with a mesoscopic thin film. In this situation no dry regions are present.

Chapter 6 describes the temperature effect of a polymer droplet on top of a brush. At a grafting density of 0.55 nm^{-2} , the droplet shows a decreased contact area at increasing temperatures. A brush consisting of chains with a grafting density of 1 nm^{-2} showed no effect of temperature. The former brush can be considered as a 'soft' brush in which the melt chains can partially mix with the brush. At elevated temperatures the chains are expelled from the brush and the droplet reduces its contact area. A 'hard' brush does not show this behaviour. In this chapter, also the wetting behaviour of a bimodal brush by a melt is described. Incorporating very few long chains into a soft brush shifts the wetting behaviour from dewetting to complete wetting. However, at high amounts of long chains (~60%) autophobic dewetting is again observed.

The deformation of the adsorbed PVP/PS polymer films by the low tip-to-sample forces in the AFM is described in chapter 7. The contact mode AFM experiments showed that the AFM tip produces rims oriented perpendicularly to the scanning direction. A wide range of molar masses of both blocks was investigated to check if there is a dependence of the rim distance of the block copolymers on the size of the PVP block copolymer. A linear relation between the composition of the polymer at a constant length of the polymer was found. A tentative explanation is proposed.

In chapter 8 we present some observations using three different systems for adsorption and wetting experiments. The first is a polystyrene layer on a brush of a triblock copolymer of vinylpyridine (end blocks) and styrene (middle block). The triblock copolymer shows complete wetting behaviour when the triblock

copolymer layer is annealed after its deposition, whereas there is partial wetting on a not annealed film. In the former case, peculiar needle like structures became visible when the sample with its overlayer of free chains, was annealed.

The second system investigated in this chapter is film formation and wettability of PS on top of a layer of a polypropylene imine dendrimer with a attached chain of PS. In all cases dewetting was observed, probably due to the relatively low amounts of hairs onto the surface. Finally, the adsorption of poly-2-vinylpyridine-polycaprolactone (PVP/PCL) block-copolymers onto silicon oxide surfaces is described, as well as the wettability of the homopolymer polycaprolactone onto such adsorbed layers. In this case the partial crystallinity of the polymer is a complicating factor.

Samenvatting

Sterische stabilisatie van polymeren wordt vaak toegepast om deeltjes te stabiliseren in een matrix. Homopolymeren worden veel gebruikt maar kunnen als nadeel hebben dat ketens een twee deeltjes adsorberen en er flocculatie optreedt. Het bevochtigingsgedrag van een oppervlak dat bezet is met polymeren kan verrassend zijn. Het oppervlak is nu bezet met polymeren en is dus niet perfect glad en ondoordringbaar. Deze polymeerketens aan een oppervlak vertonen vaak ander gedrag dan dezelfde moleculen in een bulk. Dit kan tot gevolg hebben dat chemisch identieke moleculen door entropische interacties van de moleculen aan het oppervlak elkaar afstoten. Dit zogenaamde autofobe gedrag is meer dan 40 jaar geleden voor het eerst waargenomen voor kleine moleculen op hoogenergetische oppervlakken. Het aanbrengen van polymeren aan oppervlakken kan door een copolymeer, bestaande uit een oppervlakte-actief blok ('anker') en een blok dat geen affiniteit heeft voor het oppervlak ('boei') fysisch vast te zetten. Het polymeer adsorbeert dan aan het oppervlak met het ankerblok, terwijl het boeiblok uitsteekt. Een tweede methode is, chemische verankering. Hierbij heeft het polymeer een reactieve eindgroep die reageert met het oppervlak. In beide gevallen ontstaat een polymere borstel met uitstekende haren. In dit onderzoek staat beschreven hoe zulke borstels gemaakt kunnen worden, en wat het bevochtigingsgedrag van een polymere smelt hierop is.

In hoofdstuk 2 worden diblokcopolymeren van het type poly-4-vinylpyridine-copolystyreen besproken. De adsorptie aan het oppervlak vanuit een niet-selectief oplosmiddel en vanuit de smelt is onderzocht. De geadsorbeerde hoeveelheid vanuit de smelt is een factor twee hoger dan de geadsorbeerde hoeveelheid vanuit een goed oplosmiddel. De snelheid waarmee vanuit een oplossing polymeren adsorberen is onderzocht met ellipsometrie. Gebleken is dat bij de gebruikte concentraties het oppervlak in korte tijd (ongeveer 10 seconden) verzadigd is met het polymeer. De uitkomsten van beide methoden zijn vergeleken met een door Joanny en Marques voorgestelde schalingswet en blijken daaraan beide te voldoen. Hieruit kunnen we

concluderen dat de borstels verkregen met beide methoden redelijk dicht bij thermodynamisch evenwicht zijn.

De chemische verankering van polystyreen met een eindstandige vinylgroep is onderzocht in hoofdstuk 3. De reactieve eindgroep reageert met een waterstof-getermineerd siliciumoppervlak. De ontstane verbinding bevat een silicium-koolstof binding met een grote stabiliteit. Gebleken is dat het gefunctionaliseerd polystyreen ook reageert met een silica-oppervlak en dat daarbij een silicium-zuurstof verbinding wordt gevormd. Deze ether-achtige binding kan gehydrolyseerd worden met kokend water of basische oplossingen. In dit hoofdstuk wordt ook een combinatie van deze twee verschillende covalente bindingen besproken. Het waterstof-getermineerde silicium kan namelijk met UV-licht geoxydeerd worden tot silica. Door met behulp van een masker een belichtingspatroon te maken is het mogelijk om patronen te maken, in een polymere borstel.

Hoofdstuk 4 beschrijft de bevochtiging van hydrolyseerbare en stabiele gebonden ketens door vrij polystyreen. Dit systeem werd onderzocht met Atomic force microscopy (AFM), ellipsometrie en optische microscopie. Bij een lage oppervlaktebezetting van de borstel vertoont het vrije polystyreen partiële bevochtiging (het zogenaamde allofobe gebied). Bij een hogere bezettingsgraad van de borstel treedt complete bevochtiging op. Bij zeer hoge oppervlaktebezetting van de borstel en hogere molmassa's in de smelt laat het systeem weer partiële bevochtiging zien. Numerieke berekeningen met een theorie gebaseerd op een zelf-consistent veld, voor systemen van verankerde en vrije ketens ondersteunen de experimentele resultaten.

De overgang van complete naar partiële bevochtiging wordt gekarakteriseerd door twee tussenliggende gebieden met speciale patronen. Deze patronen worden besproken in hoofdstuk 5. Het eerste tussenliggende gebied bestaat uit druppels bulkmateriaal coëxisterend met een nagenoeg kaal oppervlak en een mesoscopische film. Het tweede

gebied bestaat uit druppels polymeer in evenwicht met een mesoscopische film. Het ontstaan van deze patronen is mogelijk doordat de curve van de vrije energie als functie van de filmdikte een speciale vorm heeft, zoals aangetoond met numerieke berekeningen. In deze curve is namelijk een tweede minimum aanwezig dat invloed heeft op het mechanisme van de destabilisatie. Dit leidt tot deze speciale patronen.

In hoofdstuk 6 wordt de temperatuursafhankelijkheid van de randhoek van een druppel polymeer op een chemisch identieke borstel beschreven. Uit experimenten is gebleken dat bij verhoging van de temperatuur de randhoek op een borstel met een bezettingsgraad van 0.55 nm^{-2} een heel klein beetje toeneemt. Verlaging van de temperatuur naar de oorspronkelijke waarde geeft een daling van de randhoek, terug naar de beginwaarde. Dit proces is dus reversibel en uitsluitend een puur entropisch effect. Op een borstel met een bezettingsgraad van 1 nm^{-2} is deze thermische contractie niet aanwezig. De contractie is een anomalieit omdat meestal de randhoek afneemt met stijgende temperatuur. Een mogelijke verklaring is dat er een menging moet zijn tussen de borstel en de vrije smelt. Bij een temperatuurverhoging wordt de smelt uit de borstel gedreven en is er een aanpassing van de randhoek. Het eerste borsteltype duiden we aan met een 'zachte' borstel en het tweede als een 'harde' borstel.

Ook staat in dit hoofdstuk beschreven hoe het bevochtigingsgebied kan worden veranderd door het gebruik van bimodale borstels. Dit zijn borstels bestaande uit twee polymeren met verschillende ketenlengtes. Gebleken is dat het gebruik van bimodale borstels het venster van bevochtiging enorm vergroot. Een borstel bestaande uit veel relatief kleine ketens (20 monomere eenheden) met een kleine fractie (5%) aan lange ketens (200 eenheden) geeft reeds een omslag van partiële naar volledige bevochtiging. Partiële bevochtiging werd weer waargenomen bij 60 % lange ketens.

De Atomic Force Microscopy (AFM) kan gebruikt worden om de structuren van oppervlakken mechanisch te veranderen door een kracht uit te oefenen met de AFM-tip. Het aftasten van het een poly-4-vinylpyridine polystyreen oppervlak met een AFM tip in de zogenaamde contact mode staat beschreven in hoofdstuk 7. Bij deze

bewerking worden ribbels gevormd op het oppervlak waarvan de richting loodrecht op de aftastrichting van de tip staat. Deze structuren zijn een functie van de lengte van het totale polymeer en de fractie polystyreen in het polymeer.

In het laatste hoofdstuk staan enkele waarnemingen beschreven met borstels gemaakt met behulp van andere blokcopolymeren en smelten. Films van een triblokcopolymeer met twee vinylpyridine ankerblokken en een polystyreen middenblok zijn onderzocht, alsmede de bevochtiging van polystyreen op deze films. Gebleken is dat de voorbehandeling van de borstel een enorme invloed heeft op de bevochtigingsverschijnselen. Een niet verwarmde borstel vertoonde partiële bevochtiging en verwarmde borstels volledige bevochtiging.

Het tweede systeem beschreven in dit hoofdstuk betreft films van polypropyleen imine dendrimeren waar een polystyreen keten aan zit. Het ankerblok van dit polymeer is dusdanig groot dat de bezettingsgraad van de borstel niet erg groot wordt. Een polystyreenlaagje op deze borstel vertoonde dan ook partiële bevochtiging (allofoob gebied).

Het laatste deel van dit hoofdstuk beschrijft de adsorptie en bevochtiging van poly-2-vinylpyridine-polycaprolacton en de bevochtiging van deze borstels met het homopolymeer polycaprolacton. De samenstelling van de borstel had weinig effect op de bevochtiging, mogelijk vanwege de polydispersiteit van de borstels. De molaire massa van de smelt heeft wel invloed: er is een competitie tussen partiële bevochtiging en kristallisatie van het polycaprolacton. Lineair hoogmoleculair polycaprolacton ($M_n=80$ kg/mol) vertoonde dendriet-achtige structuren. Lineair laagmoleculair Polycaprolacton vertoonde eilandstructuren op het oppervlak, en bij het niet lineaire polycaprolacton triol polymeer (tri ester van polycaprolacton met trimethylolpropan) ontstonden terrassen van polycaprolacton van ongeveer 11 nm hoog.

Curriculum vitae

De schrijver van dit proefschrift werd samen met zijn broer op 26 mei 1970 geboren te Eindhoven. Het VWO diploma werd in 1990 behaald aan het toenmalige GSW (nu stedelijk college) in Eindhoven. In hetzelfde jaar begon hij met de studie scheikundige technologie aan de Technische Universiteit Eindhoven. Enkele onderdelen van het afstudeer opdracht werden uitgevoerd bij het Philips Natuurkundig Laboratorium te Eindhoven en het Interdisciplinary Research Centre in Polymer Science and Technology aan de universiteit van Durham (UK). Het doctoraal examen werd eind 1996 behaald en in januari 1997 begon hij met zijn promotieonderzoek bij de leerstoelgroep Fysische Chemie en Kolloïdkunde van Wageningen Universiteit. De resultaten van dit onderzoek zijn vastgelegd in dit proefschrift. Vanaf maart 2001 is hij werkzaam bij Hercules B.V. in het application and development laboratorium te Middelburg.

Dankwoord

Terugblikkend op mijn promotietijd in Wageningen zie ik mezelf vier jaar geleden voor het eerst naar Wageningen gaan. De eerst indrukken van de toenmalige vakgroep en de stad hadden een positief beeld achtergelaten. Nu een aantal jaren later is met het schrijven van dit proefschrift mijn AIO-bestaan beëindigt en was mijn eerste gevoel een juiste. Dit proefschrift is dan ook een afsluiting van een mooie tijd. Eenmaal aan de slag merk je al snel dat zonder de hulp van andere mensen je niet veel verder komt en zonder deze hulp zou dit proefschrift niet zijn geworden zoals het nu is.

Allereerst wil ik mijn beide promotoren, Martien Cohen Stuart en Gerard Fleer, bedanken voor het vertrouwen, de onophoudelijke stroom van ideeën, de intensieve discussies en de snelle correcties aan de manuscripten.

In het begin had ik enige skepsis om zelf rekenwerk te doen, maar na de eerste aarzelende pogingen ben ik nu dan ook helemaal om en zie ik de kracht en mogelijkheden van de 'sfbbox'. Frans Leermakers wil ik bedanken voor de enthousiaste begeleiding die ik kreeg en ongeacht hoe druk je het had kon ik altijd bij je terecht.

Rob van der Linde en Francis Duivenvoorde wil ik bedanken voor de samenwerking in dit duoproject waarbij de meetings in Eindhoven en Wageningen altijd zeer open en constructief waren. Ook uit Eindhoven wil ik een aantal mensen bedanken van de vakgroep Supramoleculaire en Organische Chemie. Brigitte Folmer, Marcel van Genderen en Cristina Román Vas voor de dendrimeren. Het schoonmaken van wafers heeft in ieder geval een mooie anekdote opgeleverd.

Van het Laboratorium voor Organische Chemie wil ik Alex Sieval en Han Zuilhof bedanken voor de introductie in de covalent gebonden moleculen op waterstof getermineerde wafers. Er zijn inderdaad hele mooi resultaten uitgekomen en door deze techniek hebben we gebieden onderzocht die anders niet of moeilijk toegankelijk zouden zijn geweest.

Antonie Stuiver wil ik bedanken voor al het werk dat hij in korte tijd verzet heeft. Er is niet zo heel veel van terug te vinden in het proefschrift maar je werk heeft veel

helderheid geschapen zowel in de kinetiek als in het bevochtegingsgedrag van smelten op borstels.

Als ik iets nodig had stond Ben altijd klaar met raad en daad. Ben je kent niet alleen iedereen maar regelt ook nog eens alles in zeer korte tijd en daar ben ik je reuze dankbaar voor.

Mijn kamergenoten Marcel van Eijk en Mireille Claessens wil ik bedanken voor de prettige sfeer en het oogsten van noten, appels en peren op onze tijdelijke locatie bij tuinbouwplantenteelt. Ik weet nu ook wat organellen zijn (of toch niet). Marijn bedankt voor alles; vriendschap is een kostbaar bezit. Verder wil ik Hanneke, Maarten, Martijn, Bert, Desiree, Joanne, Remco, Carla, Josie, Willy en alle andere collegae bedanken voor de goede sfeer in Wageningen.

Financial support from the Dutch National Research School Polymeren-PTN is gratefully acknowledged.